Medicine PhD program

Department of Medicine

Universitat Autònoma de Barcelona

Development and characterization of a new hydrogel for endoscopic resection. Efficacy as a drug-delivery platform for local therapy in colorectal cancer and experimental colitis animal models

Ignacio Bon Romero

Institut de Recerca Germans Trias I Pujol (IGTP)

Translational Endoscopy Research Group

April 2019

Thesis to obtain PhD degree by the Universitat Autònoma de Barcelona

Dr. Vicente Lorenzo-Zúñiga   Dr. Ramon Bartolí   Dr. Jordi Tor

(Director)   (Director)   (Tutor)

A Eva, Carmen, Vicente y Rafael,

cuyas manos solo se han podido desgastar por todo el cariño que me han dado.

AGRADECIMIENTOS

En primer lugar, me gustaría agradecer muchas cosas al Dr. Bartoli y al Dr. Lorenzo-Zúñiga. A Ramon y a Vicente. Gracias por darme esta oportunidad, y hacer caso a un e-mail de un chaval que no conocíais de nada. No solo me habéis ayudado a obtener este titulo, sino que también me habéis dado la oportunidad de formar parte activa de un grupo de investigación, en el que he sentido que hemos trabajado codo con codo, en el que he sentido que mis ideas eran escuchadas, y en el que he aprendido muchísimo, a nivel científico y personal. Espero que podamos seguir trabajando en futuros proyectos.

Por supuesto, gracias a los compañeros del IGTP, a los de la unidad de endoscopia y del servicio de digestivo del hospital.

Hay mucha gente con la que he contado durante este tiempo, mis amigos o esa familia que se escoge. He preferido dedicaros unas palabras de Jorge Guillén que, a mi entender, describen muy bien una relación de amistad. Así que amiga, amigo, si estas leyendo esto quiero que sepas que también va dirigido a ti, ¡muchas gracias!

Amigos. Nadie más. El resto es selva.

A mis amigos les adeudo la ternura
y las palabras de aliento y el abrazo,
el compartir con todos ellos la factura
que nos presenta la vida paso a paso.

A mis amigos les adeudo la paciencia
de tolerarme las espinas más agudas,
los arrebatos del humor, la negligencia
las vanidades, los temores y las dudas.

Y a ti Eva, gracias por ser tanto. Una de mis mentoras, ese chute de cafeína y credibilidad que he necesitado tantas veces, compañera de incontables copas, apoyo y tortazo de realidad cuando también los he necesitado. Esto es muy

típico, pero media tesis debería ser tuya. Gracias por ser tan buena persona, amiga y científica.

Gracias a esa familia que no escogí, sino que tuve la suerte que me tocara. Gracias mamá y papá por todo, por haber luchado para que haya tenido una buena educación, por haber inoculado en mí las ganas de viajar y ver mundo (aunque eso haya implicado estar mas alejado de vosotros). En una de las veces que estaba fuera me escribisteis que os acordabais de mi, de pequeño, diciendo que quería ver mundo; bueno, gracias a vosotros lo he conseguido, y lo seguiré haciendo. Gracias Víctor, tíos, abuelos y yayos. Como familia nos encanta discutir, pero si miro atrás solo me acuerdo de los sábados y domingos comiendo juntos, las paellas, los cocidos, o las cenas de nochebuena y navidad. Y a Taq, gracias también, el ser vivo que mas tiempo ha pasado conmigo en los últimos 6 años.

Of course, I couldn't forget to thank the Hawkins family, my family after all. Jamie and Marvin, thanks for taking in that weird Spanish boy all those years ago. You have helped me in so many ways, I just don't know how to thank you enough. I feel a part of the family, as you always tell me, and I think that is the most important thing. Thanks to the rest of the clan as well. I hope we have more chances to see each other from now on.

Por fin tengo la oportunidad de escribir esta parte de la tesis, que no significa otra cosa que el final. El final de 8 años de formación universitaria, de un sueño desde bien pequeño y de mucho trabajo y esfuerzo. Y el comienzo de muchas nuevas aventuras y proyectos. Así que, de nuevo, muchas gracias a todos por todo.

Bon vent i barca nova.

RESUM

L'endoscòpia és un procediment mínimament invasiu que permet diagnosticar condicions dins del tracte gastrointestinal, respiratori o urinari, mitjançant un endoscopi que s'insereix a través d'un orifici corporal. Els avenços en la medicina endoscòpica han conduït al desenvolupament d'una endoscòpia terapèutica que permet als metges tractar nombroses condicions mitjançant tècniques endoscòpiques com l'eliminació de pòlips i tumors primerencs.

La resecció endoscòpica de lesions grans condueix a defectes extensius de la mucosa i exposició submucosa, amb un risc substancial de complicacions (hemorràgia, estenosi i perforació), ja que els nostres enfocaments mecànics i tèrmics actuals són ineficaços en el tancament i resolució de les lesions produïdes per la resecció endoscòpica. D'altra banda, hi ha una creixent demanda de procediments endoscòpics secundaris als programes de detecció colorectal, a causa de la incidència creixent de càncer colorectal (CCR) i malaltia inflamatòria intestinal (MII) i no hi ha solució per a l'administració sostinguda de teràpies bioactives per al tractament local de lesions inflamatòries o tumorals.

Per resoldre aquestes necessitats de l'endoscòpia terapèutica hem desenvolupat un nou hidrogel, Covergel, que s'aplica directament a través de l'endoscopi sobre les lesions de la mucosa després dels procediments endoscòpics terapèutics. Covergel ha demostrat sòlides propietats curatives en models preclínics. Covergel és biocompatible, biodegradable i bioactiu; té una viscositat i capacitat d'adhesió apropiades, es pot aplicar fàcilment a través de l'endoscopi i promou la reepitelització fisiològica.

Aquesta composició s'ha desenvolupat buscant les substàncies i les seves proporcions que millorarien la viscositat, l'adherència i la resistència a la degradació bacteriana. La solució optimitzada resultant presenta la interessant propietat de convertir-se en un gel a l'entrar en contacte amb les mucoses, el que s'aconsegueix mitjançant un augment de la seva viscositat inherent amb la temperatura. En la seva forma de gel, el hidrogel pot romandre adherit a la mucosa durant un llarg període de temps (almenys 36 h), actuant així com un escut per evitar lesions tèrmiques després de EMR o ESD. Hem obtingut resultats positius en estudis de prova de concepte de lesions induïdes per dany tèrmic derivat de EMR en rates i porcs que mostren una eficàcia estadísticament significativa en la curació de la mucosa del nou hidrogel.

A mes a mes, també hem testat la capacitat d'administració sostinguda de fàrmacs del nostre hidrogel, actuant com una plataforma alliberadora de fàrmacs per administrar molècules petites i anticossos monoclonals per tractar localment les lesions de la mucosa en CRC o IBD. Els resultats obtinguts han sigut prometedors ja que, no nomes hem demostrat que la aplicació d'una plataforma alliberadora de fàrmacs a traves de l'endoscopi es possible, sinó que a mes a mes es efectiva en la resolució de les malalties en els models animals testats.

Aquest estudi suposa la creació d'una nou hidrogel per a millorar l'endoscòpia terapèutica i dotar-la de noves eines per a incrementar els casos en el que es possible fer servir endoscòpia evitant així altres procediments terapèutics mes invasius.

ABSTRACT

Endoscopy is a minimally invasive procedure that allows diagnosing conditions inside the gastrointestinal, respiratory or urinary tract, by means of an endoscope which is inserted through a body passageway. Advances in endoscopic medicine have led to the development of therapeutic endoscopy that enables physicians to treat numerous conditions using endoscopic techniques such as the removal of polyps and early tumors.

Endoscopic resection of large lesions leads to extensive mucosal defects and submucosal exposure, with a substantial risk of complications (haemorrhage, stenosis and perforation), as our current mechanical and thermal approaches are ineffective in the closure and resolution of injuries produced by endoscopic resection. On the other hand, there is a growing demand for endoscopic procedures secondary to colorectal detection programs, due to the increasing incidence of colorectal cancer (CCR) and intestinal inflammatory disease (IBD). Moreover, there is no solution for sustained administration of bioactive therapies for the local treatment of inflammatory or tumoral lesions.

To solve these needs of therapeutic endoscopy we have developed a new hydrogel, Covergel, which is applied directly through the endoscope on mucous lesions after endoscopic therapeutic procedures. Covergel has demonstrated solid healing properties in preclinical models. Covergel is biocompatible, biodegradable and bioactive; it has an appropriate viscosity and adhesion capacity, it can be easily applied through the endoscope and promotes physiological re-epithelialization.

This composition has been developed looking for the substances and their proportions that would improve viscosity, adherence and resistance to bacterial degradation. The resulting optimized solution presents the interesting property of becoming a gel when it comes into contact with the mucous membranes, which is achieved by increasing its viscosity with temperature. In its gel form, the hydrogel can remain attached to the mucosa for a long period of time (at least 36 hours), acting as well as a shield to avoid thermal injuries after EMR or ESD. We have obtained positive results in studies of evidence of lesions induced by thermal damage derived from EMR in rats and pigs that show a statistically significant efficacy in the cure of the mucosa of the new hydrogel.

In addition, we have also tested the ability of sustained drug administration of our hydrogel, acting as a drug-delivery platform to administer small molecules and monoclonal antibodies to locally treat mucous injuries in CRC or IBD. The results obtained have been promising since, not only have we shown that the application of a drug-delivery platform through the endoscope is possible but is also effective in the resolution of diseases in animal models tested.

This study involves the creation of a new hydrogel to improve therapeutic endoscopy and provide it with new tools to increase the cases in which it is possible to use endoscopy thus avoiding other more invasive therapeutic procedures.

ABBREVIATIONS

5-ASA	Mesalazine
5-FU	5-fluorouacil
A	Aflibercept
ADAs	Anti-drug antibodies
AE	Adverse events
ALG	Alginate
AOM	Azoxymethane
APC	Adenomatous polyposi coli
ASGE	American Society for Gastrointestinal Endoscopy
ATIs	Antibodies to infliximab
B	Bevacizumab
BCA	Bicinchoninic acid
BER	Base excision repair
BRAF	B-Raf proto-oncogene
BSA	Bovine serum albumin
C	Cetuximab
CD	Crohn's disease
CDEIS	Crohn's disease endoscopic index of severity
CE	Capsule endoscopy
CFU	Colony formation units
CIMP	CpG island methylator phenotype
CIN	Chromosomal instability
CMT	Critical micelle temperature
CRC	Colorectal cancer

CRP	C-reactive protein
CS	Coagulation syndrome
CTE	Computerized tomography enterography
DAP-F127	Di-acrylate pluronic F-127
DMH	1,2-dimethylhyrazine
DSS	Dextran sodium sulfate
EC	Experimental colitis
ECCO	European Crohn's and Colitis Organisation
ECM	Extra cellular matrix
EDU	Electrosurgical unit
EGF	Epidermal growth factor
EMR	Endoscopic mucosal resection
ESD	Endoscopic submucosal dissection
EUS	Endoscopic ultrasonography
FAP	Familial Adenomatous Polyposis
GC	Glyceol®
GI	Gastrointestinal
GP	Gelaspan
GS	Glucosated serum 10%
HA	Hyaluronic acid
HNPCC	Hereditary non polyposis colorectal cancer
I	Irinotecan
IBD	inflammatory bowel disease
IC	Indeterminate colitis
ICN2	Catalan Institute of Nanoscience and Nanotechnology

IFX	Infliximab
IPB	Intra-procedural bleeding
ITLs	Infliximab trough levels
KI	Knock-In
KO	Know-Out
LB	Luria-Bertani
LOH	Loss of heterogeneity
mAB's	Monoclonal antibodies
MAP	MYH-associated polyposis
MC	Methylcellulose
MLH1	mutL homolog 1
MMR	DNA mismatch repair
MRI	Magnetic resonance imaging
MSI	Microsatellite instability
MUTHY	mutY DNA glycosylase
NOD2	Nucleotide-binding oligomerization domain containing 2
P	Panitumumab
P-F127	Pluronic F127
PDGF	Platelet deriver growth factor
pEMR	Piecemeal EMR
PEO	Polyoxyethylene
PGA-FG	Polyglycolic acid sheets with fibrin glue
pHEMA	Poly (2-hydroxumethyl methacrylate)
PL	Pluronic-F127 20%
PPAR-γ	Peroxisome proliferator-activated receptor gamma

PPB	Post-procedural bleeding
PPO	Polyoxypropylene
PRP	Platelet-rich plasma
R	Resistivity
RFU	Relative fluorescence units
S	0.9% Saline
s.c.	Subcutaneous
SEM	Scanning electron microscopy
SSA	Sessile serrated adenomas
TA	Transit amplifying
TB	Hydrogel
TCF	T-cell factor
TGF	Transforming growth factor
TNBS	2,4,6-Trinitrobenzenesulfonic
TNFα	Tumor necrosis factor α
UC	Ulcerative colitis
UCCIS	Ulcerative colitis colonoscopic index of severity
VDZ	Vedolizumab
VEGF	Vascular endothelial growth factor
VEGFR	Vascular endothelial growth factor receptor
WBC	White blood cells

INTRODUCTION

1. Colon

The human colon is a tubular organ that extends from the ileocecal valve to the rectum. Its length ranges from 90 to 150 cm and its primary functions are water and electrolytes absorbance and storage of feces for the subsequent controlled excretion[1]. This organ is divided into four segments: ascending colon, transverse colon, descendent colon and sigmoid colon[1] (Figure 1).
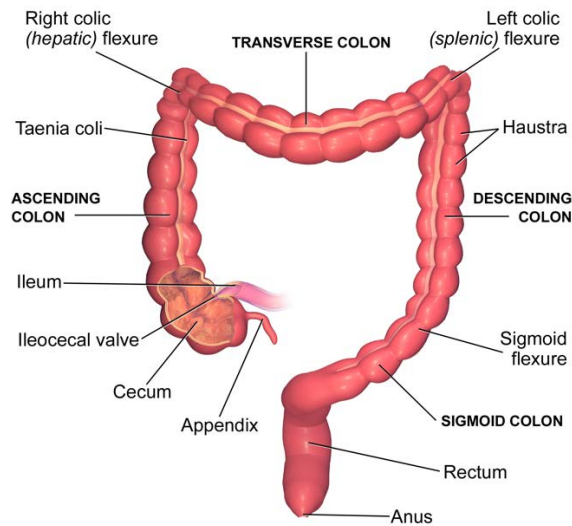
Figure 1. Anatomy of the colon[1].

The ascending colon occupies a vertical position on the right side of the abdominal cavity, going upwards until it reaches the inferior part of the liver known as the hepatic flexure. The transverse colon crosses the abdominal cavity horizontally just below the liver, stomach and spleen and on top of the small intestine. This section of the colon goes from the hepatic flexure to the splenic flexure. At both flexure points, the colon turns on itself 90°. The descending colon is also in a vertical position on the left side of the abdominal cavity, descending from the splenic flexure to the iliac crest where it connects with the Sigmoid colon. The sigmoid colon forms a loop shaped like an S, laying within the pelvis, and ends in the rectum[1]. Although constituting only

one organ, the ascending and transverse segments are grouped together as the "right colon" and the descending and sigmoid segments as the "left colon". These subgrouping of the right and left colon arises from different embryological origins and the differences in blood supply and innervation[1].

Histologically, the wall of the colon consists of 4 different layers: mucosa, submucosa, muscular and serosa (Figure 2).
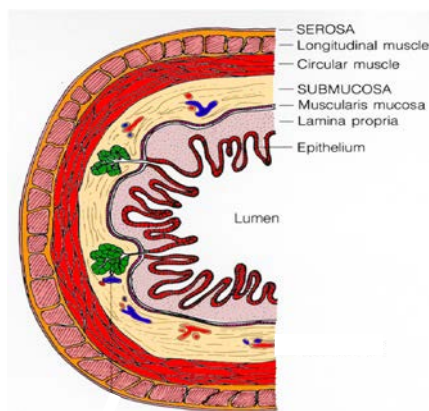
Figure 2. Colon histology. Extracted from Fiser *et al*[2].

The mucosa layer consists of a simple columnar epithelium that lies on top of connective tissue called the lamina propria, and then a thin layer of smooth muscle called the muscularis mucosae, which separates the mucosa and submucosa[3]. The epithelial cells, which form finger-like invaginations into the underlying connective tissue of the lamina propria, constitute the basic functional unit of the intestine, the Lieberkühn crypts or Colonic crypts[3]. The submucosal layer is formed by connective tissue where a network of blood and lymphatic vessels settle[3]. The muscular layer consists of smooth muscle in two different orientations, thus creating one layer of muscle in a circular fashion on the inner part of the wall and a longitudinally layer on the outer part of the wall. Finally, the most extern layer of the wall is the serosa layer, a smooth tissue membrane consisting of two layers of mesothelium[3,4].

In rats, the colon does not encircle the internal organs in the same way it does humans. Therefore, a different nomenclature is required. Authors in the community have labeled the four segments in a rat colon as: caecum, proximal colon, distal colon and rectum[5,6] (Figure 3).
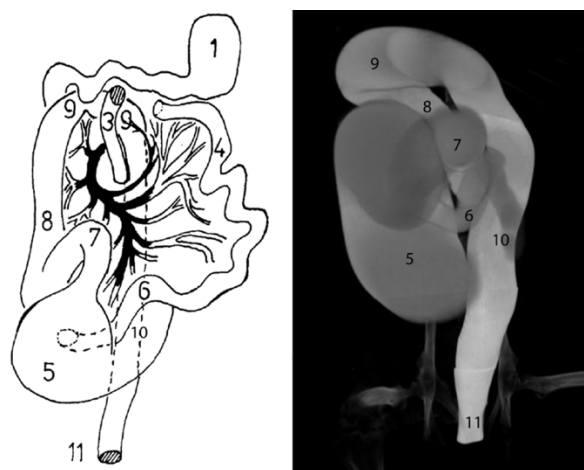
Figure 3. Colon of the rat. Left, diagram of the colon[5] and right, tomographic image. 1) stomach, 2) descending duodenum, 3) ascending duodenum, 4) small intestine, 5) caecum, 6) distal ileum, 7) small flexure of the proximal colon, 8) proximal colon, 9) major flexure, 10) distal colon, 11) rectum.

The colon of an adult rat measures around 25 cm in length. The first part, the caecum, measures approximately 4-5 cm and presents a kidney like structure with a minor curvature where the outlet of the distal ileum is located, and a convex major curvature. The colon adopts a tubular form right next to the minor curvature, on the distal pole of the caecum. Rats do not have vermiform appendix[5–7]. The proximal colon measures around 6 cm and presents a marked oblique folding of the mucosa. This characteristic mucous membrane pattern changes in the major flexure as a transition zone to the distal colon where a more protuberant mucous membrane can be found as the wall thickness of the colon decreases from the rectum to the caecum. The distal colon has a length between 7-9 cm and runs straight to the rectum which has a length of 3-5 cm[5–7]. Histologically, the colon of the rat doesn't present major differences that of a human's colon[5].

1.1. Colonic crypts

Liberkühn crypts or Colonic crypts house the tissue-specific multipotential stem cells. These stem cells are located in the niche at the base of the crypt and they hold the ability to regenerate all colonic epithelial cell types[8].

There are four major fully differentiated epithelial cell types found in the colon (Figure 4): colonocytes or absorptive cells, mucus-secreting Goblet cells, peptide hormone-secreting endocrine cells and Paneth cells. Intestinal crypts are clonal populations which ultimately derive from a single cell during development[9].
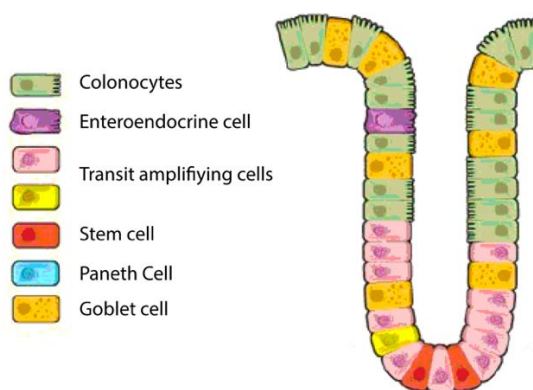
Figure 4. Structure of a colonic crypt. Adapted from Medema *et al*[10].

The niche of a colon crypt can be found by a different gradient of gene expression throughout the crypt[11]. Stem cells inside the crypt will express unique markers such as LGR5+ or ASCL2 that can only be found in these stem cells[11]. Furthermore, stem cells and transit amplifying (TA) cells show a gradient of proliferation genes such as EPHB2 or OLFM4 which grows weaker the higher you look onto the crypt[11]. Differences regarding molecular biology of cells can also be found throughout the different parts of a crypt. In the proliferative area of the crypt where TA cells are, WNT signaling pathway is more activated. This activation decreases towards the top of the crypt where BMP signaling pathway is more active[11] (Figure 5).
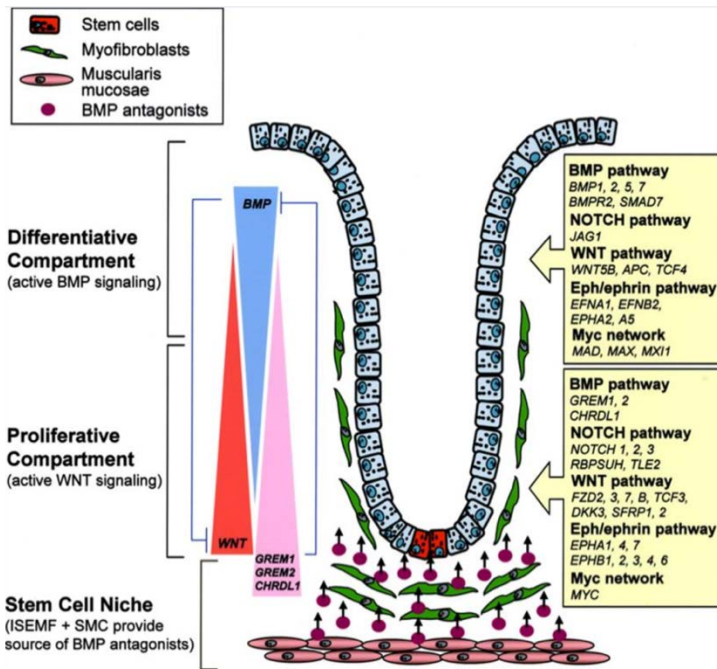
Figure 5. Gene pattern of colonic crypts[11]. Intestinal epithelial cell development and stem cell niche maintenance.

At the top of the crypt, the ratio of the different mature cells is also important[8]. The proportion of Goblet cells (mucus-secreting cells) has been found to be about 20-30% on the right colon and increases towards the left colon where it can reach up to 40-50% of total cells[8]. The proportion of these Goblet cells to the other major cell type, absorptive cells, might be important for electrolyte and fluid movement[8]. The percentage of non-Goblet cells is formed on its majority by absorptive cells higher on the surface of the crypt. Entero-endocrine cells and Paneth cells (only found on the right colon) are both found in a small number at the base of the crypt[8].

No consensus has been reached on the mechanism controlling the self-renewal, proliferation and differentiation within the crypt; two major schools of thought define these theories (Figure 6):

- The Pedigree models state a hierarchical heredity on the different cell types found in the crypt. Stem cells inside the crypt would overcome an asymmetric cell division resulting in another stem cell and another cell that differentiates into a TA cell. These TA cells will then divide symmetrically, each new generation will be more differentiated than the previous one until reaching the fully differentiated cell types of the crypt. The core of this theory is that after amplifying divisions, each cell is already set to its future mature state. This model accepts that cells would not be completely exempt from the environmental effect[12].
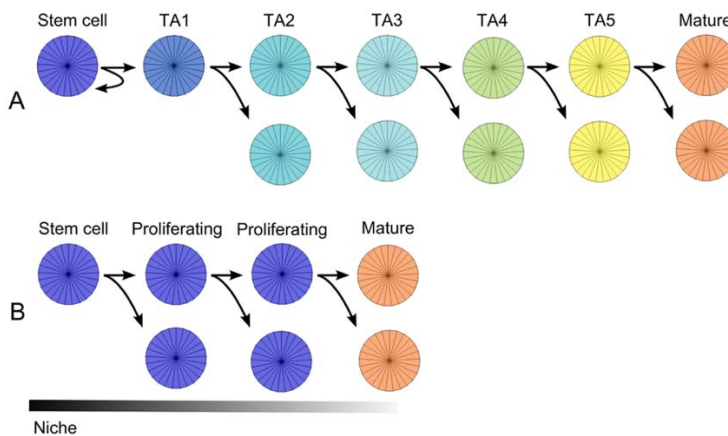
Figure 6. The Pedigree (A) and Niche (B) concept[12].

- The Niche models give all the responsibility of progression and differentiation of crypts cells to signals from the microenvironment. This microenvironment is the niche where epithelial stem cells are located. The microenvironmental conditions will change along the surface of the crypt. The bottom of the crypt is the niche where the cells would be stimulated to become stem cells and as they leave the bottom of the crypt and move upwards, the microenvironment indicates the cells to proliferate and differentiate into a fully mature state. In this model, all cell division are symmetric, but only cells

resulting from a division that stay in the bottom of the crypt will remain stem cells[12].

1.2. Mucosal healing

The mucosal barrier in the gastrointestinal tract is a defense mechanism against potentially harmful agents in the intestinal lumen such as parasites, viruses, bacteria or dietary products[13,14].

When this barrier is disrupted a biological process called epithelial restitution is activated. The extent of this response will depend on the lesion size[13,15]. Small lesions affecting one or two cells will trigger a localized effect in the surrounding epithelium[13,15]. Bigger lesions activate a more vigorous response which will enlist other cell types from the lamina propria such as myofibroblasts and immune cells[13,15]. This will lead to a secondary wound healing. Depending upon the extent of fibrous tissue accumulation, possible fibrosis and stenosis can occur[13,15]. Long lasting wounds in the intestinal barrier can lead to bacterial translocation from the gut to the peritoneum, leading to possible adverse event such as infections[13].

The wound healing process will start when an injury causes an outpouring of lymphatic fluid and blood[16], and 4 phases are well distinguished (Figure 7):

- Hemostasis phase. The wound is rapidly closed by clotting. Blood vessels constrict to restrict blood flow. Platelets stick together to seal the break in blood vessels, this is caused by the release of adenosine 5' diphosphate. Then coagulation occurs by the deposit of fibrin in the clot. Both intrinsic and extrinsic coagulation pathways are activated. This is a really quick process within the first minute after the injury. The initial vasoconstriction is followed by a vasodilatation to allow the influx of white blood cells (WBC) and the beginning of the next phase[16].
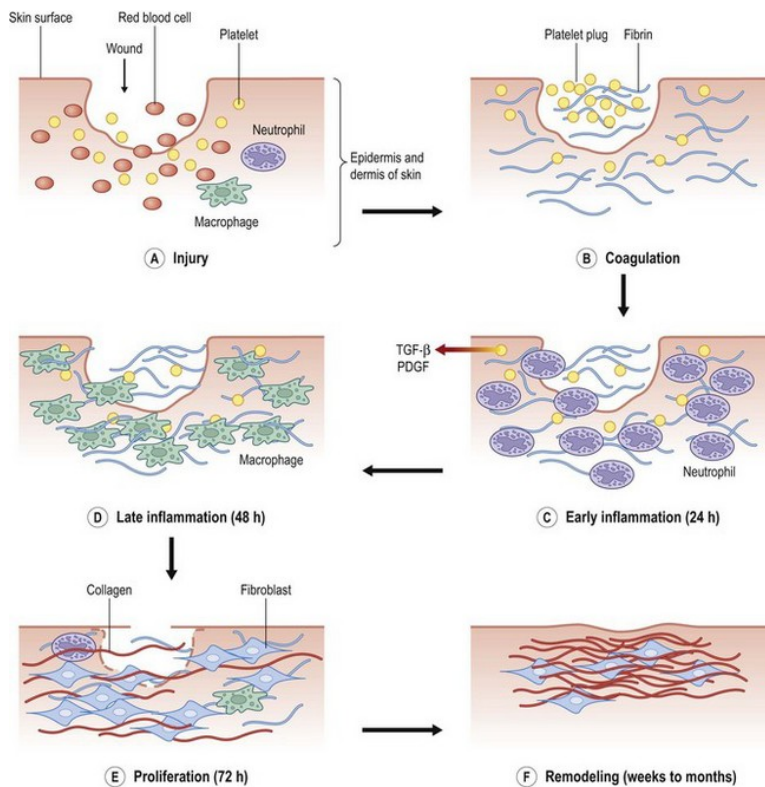
Figure 7. Wound healing phases[16].

- Inflammation phase. Injured blood vessels will leak transudate (water, salts and proteins) causing localized swelling. This phase will start with hemostasis and chemotaxis. WBC and thrombocytes release mediators and cytokines. Platelets release mediators like histamine and serotonin which increase cellular permeability, or platelet deriver growth factor (PDGF) which attracts fibroblasts and along with transforming growth factor (TGF) enhance their multiplication. Fibroblasts are in charge of collagen synthesis. WBC adhere to the fibrin clot. Neutrophils decontaminate the wound by phagocyting cellular debris and bacteria. Inflammation is seen by swelling, heat, pain and redness in the area, all caused by cells and growth factors[16].

- Proliferative or granulation phase. This phase starts around day 5 to 7. The wound is now stabilized thanks to the collagen and the extra cellular matrix (ECM) secreted by fibroblasts. To maintain this new tissue, neovascularization occurs both by angiogenesis and vasculogenesis. All the collagen and ECM help in contracting the wound. Reepithelization or epithelial restitution finally occurs with the migration of epithelial cells from the wound edges and periphery[16].

- Maturation or remodeling phase. This phase starts around week 3 and can last up to a year. Collagen starts remodeling from type III to type I and excess collagen is degraded. Wound contraction is faster. Collagen starts organizing along tension lines. Water is reabsorbed so collagen fibers can lay closer and cross-link. Excess cells not needed anymore undergo apoptosis. Healed wound areas will have about 80% of the tensile strength of unwounded skin[16].

Epithelial restitution has traditionally been divided into three different and overlapping phases. First the cells on the edge of the wound undergo a de-differentiation state and migrate to the wound. This migration is followed by a cellular proliferation and finally re-differentiation. The goal is to obtain a new epithelial cell monolayer and reestablish tight and adherent junctions for the intercellular communication. This process is regulated by growth factor, chemokines, cytokines and other factors[13,15,17].

2. Colorectal cancer

According to the WHO[18], colorectal cancer (CRC) is the 3rd most common cancer worldwide with an estimated incidence rate of 19.7 per 100,000 person/year (1,849,518 new cases in 2018) and the second according to mortality (880,792 deaths in 2018)[18].

Many risk factors account for CRC, being the two most important age and male gender, followed by family history, inflammatory bowel disease (IBD), smoking or excessive alcohol consumption.

The first variation observable in a normal epithelium that can lead to CRC are aberrant crypt foci, which are clusters of abnormal tubular-like glands in the epithelium of the colon and rectum and are considered to be the precursors of adenomas. These adenomas, adenomatous polyps or most commonly known as simply polyps can grow for a long period of time and is estimated that up to one third of population will develop polyps along their life. Nevertheless, and besides the potential to become cancerous of all polyps, only about a 10% will evolve into invasive cancer. The larger the polyp and the longer it grows, the more probability to become a cancer lesion, a carcinoma. CRC developed from polyps accounts for 96% of all cases. Once the carcinoma has penetrated into the deeper layers of the colon wall, it can reach blood and lymphatic vessels spreading first to nearby lymph nodes and later to other organs or tissues causing metastasis[18–21] (Figure 8: evolution of CRC. Adapted from Cox *et al*[22].

Figure 8: evolution of CRC. Adapted from Cox *et al*[22]

CRC is classified by three different aspects: local invasion depth (T stage), lymph node involvement (N stage) and distant metastases (M stage). Together all these stages combine into an overall stage of the tumor that will lead the therapeutic decisions (Table 1 and Table 2).

Table 1: Classification of colorectal cancers according to local invasion depth (T stage), lymph node involvement (N stage), and presence of distant metastases (M stage)[23].

T Stage	
Tx	No information about local tumor infiltration available.
Tis	Tumor restricted to mucosa, no infiltration of muscularis mucosae.
T1	Infiltration through muscularis mucosae into submucosa, not into muscularis propria.
T2	Infiltration into, but not beyond, muscularis propria.
T3	Infiltration into subserosa, non-peritonealised pericolic or perirectal tissue or both; no infiltration of serosa or nearby organs.
T4a	Infiltration of the serosa.
T4b	Infiltration of nearby tissues or organs.
N Stage	
Nx	No information about lymph node involvement available.
N0	No lymph node involvement.
N1a	Cancer cells detectable in 1 regional lymph node.
N1b	Cancer cells detectable in 2-3 regional lymph nodes.
N1c	Tumor satellites in subserosa or pericolicor perirectal fat tissue, regional lymph nodes not involved.
N2a	Cancer cells detectable in 4-6 regional lymph nodes.
N2b	Cancer cells detectable in 7 or more regional lymph nodes.
M Stage	
Mx	No information about distant metastases available.
M0	No distant metastases detectable.
M1a	Metastasis to 1 distant organ or lymph node.
M1b	Metastasis to more than 1 distant organ or lymph node or peritoneal metastasis.

2.1. Etiology

CRC is the result of an accumulation of genetic and epigenetic alterations which causes the transformation of normal colonic mucosa into invasive cancer. Pre-existing adenomas harboring some of these genetic mutations might finally give rise to CRC in a process that can take about 10 years. It is thought that up to a 35% of all CRC can be attributed to heritable factors although nowadays and approximately 70% of CRC cases are sporadic[19].

Table 2: Overall Union Internationale Contre le Cancer stage classification of CRC[23].

		T stage	N stage	M stage
Stage 0		Tis	N0	M0
Stage I		T1/T2	N0	M0
Stage II		T3/T4	N0	M0
	IIA	T3	N0	M0
	IIB	T4a	N0	M0
	IIC	T4b	N0	M0
Stage III		Any	N+	M0
	IIIA	T1-2	N1	M0
		T1	N2a	M0
	IIIB	T3-4A	N1	M0
		T2-3	N2a	M0
		T1-2	N2b	M0
	IIIC	T4A	N2a	M0
		T3-4a	N2b	M0
		T4b	N1-2	M0
Stage IV		Any	Any	M+
	IVA	Any	Any	M1a
	IVB	Any	Any	M1b

2.1.1. Hereditary CCR

Germline mutation in genes involved in colorectal carcinogenesis give hereditary CRC. Although it is believed that up to 35% of all cases are hereditary, only a 5% can be explained nowadays. Different syndromes are associated with hereditary CRC.

Familial Adenomatous Polyposis (FAP)

FAP is an autosomal dominant disorder characterized by a germline mutation in the *Adenomatous Polyposi Coli (APC)* gene. FAP accounts for less than 1% of all cases of CRC. Patients with FAP present hundreds to thousands of adenomatous polyps during adolescence and young adulthood. The location of the mutation in the *APC* gene seems to correlate with the severity of the syndrome and the extracolonic manifestations present. APC has an important role in maintaining the homeostasis of the colonic epithelium and is an important component in the canonical Wnt/β-catenin pathway. Mutations in

APC cause an accumulation of β-catenin which will bind to the T-cell factor (TCF) family of transcription factors altering the expression of different genes involved in proliferation, differentiation, migration and apoptosis[19,24,25].

Hereditary Non Polyposis Colorectal Cancer (HNPCC) or Lynch Syndrome

HNPCC or Lynch syndrome is an autosomal dominant condition caused by germline mutations in the DNA mismatch repair (MMR) system. The MMR system is in charge of repairing mistakes in the DNA replication and thus, a fault in the system will eventually lead to an accumulation of errors, an increase rate of mutations and finally a higher risk of malignancy[19,24,25].

MYH-Associated Polyposis (MAP)

MAP is caused by an autosomal recessive mutation in the *mutY DNA glycosylase (MUTYH)* gene, which encodes an enzyme called MYH glycosylase, a base excinsion repair (BER) that targets oxidative DNA damage. This carcinogenesis pathway seems to be different that of chromosome instability (CIN) pathway or microsatellite instability (MSI) pathway[24].

Hamartomatous polyposis syndromes

Hamartomatous polyposis syndromes include Peutz-Jeghers syndrome, Juvenile Polyposis syndrome and Cowden syndrome.

2.1.2. Sporadic CRC

There are three major genetic mechanisms responsible for sporadic CRC:

Chromosomal instability (CIN) pathway

This pathway account for the majority (up to 65%) of sporadic CRC. It follows a classical adenoma-carcinoma progression, and the tumorigenic process involves activation of oncogenes and inactivation of tumor suppressor genes. CIN is a result from defects in chromosome segregation that causes aneuploidy, telomere dysfunction and loss of heterogeneity (LOH). One of

the key alterations is the suppression of the tumor suppressor *APC* gene. Mutation in APC will cause a dysregulation in the canonical pathway of Wnt/β-catenin pathway as it happens in FAP. Other common mutation in the CIN pathway are mutations in the *KRAS* protooncogene, tumor suppressor p53 and heterozygosity for the long arm of chromosome 18 (18qLOH)[24–26].

Microsatellite instability (MSI) pathway

This pathway account for about 10-15% of all sporadic CRC and is the form of genetic instability present in about 95% of HNPCC. MSI pathway is primarily caused by deficiencies in the MMR system. Deficiencies in MMR system causes a 100-fold increase mutation rate in colorectal mucosal cells. Depending on how many microsatellite loci are affected by instability, MSI can be differentiated between high, low or microsatellite stable. MSI-high processes with a hypermethylation silencing of *mutL homolog 1 (MLH1)* gene promoter[24–26].

CpG Island Methylator Phenotype (CIMP)/Serrated Pathway

This pathway consists on aberrant hypermethylation of CpG sequences in the promoter regions of genes involved in cell cycle regulation, apoptosis or DNA repair. Hypermethylations cause silencing and thus, loss of gene expression. CIMP phenotype can also be divided in high or low according to the number of methylated markers. Mutation in *B-Raf proto-oncogene (BRAF)* gene are usually found in CIMP-High CRC. Moreover, BRAF mutation have been found in 90% of CRC cases with sessile serrated adenomas (SSA)[24–26].

2.2. Treatments

Surgically, the gold standard practice for the treatment of rectal cancer is the removal of the rectum along the mesorectum and the mesorectal fascia to avoid leaving any lymph nodes possibly affected behind. When facing colon cancer, the tumor and the corresponding lymph nodes must also be retrieved. Imitating the complete mesorectal removal in rectal cancer, some experts have

proposed a complete mesocolic excision, which would aid in the resection of a greater amount of mesocolon and lymph nodes[19,20]. When carcinoma in situ is present, endocopic removal of polyps might be sufficient if no tumor cells are found in the surrounding tissue after polypectomy.

Adjuvant chemotherapy after surgical resection of tissue is recommended in patients with high risk of recurrence, such as patients in Stage II-III, which have a 15-50% risk of recurrence. This adjuvant therapy is usually based on 5-fluorouacil (5-FU), but other drugs have been tested such as Capecitabine (and oral prodrug of fluorouacil), Oxiplatin or Irinotecan[19,20].

Radiotherapy, as a neoadjuvant therapy, is being tested both before surgical removal of tumors in order to reduce their size, and after surgery alone or in combination with chemotherapy, but the effect of radiotherapy is no yet all clear and further clinical research has to be carried out[19,20].

Biological targeted therapy is directed to molecules involved in the carcinogenesis of CRC that aims to reduce toxicity and adverse effects of chemotherapy. This therapy is based in monoclonal antibodies that can be given alone or in combination with some chemotherapy. The two main molecules targeted are epidermal growth factor (EGF) and vascular endothelial growth factor (VEGF)[20,26].

2.3. Animal models of CRC

Different CRC models have been developed to help in research and drug discovery. These models offer the ability to mimic genetic, histologic and molecular features of human CRC but not fully reaching an optimal imitation of the disease[27] (Table 3).

In vitro models represent the first model used when developing and testing new drugs against CRC. Basically, we have human and mouse CRC cells lines and organoids[27].

Table 3: Overview of the advantages and disadvantages of *in vitro* and *in vivo* colorectal cancer models[27].

Model type	Model	Advantages	Disadvantages
In vitro	Cell lines	Easy to culture. Many well-characterized lines available. Easy to model multiple genetic mutations.	Monoclonal cells poorly represent heterogeneity of tumor.
	Organoids	Possibility for personalized treatment. Ability to model normal intestinal tissue. Easy to model multiple genetic mutations.	Can be costly to culture.
In vivo	Xenografts, Organoid xenograft, Patient-derived xenograft	Easy to establish, rapid tumor onset. Can be used with most human cell lines. Recapitulates histology of human CRC. Can be derived from patient tumor or from genetically altered normal tissue for personalized therapy. Therapy tailored for individual patients. Tumor histology and genetic heterogeneity is similar to original tumor.	Requires immunodeficient host. Non-colon microenvironment. Homogeneous cell population does not reflect tumor heterogeneity. Can be used with most human cell lines. Potentially long tumor latency.
	Orthotopic transplantation	Uses the same microenvironment (colon) as human cancer. If transplanted into distal colon, optical colonoscopy can be used to monitor growth and response to therapy.	Technically challenging to perform. If human cells are used, requires immunodeficient animal.
	Carcinogen-induced	Near 100% efficiency in tumor formation. Ability to induce tumors in most mouse strains. Correct tumor	Models inflammatory bowel disease-mediated CRC rather than sporadic CRC. Long tumor latency.

		microenvironment. Recapitulates human adenoma histology.	Time consuming and expensive to model multiple mutations.
In vivo metastasis	Genetically engineered, Splenic transplantation, CCR9-mediated liver metastasis	Correct tumor microenvironment. Recapitulates human adenoma histology. Histologically accurate liver metastases. Reproducible liver metastasis or seeding. Liver metastasis form from primary intestinal tumors	Most tumors are adenomas, not carcinomas. Long tumor latency and poor penetrance make this model impractical for largescale study. Requires technically challenging surgery in Apc loxp14/loxp14LSLKras G12D/+ mice. Does not model true metastasis from primary tumor. Requires genetically manipulated cell lines.

In vivo models are essential to study CRC on a tumor environment way, as they are a more reliable way to mimic all the microenvironment signals that have a role on the outcome of the disease[27]. Some common *in vivo* models are the ones created by transplant, specially cell line xenografts from both murine and human CRC cells lines, but also organoid xenografts. Most recently, patient-derived xenografts, which are samples of a patient tumor injected onto a immunodeficient mouse allowing the tumor to grow have been used, allowing researchers to experiment with the exact tumor that a patient has[27].

Carcinogen induced models are developed by the application of a carcinogenic substance. These models show high reproducibility and are an inexpensive for tumor initiation[27]. 1,2-dimethylhyrazine (DMH), or its metabolite, azoxymethane (AOM) are used. AOM is N-oxidated and hydroxylated in the liver, then excreted in the bile. In the colon, microbial flora then metabolizes the agent into a form that promotes carcinogenesis. AOM administration results in tumors that often have mutations in KRAS and CTNNB1 (encoding β-catenin). However, mucosal invasion and distant metastasis is rarely seen in

this model[27]. The main disadvantage of the AOM model is the latency time that can take more than 30 weeks for tumors to appear. An alternative is the addition of dextran sodium sulfate (DSS), an agent that causes colitis. The combination of both lowers latency time to approximately 10 weeks, although this model is more representative of IBD induce CRC than sporadic CRC[27].

3. Inflammatory Bowel Disease

Inflammatory bowel disease (IBD) is the name applied to a class of conditions that share the main characteristic of chronic inflammation of the gastrointestinal tract. These affectations show a variety of phenotypes, clinical behaviors and severity. Most common classification is: Crohn's disease (CD), Ulcerative colitis (UC) and Indeterminate colitis (IC)[28,29].

Crohn's Disease is characterized by a chronic inflammation that can affect any part of the digestive tract from mouth to anus. However, the vast majority of patients have affectations in the ileum and colon. This disease shows a segmented distribution, meaning that some areas of the gastrointestinal (GI) tract might be affected and not others. It has been observed that there are healthy sections between affected areas. The inflammation can be asymmetric throughout the circumference of the wall, but it is transmural, meaning that it affects all the layers of the wall in the affected area. Therefore, the swelling of the intestinal wall will affect the mucosa, submucosa, muscular and serosa layers. This phenomenon accounts for some of the clinical manifestations of the disease such as stenosis or fistulas.

The most characteristic histological finding in these patients is the presence of noncaseating granulomas - an ensemble of epithelial cells, macrophages and lymphocytes, mainly T lymphocytes[30–32].

Ulcerative Colitis affects only the colon, starting on the rectum it can affect up to the cecum in the most extreme cases. In UC the affectation is continuous but is limited to the mucosal layer of the wall. Therefore, the appearance of

penetrating manifestations, such as transmural swelling, stenosis or fistulas, are extraordinary.

Histologically, the most unique features of this disease are the limitation of the inflammation to the mucosal layer, congestive alterations on the lamina propria with an increase on the inflammatory infiltrate, distortion of the colonic crypts and neutrophil infiltration on them, architectonic deformation of the mucosal layer and overall a diminution of the mucus barrier[30,33,34].

Indeterminate Colitis is defined by the presence of a chronic colitis of unknown etiology which, after histological study, cannot be differentiated between CD or UC[28,29].

3.1. Etiology

The cause of IBD is not fully understood yet. The main consensus settles on a combination of genetic, endogenous and environmental factors that together causes this disease. Important changes, such as dysbiosis, increased mucosal barrier permeability and bad regulation of the gut immunity trigger an exacerbated immune response and a chronic inflammatory state. A clear alteration in the interaction between host microbiome and the mucosa is seen, as a result of both genetic inheritance at several susceptibility loci and environmental factors. These susceptibility loci are mainly related with barrier function, innate and adaptive immunity[35].

UC and CD are polygenic diseases. Genome-wide scans have found susceptibility regions on 12 different chromosomes. However, no single locus has been reported in all genome scans carried out[35]. One of this susceptibility locus affects the nucleotide-binding oligomerization domain containing 2 gene (*NOD2*). Mutations affecting NOD2 hinder its ability to recognize ligands and are thought to cause a disturbance in the normal unresponsiveness of the gastrointestinal mucosa to host microbiota[35].

What is seen in IBD is a loss of control of the intestinal immune system at

different levels. The increased permeability of the mucosa allows the passage of luminal antigens towards the underlying tissue accompanied by an affection on innate and adaptive immune cells which will express a different profile of pattern-recognition receptors and thus, help on the activation and maintenance of an inflammatory response towards one's own microbiota. The inflammatory microenvironment created on the mucosa promotes differentiation of naive T cells into effector T cells (Th1, Th17, and Th2) and natural killer T cells. Intestinal epithelial cells will also start expressing costimulatory molecules enabling them to function as antigen-presenting cells and further contributes to the effector T-cell response. The effector T-cell response causes a secretion of different proinflammatory cytokines that will stimulate macrophages to secrete tumor necrosis factor α (TNFα), interleukin 1 and 6. The release of such numerous noxious mediators is responsible of tissue damage[35–38].

3.2. Treatments

Current treatments used in IBD focus on inducing and maintaining a remission state of the disease and ameliorating effects secondary to IBD. Since the exact mechanism of the disease is not yet known, treatments are not working on modifying or reversing the underlying pathogenic mechanism.

- Aminosalicylates: They derive from Mesalazine (5-ASA), an anti-inflammatory agent. Its mechanism is based on a topical anti-inflammatory effect due to a diminution of leukotriens and prostaglandins synthesis through the increased expression of peroxisome proliferator-activated receptor gamma (PPAR-γ). Their main adverse effects, although rarely frequent, are: diarrhea, headaches, skin rash and hematologic alterations. They are mainly used in UC, on the remission induction phase and on the maintenance phase at a lower dose[39,40].

- Corticoids: This is the most commonly used group of drugs to treat moderate and severe flares both in CD and UC. They have a significant potential to inhibit the inflammatory response at different levels by reducing the vascular permeability and proliferation, neutrophil migration, and collagen deposits. Intracellularly they inhibit the NF-κB factor and the arachidonic acid pathway. Corticoids are indicated during the remission induction phase but not during the maintenance phase due to their adverse effects[28].

- Immunosupressants: The most commonly used immunosupressants for the treatment of IBD are the thiopurines. Thiopurines are primarily used in the maintenance phase and to avoid recurrence of patients. The classical understanding of the mechanism of action was thought to be the inhibition of nucleotide synthesis which decreased the production of B and T lymphocytes, and hence, the immune response. Recent work, however, shows that immunosupressants inhibit the coestimulation of lymphocytes thought their effect on the protein RAC1[28].

- Biologics: This term is used to refer to monoclonal antibodies (mAb's) against inflammatory cytokines. Biologics are drugs derived partly or completely from living biological sources, like animals or humans. The most extensively used group of biologics is the one that targets TNFα, a proinflammatory cytokine, such as Infliximab (IFX) or Adalidumab. Another group is the antibodies that target integrins, such as Vedolizumab (VDZ). They inhibit lymphocytes migration towards the gut. Recommendations on the use of biological therapy is for patients with moderate to severe disease that don't respond, or are intolerant, to conventional therapy[28,41].

3.2.1. Immunogenicity of biologics in IBD

Biologics are big, complex proteins that have the risk of triggering an immunogenicity reaction in the body, and this could explain why up to a 30% of patients treated with biological therapy fail to meet desired endpoints or lose effectiveness towards the drug over time. This immunogenicity reaction will eventually lead eventually to the creation of Anti-Drug Antibodies (ADAs) and consequent loss of response[42].
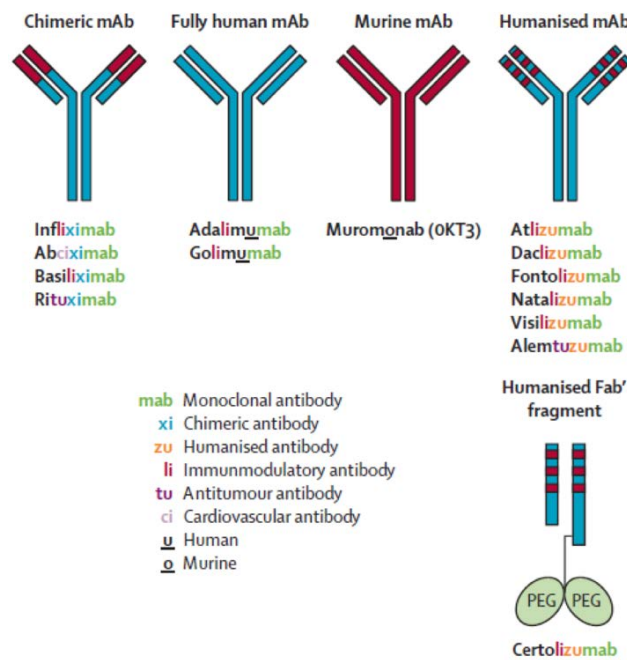
Figure 9: US FDA nomenclature for biologics used in IBD and other diseases[39].

Vermeire *et al*[42] carried out a systematic review evaluating immunogenicity publications of biologics used to treat IBD and concluded that all 6 drugs evaluated (IFX, Adalimumab, Certolixumab pegol, VDZ, Golimumab and Ustekinumab) triggered immunogenicity reactions in patients with IBD. Nevertheless, the immunogenicity rate oberserved presented a huge variability accountable to the drug, the time of the study, evaluation techniques or the

criteria for positive findings[42]. Therefore, these findings must be taken carefully when interpretations and comparisons are made.

Casteele *et al*[43] related Infliximab trough levels (ITLs), antibodies to Infliximab (ATIs) and disease activity. Their study evaluated samples from 483 patients who received maintainance therapy for CD, and concluded that there was a strong inverse correlation between ITL and C-Reactive Protein (CRP) defined remission of the disease. CRP is commonly used to evaluate inflammatory responses. Moreover, they also found a strong correlation between the presence of ATIs and the probability of active disease defined by CRP > 5 mg/L.

Their findings showed that ATIs negatively affect the efficacy of IFX even at low concentrations of ATI and an adequate concentration of ITLs. Another important finding was that ATIs seemed to have two mechanisms of action, not only by increasing the clearance of the drug as previously thought, but also by impairing the binding of IFX to TNFα, thus directly neutralizing the drug's activity by coexisting both mechanisms in patients[43].

3.3. Animal models of IBD

There is a wide variety of animal models that try to mimic IBD (Figure 10) but none of them are a complete replica of the disease, since the etiology of this disease is not yet fully understood.

The two groups of animal models most used are the chemically induced and the genetically engineered models.

Genetic engineering animal models can be further classified depending on the technique used to develop them. Conventional transgenic or Knock-Out (KO) models are genetically engineered to carry an overexpression or lack of certain gene in all cell types. Conditional Transgenic or KO models are engineered to overexpress or lack a gene in a specific cell type or under specific conditions that can be inducible. Knock-In (KI) models are characterized by

carrying a mutation in a gene of interest. Innate models are immune-deficient mice that lack both T and B cells and are able to develop spontaneous colitis[44].
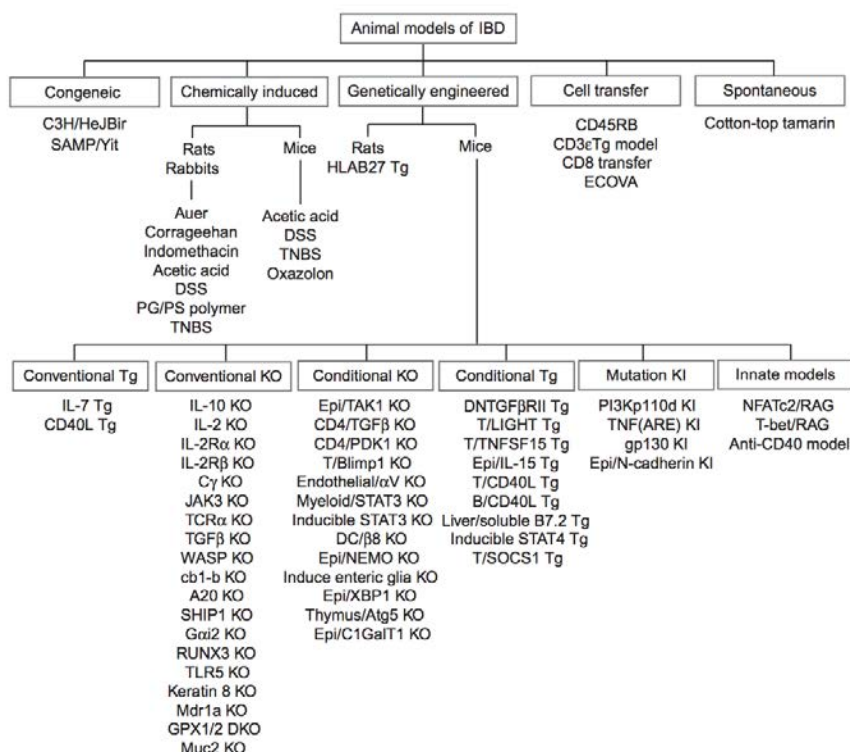
Figure 10: Classification of IBD animal models[44].

Chemically induced animal models represent a cheap method of imitating IBD. They are an easy, rapid way of studying specifically the innate immunity, inflammation and repair mechanism of the disease. However, since they are caused by an exogenous aggression, the condition is not long lasting and normally is resolved by the animal model itself. Therefore, the chemically-induced animal model is not a great representative model of a chronic disease, but a more useful model for acute outbreaks of the disease[45].

- The 2,4,6-Trinitrobenzenesulfonic (TNBS) acid model. Consists on the application of TNBS diluted in 50% ethanol through an enema. This model has been achieved in mice, rats, rabbits and pigs and

causes an acute colitis that courses with diarrhea, ulcerations and granulocytes infiltrate. The highest inflammation obtained with this model is reached at about 3-4 days after administration[44]. A closer model of chronic inflammation can be achieved by a regime of repeated administrations of TNBS, although this cannot be maintained for a long period of time.

- The Dextran Sulfate Sodium (DSS) model. Consists on the administration of 1-5% DSS in drinking water that causes acute colitis after 7-10 days. This model is characterized by bloody diarrhea, ulcerations, intestinal inflammation, body weight loss, and shortening of colon length. Damage seems to be caused by a hyperosmotic insult to epithelial cells, thus, the animal recovers spontaneously after DSS treatment, allowing to study the mechanism of recovery processes from intestinal inflammation.

4. Endoscopy

Endoscopy is a diagnostic tool consisting of the introduction of a camera or lens inside a tube or an endoscope through a natural orifice or surgical incision for the visualization of a hollow organ or a body cavity. Various names can be given to endoscopy, depending on the cavity explored: enteroscopy for the small intestine, colonoscopy for the large intestine, rhinoscopy for the nose, bronchoscopy for the lower respiratory tract, citoscopy for the urinary tract, gynoscopy for the female reproductive system or laparoscopy for the abdominal or pelvic cavities.

Endoscopy was initially established as a purely diagnostic procedure but has evolved to an important therapeutic modality over the last years[46]. The evolution of endoscopy has been marked by the vast improvements of visualization fidelity and the development of resection techniques that have given a therapeutic role to endoscopy. The growing capabilities of therapeutic endoscopy have ushered in a new era in the treatment of gastrointestinal

conditions. Significant technological advancements in endoscopic resection techniques have led to a rapid expansion of the indications of therapeutic endoscopy[47]. Colonoscopy itself is a commonly performed procedure for the diagnosis and treatment of a wide variety of affections to the colon as well as for the screening and surveillance of colorectal neoplasias[48].

4.1. Endoscopic resection techniques

Several endoscopic resection techniques are used as a tool of local excision of neoplastic lesions confined to the mucosal layer (Figure 11).

Polypectomy is a technique for the removal of polyps. When routine surveillance colonoscopy is performed, the majority of polyps found are < 10 mm. This type of small lesions, especially the ones without submucosal invasion of the tumor lesion, can be easily handle with polypectomy[49]. Lesions smaller than 5mm can be removed with biopsy forces whereas with larger lesions up to 20 mm, a snare is used in polypectomy to loop a thin wire around the polyp and cut it[49].

Unlike in endoscopic polypectomy, in endoscopic mucosal resection (EMR) and endoscopic submucosal dissection (ESD), a physiological saline solution or a sodium hyaluronate solution is locally injected into the submucosa of a superficial-type tumor through an injection needle in order to elevate the mucosa and facilitate the control of the resected margins, often difficult to control accurately through polypectomy[50]. In EMR the lesion is strangled with a snare and then resected by applying high frequency current[51]. One of EMR limitations is the size of lesions in which it can be performed, < 20 mm. For larger lesions, piecemeal EMR (pEMR) is a possibility. The low number of cases in which *en bloc* resection can be performed by EMR translates into a greater rate or recurrence of tumor lessions[49]. Nevertheless, this should not be considered as failure of the technique. ESD is a knife-based dissection procedure in which the circumference of the lesion is incised using a needle-type knife with electrical cutting current. The submucosal layer is then

dissected. The major advantage of ESD is that the lateral margin is sufficiently preserved[50]. This technique can resect the lesion in one piece regardless of its size[51]. ESD is considerably a more time consuming and difficult technique[49].
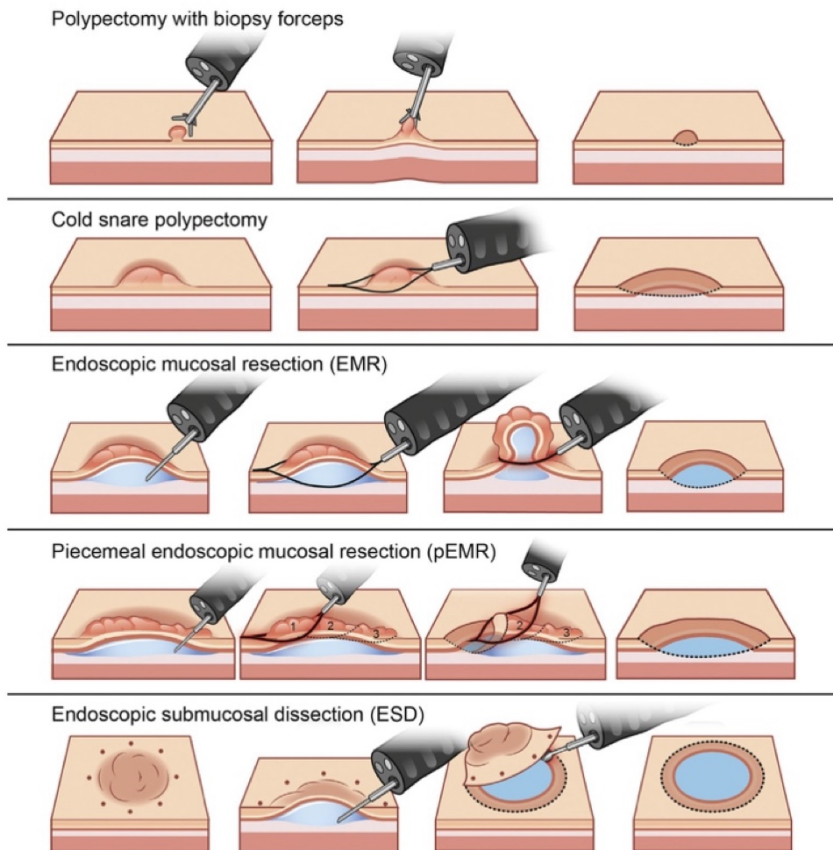
Figure 11. Endoscopic resection techniques[52].

The mucosa and muscularis propria are attached to each other by the loose connective tissue of the submucosa. Submucosal injection of a fluid creates a space between them (Figure 11), which allows resection of the mucosa alone leaving the muscularis propria layer intact. Lifting of the mucosal surface can be achieved after appropriate submucosal injection in any part of the gastrointestinal tract. After a sufficient volume of solution has been injected, the mucosa, including the target lesion, can be safely captured and resected by

electrocautery (EMR) or can be dissected by cutting submucosal tissue with an electrocautery knife (ESD)[50].

4.1.1. Adverse events in endoscopic resection

The most significant complications related to endoscopic resections are bleeding and perforation. These adverse events (AE) can be treated and resolved with endoscopic methods in the majority of cases. However, surgery might be required in other cases such as in the case of a perforation.

Bleeding is the most frequent complication related to this procedure. Bleeding can occur anytime within the first 48 hours and occasionally up to 14 days after the resection. In most cases, however, bleeding is self-limited and does not require treatment resulting in an almost null associated mortality rate.

Intra-procedural bleeding (IPB) is bleeding occurring during the procedure which persists for more than 60 seconds or requires endoscopic intervention. IPB occurs in 2.8% of patients undergoing standard polypectomy[53] and 11.3% of patients with lesions $\geq$ 20 mm treated with EMR[54] and is rarely serious. Diluted adrenaline injection may be used to gain initial control of active bleeding but should always be used in combination with a second mechanical or thermal hemostatic method.

Post-procedural bleeding (PPB) can be immediate or delayed, occurring after the procedure and up to 30 days, resulting in an unplanned medical presentation such as emergency department visit, hospitalizations or re-intervention. The incidence of PPB ranges from 0 to 9.7%.

Perforation has a rate of 0.03-0.8% during diagnostic procedures and 0.15-3% during therapeutic procedures[55]. Early diagnosis is crucial in the management of a perforation and determines the best therapeutic strategy for an optimum patient prognosis. Almost a third of the cases are detected immediately and the remaining are detected one to two days after the procedure. Risk factors for deep mural injury include attempted *en bloc* snare excision for lesions $\geq$ 25

mm, high grade dysplasia/early cancer and transverse colon location.

After an endoscopic resection technique, it is essential to inspect the mucosal defect and rule out the existence of the target sign - the presence of muscular tissue at the base of the resected lesion surrounded by submucosa. In these cases, the eschar should be closed with clips in order to avoid delayed perforation. However, clip closure is inefficient for mucosal defects greater than 30 mm due to the limited size of clips. New protocols to prevent delayed perforations in these cases are needed[56].

Another typical AE is coagulation syndrome (CS). CS occurs when the bowel wall suffers an electrocoagulation injury, which induces a transmural burn, localized peritonitis and serosal inflammation. CS can occur after any resection technique. After polypectomy and EMR, according to literature, there is a 1% chance of CS. The possibility of CS increases with ESD up to a 9% of cases[57].

4.1.2. Submucosal injection

Submucosal injection of a solution is aimed to separate the muscular and the mucosal layers in order to isolate the lesion to be resected on the mucosal layer. At the same time, the injection protects the muscularis propria from the potential damage derived from the endoscopic procedure, such as thermal and/or mechanical injury. Protection of the muscularis propria decreases the risk of adverse events such as bleeding and perforation[58].

Endoscopic resections techniques are carried out using an electrosurgical unit (ESU) which works by applying and electrical current through an electrode in contact with the tissue. Depending on the setting of the machine, ESU performs either coagulation or cutting procedure. The electric circuit that forms between the ESU, the electrode and the colon tissue can be affected by many variables. These variables can greatly alter the outcome of the procedure. Thus, electrical characteristics of the submucosal injection solution used also has an effect on this outcome[59]. Resistivity is a property of a material that

quantifies the opposition of a material to the flow of an electric current. Osmolarity is a measure proportional to solute concentration - the number of osmoles of solute particles per unit of volume in a solution. This value is indicative of the osmotic pressure of a solution which will determine how the solution will diffuse across a semipermeable membrane (osmosis). Viscosity is often referred to as the thickness of a fluid. At a molecular level, viscosity is the result of the interactions between the different molecules in a fluid and will determine the energy needed to make a fluid flow. Viscosity of a fluid, in particular blood, has been linked to its resistivity in studies where they examined the influence of fibrinogen on blood viscosity and its electrical resistivity[60,61]

The ideal submucosal injection solution should: achieve and maintain a long-lasting cushion remaining in the submucosal space long enough to safely allow the physician to perform the techniques needed, be a non-toxic solution therefor not influencing histological evaluation and should be an inexpensive, readily available and easily administered solution[58,62–65].

Saline is the most commonly used solution when performing a submucosal injection due to its low price and availability in all endoscopic units and its ease of use. Saline solutions are hindered by the quick absorption by the surrounding tissue. As a result, repeated saline solution injections are required during each procedure increasing the probability of AE[66].

In general, increasing the osmolarity of the solution also increases the duration of the submucosal cushion. However, the chance of tissue damage is increased due to osmotic pressure differences, and the greater force needed to inject more viscous solutions[58]. Some viscous and hypertonic solutions have been used in order to increase the feasibility of EMR or ESD by facilitating the formation and maintenance of the mucosal elevation[67].

Huai *et al*[58,] carried out the first meta-analysis exploring the influence of different classes of submucosal injection solutions. They identified a distinct

advantage of other solutions when compared to saline. These new viscous solutions represented an improvement in the clinical outcome of the procedure such as a higher *en bloc* resection and complete resection rates. However, there was no significant difference between the new submucosal injection solutions and saline in the prevention of AE[62,67]. Some examples of the new kind of solutions being studied are:

- Glyceol®: a hypertonic solution which consists of 10% glycerin and 5% fructose in normal saline. Uroka *et al*[68] proved that glyceol was able to maintain a higher and longer submucosal cushion than saline[68].

- Dextrose water: a hypertonic solution able to maintain a cushion longer that saline, but with possible histopathological effect on samples if the concentration of dextrose is higher than 15%[63,64].

- Hyaluronic acid: a glycosaminoglycan with high viscosity and ability to retain water that doesn't cause allergy or toxicity in humans. It is the substance that has maintained the submucosal cushion the longest and with the highest rate of *en bloc* resection in different studies[58,63–65].

- Fibrinogen mixture: this solution shows a high ability to maintain a submucosal cushion and facilitate *en bloc* resection. It also helps in the visualization through the endoscope after EMR since it can help in micro-bleedings coagulation[69,70]. One of the concerns about this solution is the possibility of cross-contamination from the blood from which the fibrinogen has been extracted.

- Cellulose substances: such as hydroxypropyl methylcellulose or carboxymethylcellulose. Both are viscous solutions capable of maintaining the submucosal cushion in a similar fashion as hyaluronic acid, but with a reduced price. Special needles might be necessary due to the high viscosity of the solutions. Moreover, further safety and efficacy studies are required as these are synthetic solutions and might give rise to antigenic reactions[63,71–73].

4.2. Endoscopic Shielding Technique

Current resolutions to adverse events derived from endoscopy are inefficient and unable to prevent all possible complications. Endoscopic shielding technique has been incorporated lately as an easy and feasible technique to better improve the outcome of endoscopic procedures and endoscopic resection techniques. Endoscopic shielding technique refers to the endoscopic application of biocompatible substances with a known biological activity to cover lesions after therapeutic endoscopy, thus providing protection of a resected area and preventing AE[74]. Endoscopic shielding technique has been shown to avoid AE and indirect cost derived from hospitalizations to treat these AE[74].

Both experimental and clinical studies have been carried out to implement this technique and asses its efficacy and feasibility. Some of the substances that have been used are Chitosan hydrogel with EGF[75] and Polyglycolic acid sheets with Fibrin Glue (PGA-FG)[76–79] among others. All of the studies were carried out to try to increase mucosal healing and prevent delayed complications of resection techniques. These studies showed an efficacy greater than 80% in all cases by the final endpoint of the study.

4.3. Endoscopy in CRC

Endoscopy has a multitask role in CRC, from simply localizing tumors to therapeutic endoscopy. Based on the American Society for Gastrointestinal Endoscopy (ASGE) guideline "Role of endoscopy in the staging and management of colorectal cancer"[80]:

- Presurgical localization of lesions is performed endoscopically. Malignant lesions are marked by endoscopic tattooing or metallic clips for the subsequent localization during surgery. This is especially important in flat, small colonic lesions difficult to find by simple visualization or palpation.

- Staging of CRC. Correctly staging the local invasion depth (T stage) of the tumor is of great importance for the first steps to take when CRC is diagnosed. Endoscopic ultrasonography (EUS) has shown, in different studies, a high specificity and sensitivity for the staging of T0 to T3 diseases, comparable to other visualizing techniques such as MRI or CT. Nevertheless, some limitations are still present, such as the understagement of T4 diseases, modest accuracy when evaluating N stage, or the advantage of MRI when guiding surgery due to the capacity of visualizing the anatomic position and relationship of tumors.

- Endoscopic management of malignant obstructions. Endoscopy presents some alternatives, or previous steps before surgery in the management of colonic obstructions. Some alternatives are self-expandable metal stents, tumor debulking or decompression tubes. Nevertheless, these techniques present some risk of AE such as obstruction, migration of the objects and perforation. Endoscopy should not be performed in patients with suspicion of perforation.

- Endoscopic resection of neoplasia. Depending on the type of lesion found and the risk of recurrence, the choice of the resection technique can vary, but generally, flat and polypoid lesions found during endoscopy should be removed. Pedunculated lesions can easily be removed by polypectomy as long as the cancer is confined to the submucosa ad there is no evidence of unfavorable histological factors, otherwise, surgical removal might be necessary.

Endoscopic removal of larger sessile or flat lesions will requires more advance techniques such as EMR or ESD. EMR is usually indicated for sessile or flat lesions confined to the mucosa or submucosa layers; lesions 2 cm or smaller can be resected *en bloc*, as for lesions bigger than 2 cm piecemeal resection or ESD are other options[80].

It is very important to minimize residual polyp tissue as much as possible by taking small samples of the mucosa surrounding the polyp or by tissue ablation. Tissue ablation with argon plasma coagulation is used both as prophylactic after a piecemeal removal and as treatment of visible residual polyp tissue[80]. A randomized study found a lower risk of recurrence in patients who had had prophylactic argon plasma coagulation after piecemeal resection vs the ones who hadn't (1/10 vs 7/11, P value = 0.2)[81]. A 2-6-month follow-up after lesions resection is recommended for both endoscopic and pathological evaluation of complete removal[80].

Jacob *et al*[82] performed a retrospective study on canadian population that was aimed to stablish the effect of colonoscopy on CRC incidence and mortality. For this, the authors used the health-service information of Ontario to study the incidence and mortality of CRC from 2001 to 2007 in patients aged 50-74 and free of CRC on January 1st 2001, and the variable was whether they had had a colonoscopy between 1996-2000 or not. The conclusion of this study was that an increased use of colonoscopy was associated with a reduction in the incidence and mortality of CRC in the studied population[82].

4.4. Endoscopy in IBD

The role of endoscopy in IBD has grown over the last years helping not only in the initial diagnosis to distinguish UC from CD but also in the assessment of the extent and severity of the disease, monitorization of the response to therapy, permitting surveillance of dysplasia or neoplasia and providing endoscopic treatment for complication such as strictures[83].

Colonoscopy coupled with ileoscopy allows the direct visualization and biopsy of the mucosa of the rectum, colon and terminal ileum. It has been proven as a safe procedure with a low rate of adverse events in patients with IBD[84]. Therefore, unless contraindicated, a full colonoscopy with ileoscopy should always be performed during the initial evaluation of patients with clinical symptoms suggestive of IBD[83]. Information obtained from an index

colonoscopy will be of great importance when differentiating UC and CD. There are many disease activity indexes for patients with IBD based on clinical symptoms or endoscopic imaging. However, there is still a poor correlation between existing symptoms scores for adults and the degree of endoscopic inflammation, or between clinical remission and mucosal healing[29,85]. Although no scoring system has been accepted as the standard, the existing endoscopic scoring systems for UC and CD are helpful for reporting endoscopic findings and assessing the endoscopic severity of the disease[83].

Capsule endoscopy (CE) is a wireless video-containing capsule which allows direct and minimally invasive visualization of the small-bowel mucosa. CE has become an important, first-line tool for the study of small-bowel pathologies such as CD[29,83,86]. Some of the contraindications of CE are strictures or obstructions. Therefore, some other imaging technique (MRI, Computerized tomography enterography (CTE) or barium contract) is needed before CE to ensure the patient has no contraindications that would preclude the use of CE[29]. CE is useful in the diagnosis of suspected small-bowel CD when radiology and ileoscopy are unsuccessful or have negative results. This process has given CE a higher diagnostic yield than other techniques for the small-bowel[87]. The European Crohn's and Colitis Organisation (ECCO) guidelines on endoscopy in IBD state that, with patients that are suspected to have CD but have negative ilecolonoscopy findings CE should be the first-line diagnostic tool if there are no obstructive symptoms[88].

Enteroscopy gives the opportunity to examine the small intestine not accessible by routine endoscopy. This technique permits the visualization of approximately 430 cm of the small intestine both via oral or rectum approach. This technique is useful in patients with abnormalities seen on other, less invasive, imaging techniques, since enteroscopy allows the endoscopic and histological evaluation as well as therapeutic interventions as hemostasis, stricture dilation or foreign body removal. Enteroscopy is accompanied by devices which assist on the technique and separate the technique on the basis

of which device is being used: single-balloon enteroscopy, double-balloon enteroscopy, spiral enteroscopy or intraoperative enteroscopy. Nevertheless, these different techniques show similar diagnostic yields. CD can be found mostly in the terminal ileum and for a complete evaluation a combination of enteroscopy techniques can facilitate an evaluation of about 100 cm of the bowel from the start of the terminal ileum, which is normally significant. Enteroscopy has a low post-procedure complication rate of about 1%, with pancreatitis and abdominal pain being the most common ones. Perforations have also been reported as procedure complications.[29,83,86,89].

Tharian *et al*[90] categorized the role of endoscopy in the diagnosis and management of IBD into three different stages:

- Complications that occur as a part of the natural history of IBD, such as strictures or neoplasia.
- Complications related to endoscopy like perforations.
- Complications related to surgery in patients with IBD: pouch-related complications or fistulae among others.

Endoscopy is used for documentation of the severity of the disease, presence of pseudopolyps and presence of fistulae-including perianal lesions. Furthermore, IBD-associated benign strictures with obstructive symptoms treatable with therapeutic endoscopy can be managed throughout the gastrointestinal tract. For the diagnosis of strictures, endoscopy is the principal tool used due to the capacity of obtaining a biopsy for histologic assessment and therapeutic procedures, as well as avoiding radiation risk of other available tools such as computerized tomography[90].

In patients with CD strictures, they are normally found in the terminal ileon and colon as well as at the ileocolonic anastomosis in the event of surgery. Endoscopy allows the visualization of the stricture, study of its malignancy through histology and therapy in certain cases. In patients with UC a stricture should always be considered malignant until histological studies prove it

otherwise. If the stricture can't be properly examined and biopsied, surgery should be considered[51].

Ferreira *et al*[91] found that the rates of colonoscopy/endoscopy-related complications seem to be similar between IBD patients and the general population. However, when using a Markov Monte Carlo model to estimate the Lifetime Risk of Complications, this seem to be higher in IBD patients, meaning a higher risk of developing a postprocedural complication due to the increased amount of procedures that IBD patients undergo, compared to the general population[91].

Endoscopy has a main role on monitoring the disease activity as a way of evaluating the response to treatments. For this, many scoring systems have been created that enable physicians to grade the degree of disease through endoscopy. One of the most used ones is the Mayo endoscopic subscore (Table 4) that looks for erythema, bleeding or ulcerations and at the same time is a part of the Mayo score which evaluates other features related to the disease. The Ulcerative Colitis Colonoscopic Index of Severity (UCCIS) (Table 5) was created from high-definition colonoscopic findings and it correlates with clinical indexes of disease activity and laboratory values of inflammation. The Crohn's Disease Endoscopic Index of Severity (CDEIS) (Table 6) is the first endoscopic scoring system for the evaluation of CD.

Table 4: Mayo endoscopic subscore[92].

Subscore	Disease activity	Endoscopic feature
0	Normal or inactive	----
1	Mild	Erythema decreased vascular pattern, mild friability
2	Moderate	Marked erythema, absent vascular pattern, friability, erosions
3	Severe	Spontaneous bleeding, ulceration

Table 5: Ulcerative Colitis Colonoscopic Index of Severity (UCCIS)[93].

Lesion	Score	Endoscopic feature
Vascular pattern	0	Normal, clear vascular pattern
	1	Partially visible
	2	Complete loss of vascular pattern
Granularity	0	Normal, smooth and glistening
	1	Fine
	2	Coarse
Ulceration	0	Normal, no erosion or ulcer
	1	Erosions or pinpoint ulcers
	2	Numerous shallow ulcers with mucous
	3	Deep, excavated ulcers
	4	Diffusely ulcerated with > 30% involvement
Bleeding/friability	0	Normal, no bleeding or friability
	1	Friable, bleeding to light touch
	2	Spontaneous bleeding
Grading of global assessment of endoscopic severity and segmental assessment of endoscopic severity	0	Normal/Quiescent
	1	Mild
	2	Moderate
	3	Severe

Table 6: Crohn's Disease Endoscopic Index of Severity (CDEIS) score sheet[94].

Parameter	Rectum	Sigmoid and Left colon	Transverse colon	Right colon	Total
Deep ulceration (12 if present, 0 if absent)					Total 1
Superficial ulceration 12 if present, 0 if absent)					Total 2
Surface involved by disease (in cm)					Total 3
Ulcerated surface (in cm)					Total 4

Total 1 + 2 + 3 + 4 = Total A.
Number of segments totally or partially explored (1-5) = n
Total A/n = Total B
If ulcerated stenosis is present, Total C = 3. If no ulcerated stenosis is present Total C = 0.
If non-ulcerated stenosis is present, Total D = 3, if no ulcerated stenosis is present Total D = 0.
Total B + Total C + Total D = CDEIS

5. Hydrogels

Hydrogels is a name commonly used to refer to hydrophilic gels, polymer networks highly swollen with water. Although an official definition of hydrogels doesn't exist, researchers have been addressing to them as being cross-linked polymeric three-dimensional networks which exhibit the ability to absorb up to thousands of times their dry weight in water within its structure, but will not dissolve in water[95–98].

A way of classifying hydrogels is based on the cross-linking technique chosen: physically or chemically cross-linked.

Physically cross-linked hydrogels are also known as self-assemble or reversible hydrogels. These hydrogels are held together by physical interactions between the different components of the hydrogel, and do not require the addition of a cross-linking agent. Different methods are available for obtaining a physically cross-linked hydrogel. Repetitive freeze-thaw cycles will promote the formation of microcrystals in the structure and thus, the cross-linking. They are connected by hydrogen bonds.

Stereocomplex formations refers to the dissolution of different substance in water which then, when mixed together, will form the cross-linked hydrogel. This kind of cross-linking process restricts the range of possible polymer compositions.

Ionic interactions are acquired in hydrogels that have been added di- or tri-valent counter ions, and the gelling principle is the capacity of opposite charged multivalent ions to gellify a polyelectrolyte solution. Gelation can also be acquired by heat induction.

Chemically cross-linked hydrogels have covalent bonds between the different polymer chains which offer them more stability, but at the same time they might present a relative long degradation time. Design flexibility is hindered by the difficulty to control important aspects such as gelation time, network

pore size or degradation time. This gelation can be achieved by the addition of cross-linkers such as glutaraldehyde, by the polymerization of monomers on a polymer backbone, by the addition of a radical initiator like ammonium persulfate or by enzymatic reactions.

The first time the term "Hydrogel" was cited in the literature was in 1894 to refer to a colloidal gel of inorganic salts[99], but it is not until 1960's that Wichterle and Lim[100] talk about hydrogels as we know them nowadays, in their paper about poly (2-hydroxumethyl methacrylate) (pHEMA) hydrogels as soft contact lenses. This gave rise to the first generation of hydrogels, which were relatively simple, chemically cross-linked networks of synthetic polymers. They were prepared by either polymerization of water-soluble monomers or by cross-linking of hydrophilic polymers[96].

Research in the field started evolving and hydrogels started to be able to respond to changes in environmental conditions like pH, temperature or molecules concentration[96]. Second generation hydrogels then, were able to be modulated by the environment they were placed in, and important aspect like gelation or drug release were better controlled[96]. The ones that were most studied were the temperature-sensitive hydrogels. Temperature was used to modulate the physical interactions in these hydrogels (hydrogen bonds, hydrophobic interactions and physical entanglements)[96].

Lately, a third generation of hydrogels has been developed. This kind of hydrogels are not held together only by hydrogen bonds or ionic interactions. New physical interactions have been put to use to improve the mechanical, thermal and degradation properties of hydrogels, and also allowing the *in situ* gelation of hydrogels[96].

5.1. Hydrogels in Biomedicine

In biomedicine, hydrogels have raised a lot of attention due to their unique characteristics. These polymeric networks present soft tissue-like elastic, non-

toxic and biodegradable properties while being responsive to stimulus. The classification for hydrogels in biomedicine is based on their physical state[95,98].

Solid hydrogels are able to mimic properties from biological tissues by imitating their complex architecture, thus providing the required cellular microenvironment. They are strong network structures held by ionic or covalent forces that are solid at room temperature but also able to swell when placed in an aqueous environment.

Semisolid hydrogels show strong adhesive interactions with a soft network, characteristics helpful for the controlled release of drugs during time. Besides, the adhesive forces allow them to adhere in biological tissues like mucous membranes. They are normally made out of two different materials, one of them being of biological origin, and have a molecular weight greater than 100, improving hydrogel's adhesion, wetting, absorption and release and flexibility.

Liquid hydrogels with reverse thermogelation show the ability to remain liquid at room temperature whereas, when reaching certain temperature, they acquire a soft tissue-like structure. The ease of synthesis of this kind of hydrogels also gives researchers the chance to adjust important aspects as network pore size. They are most advantageous for the possibility of placing molecules and cells within them, and the avoidance of surgery in order to place them inside the body, since injection is possible.

5.1.1. Swelling and water content of hydrogels

Practical applications of hydrogels can be hindered by the difficulty to predict their changes in structure after placing them in an aqueous solution. Three stages are normally followed by hydrogels when placed in a water-rich environment (Figure 12): first they start to absorb water until they reach an equilibrium, while continuing working. Then, degradation of hydrogels starts when the forces that held them together start vanishing, thus, hydrogels start increasing their volume and the polymer network starts degrading; this is

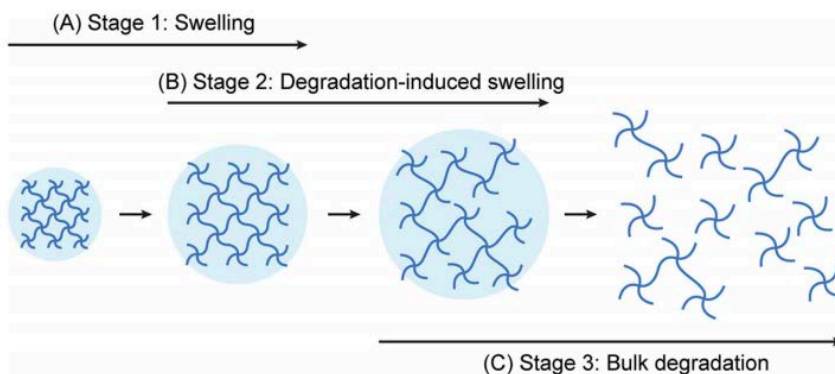known as degradation-induced swelling. This continuous swelling finally leads to a bulk degradation of the hydrogel[101].

Figure 12. Temporal changes in the shape of hydrogels after the installation. Extracted from Kamata, *et al*[101].

In hydrogels held by non-degradable unions, water will first bind to the hydrophilic groups of the hydrogel, then to the hydrophobic groups. Water bound to both types of groups is called total bound water. After, the hydrogel will still tend to swell, but this is opposed by the forces that hold the hydrogel together and it will reach a swelling equilibrium. The extra water is assumed to fill the spaces between the polymer chains and is denominated free or bulk water[95].

The content of water in a hydrogel is an important matter due to the effect that it will have into the overall permeation of substances and, ultimately, water content (or the excess of it) can also affect the structure of the hydrogel. One of the main problems derived is the possible loss of mechanical force and the possible mobilization of the hydrogel from the implanted site. Further problems arise when considering the importance of pores size within the internal structure of the hydrogel. Pores are of great importance for release and absorption of substances, cell adhesion and nutrient and waste product flow, features of great importance for the correct biocompatibility with both cells and tissues[95,101].

5.1.2. Hydrogels as drug delivery systems

Development of new drugs is a time and money-consuming procedure. Instead, adjusting the way a drug is released in the body, the location or the rate it reaches the blood stream, can be an effective solution to avoid adverse events or incorrect dosing of drugs. Hydrogels represent a promising tool to perform this controlled release thanks to the flexibility in their design, water absorbance properties and overall biocompatibility they present[102].

The release of a bioactive substance from a hydrogel can be diffusion-controlled through a membrane or the hydrogels own matrix, degradation-controlled occurring at the same pace as the hydrogel degradation, or even environmentally triggered by changes in pH, ionic strength or other features[102].

Important aspects to take into account about hydrogels when aiming a good and controlled drug release are the amount of fluid the hydrogel can take, the degree of cross-links between the different compounds of the hydrogel, or the pore size of the inner network, meaning the space between polymer chains available for diffusion[102].

5.2. Materials used in the development of hydrogels

Many polymer combinations can be used to fabricate hydrogels. Table 7 summarizes some of the most widely used combinations reported in literature. These compositions can be divided in natural or synthetic polymer hydrogels, and the combination of both.

Table 7. Hydrophilic polymers used to synthesize hydrogel matrices[95].

Natural polymers and their derivatives (± crosslinkers)	
Anionic polymers	HA, alginic acid, pectin, carrageenan, chondroitin sulfate, dextran sulfate.
Cationic polymers	Chitosan, polylysine.
Amphipathic polymers	Collagen (and gelatin), carboxymethyl chitin, fibrin.
Neutral polymers	Dextran, agarose, pullulan.
Synthetic polymers (± crosslinkers)	
Polyesters	PEG-PLA-PEG, PEG-PLGA-PEG, PEG-PCL-PEG, PLA-PEG-PLA, PHB, P(PF-co-EG) ± acrylate end groups, P(PEG/PBO terephthalate).
Other polymers	PEG-bis-(PLA-acrylate), PEG ± CDs, PEG-g-P(AAm-co-Vamine), PAAm, P(NIIPAAm-co-AAc), P(NIIPAAM-co-EMA), PVAc/PVA, PNVP, P(MMA-co-HEMA), P(AN-co-allyl sulfonate), P(biscarboxy-phenoxy-phosphazene), P(GEMA-sulfate)
Combinations of natural and synthetic polymers	
	P(PEG-co-peptides), alginate-g-(PEO-PPO-PEO), P(PLGA-co-serine), collagen-acrylate, alginate-acrylate, P(HPMA-g-peptide), P(HEMA/Matrigel®), HA-g-NIIPAAm.

Abbreviations: CD, cyclodextrin; EG, ethylene glycol; HA, Hyaluronic acid; HEMA, hydroxymethyl methacrylate; P(…), poly(…); PAAc, poly(acrylic acid); PAAm, polyacrylamide; PAN, polyacrylonitrile; PBO, poly(butylene oxide); PCL, polycaprolactone; PEG, poly(ethylene glycol); PEO, poly (ethylene oxide); PEMA, poly(ethyl methacrylate); PF, propylene fumarate; PGEMA, poly(glucosylethyl methacrylate); PHB, poly(hydroxyl butyrate); PHPMA, poly(hydroxypropyl methacrylamide); PLA, poly(lactic acid); PLGA, poly(lactic-co-glycolic acid); PNIPAAm, poly(N-isopropyl acrylamide); PNVP, poly(N-vinyl pyrrolidone); PPO, poly(propylene oxide); PVA, poly(vinyl alcohol); PVAc, poly(vinyl acetate).

Hyaluronic acid (HA) is a glycosaminoglycan type polysaccharide consisting of a basic unit of two sugars, glucuronic acid and N-acetyl-glucosamine with variable molecular weights. It is distributed along connective, epithelial and neuronal tissue and is an important part of extracellular matrix offering it an intrinsic biocompatibility[103]. HA has an important role in tissue repair due to its immunomodulatory and inductor of proliferation effects, promoting reepithelization instead of scaring. It shows high biocompatibility, this is why is has been used in some types of surgery as a main component of a hydrogel to deliver therapeutics. Different studies have focused on HA as a component

of scaffolds for wound healing. These scaffolds were able to increase dermis regeneration and wound healing[104]. HA has been widely used as a hydrogel base, and very recent reports show its benefits in different fields. Jooybar *et al*[105] have used a HA-tyramine hydrogel loaded with platelet lysate to enrich human mesenchymal stem cells for cartilage regeneration, and Garcia *et al*[106] have recently created a HA based scaffold with the ability to facilitate myogenic precursor cells for the treatment of volumetric muscle loss.

Methylcellulose (MC), a hydrophilic chemical compound derived from cellulose, is normally used as a thickener and is a non-digestible, nontoxic and non-allergenic agent. Cellulose derivatives are also used to control viscosity of solutions, improve their flow and incr/ease their UV stability[107].

First reports of HA-MC hydrogels were provided by Gupta et al[108] as vehicles to locally deliver therapeutic agents to the spinal cord. MC in a water solution shows inverse thermal gelling properties, so as the temperature increases, hydrogen bonds within the polymer break and hydrophobic junctions form to produce a gel. This process is helped by salts. The more amount of salt, the faster the gelation will be, since salts draw water molecules away from the polymer chains. HA is commercialized as a sodium salt, and thus aids in the gel formation by lowering the gelation temperature and by promoting a higher number of molecular entanglements[109].

Poloxamers are polyoxyethylene (PEO) – polyoxypropylene (PPO) – polyoxyethylene tri- block copolymers. Within poloxamers, Pluronic F127 (P-F127) has a molecular weight of 12.500 and a PEO / PPO ratio of 2:1 by weight. Solutions of P-F127 are used for their pharmaceutical advantages, specially solutions with 20% or higher, which show thermoreversible gelation properties. This thermoreversible characteristic has raised a lot of interest and different studies have clarified that when the temperature of a P-F127 solution increases the molecules that form P-F127 aggregate into micelles. It is generally accepted that micellization is due to the dehydration of the

hydrophobic PPO block with temperature; the temperature at which micelles are formed is called the critical micelle temperature (cmt). The cmt can be modified with F127 concentration; as the concentration increases, the cmt decreases[110].

Release kinetics of different drugs from P-F127 gels have also been studied and showed that diffusion coefficients of drugs in the gel decrease with higher P-F127 content, which is consequent with the increased viscosity and gel rigidity. Interestingly, although bulk viscosity of the gels has also been shown to increase with temperature, release rates actually increase with temperature[110].

HYPOTHESIS & OBJECTIVES

Endoscopy is no longer understood as a mere diagnostic tool but also as a therapeutic one. Although chiefly safe, some adverse events exist which need to be addressed in order to improve and make of therapeutic endoscopy the chosen first line treatment in those pathologies which it can be helpful. Current methods to deal with eschars after endoscopic resection techniques are done do not fulfill present needs, and thus, indirect costs due to adverse event in endoscopy are higher than they should.

Hydrogels have been on the talk for being good candidate to manage eschars and tissue after endoscopic resection, decreasing the risk of adverse event.

Moreover, these hydrogels could enable endoscopy to administer bioactive treatments directly onto mucosal lesions of the gastrointestinal tract, opening new possibilities for therapeutic endoscopy, being able to locally administer personalized treatments.

Our hypothesis is that a hydrogel could solve some of the unmet needs of therapeutic endoscopy as well as to equip it with new skills when it comes to treating gastrointestinal disorders.

Thus, we aim to:

1. Develop and characterize a new hydrogel.
2. Implement the hydrogel in therapeutic endoscopy resection techniques to cover its unmet needs.
3. Study the efficacy of the hydrogel to act as a drug-delivery platform in two animal models: CRC and experimental colitis.

MATERIALS & METHODS

1. Development and characterization of the new hydrogel

For the first part of these project we aimed to characterize and better understand the properties of this newly developed hydrogel. The tests carried out during this part were related to the future uses we wanted to give the hydrogel.

1.1. Composition of the new hydrogel

4 different combinations of materials were tested as a possible new hydrogel based on literature found on the characteristics of each material. The initial base of this hydrogel was designed to be only HA+MC, and additional modifications were done to test four prototypes. Combinations are shown in Table 8.

Table 8. Four initial hydrogel combinations tested.

Sample	HA	MC	SA-CaCl$_2$*	P-F127	Medium
CD1	0.3g	0.6g	-	-	30mL H$_2$O
CD2 (Covergel)	0.3g	0.6g	-	6g	30mL H$_2$O
CD3	0.3g	0.6g	-	-	30mL PBS
CD4	0.3g	-	0.24g–0.06g	-	30mL H$_2$O

* Sodium alginate and sodium chloride

1.2. Rheological test

Viscosity was evaluated in a rheometer Haake RheoStress (Thermo Fisher Scientific, Waltham, MA USA) with a C60/1°Ti probe and a gap set of 0.053 mm. Rotation ramp went from 0–300 s^{-1} in 30 seconds. For each study, Viscosity (η) was measured as a function of shear rate (γ) at 22°C and 37°C.

Adhesion was measured with a Texture Analyzer TA.XT Plus (Stable Micro Systems, Surrey, UK). A 40-mm (diameter) disk was compressed into the gel and redrawn. Velocity of the insertion assay was 1mm/s and withdrawn distance was 9mm. Adhesion was determined at 20°C and 37°C.

After rheological tests, the best combination was chosen to continue with the characterization study, and the hydrogel will be referred to Covergel from now on.

1.3. Preparation of the thermally-reversible hydrogel

The base of Covergel is distilled water with 20% of the thermosensible tensioactive Pluronic F127 (Sigma-Aldrich), 2% of Methylcellulose (Sigma-Aldrich) and 1% of Hyaluronic acid (TCI Europe) (Figure 13).
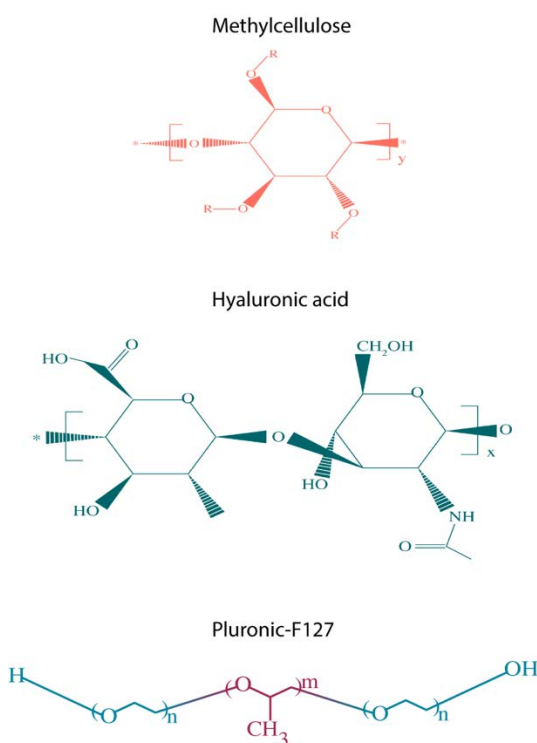
Figure 13. Materials used to develop our hydrogel

First, the desired quantity of Pluronic F127 was placed on a clean vial and the needed volume of distilled water was added; the vial was set to agitation at 500rpm until the solution was completely homogeneous. Then, Methylcellulose was added to the vial and it was put back in agitation at 500rpm until complete dissolution. Finally, Hyaluronic Acid was added

following the same agitation conditions.

This preparation was carried out at 4°C to avoid the effect of temperature which would slow the process.

We saw the need to improve the stability in aqueous medium of the Covergel, this is why it was proposed to prepare a hydrogel irreversible to gelation. For this, Dr. Mary Cano at the Catalan Institute of Nanoscience and Nanotechnology (ICN2) performed the chemical modifications necessary on the thermosensible tensioactive Pluronic F127(P-F127) to add acrylate groups (Di-Acrylate Pluronic F-127, DAP-F127) (Figure 14) and allow for the irreversible gelation when Covergel was exposed to UV light.
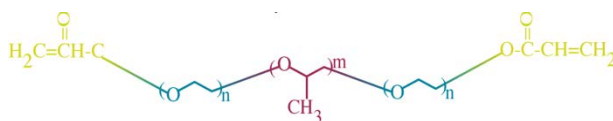

Figure 14. Di-acrylate Pluronic-F127.

1.4. Preparation of DAP-F127

In a 250 mL Florence flask 25 g of P-F127 were added to 80mL of Toluene at room temperature and under a nitrogen atmosphere. Next the mixture is cooled in an ice bath at 0°C and 1.2 mL of thiethilamine, 20 mL of dichloromethane and 0.5 mL of Acryloyl chloride previously dissolved in 20 mL of dichloromethane were added. The sample is allowed to stir for 12 hours. The mixture is then vacuum filtered to remove the subgroup of triethylammonium chloride generated during the reaction. The collected supernatant is rotavaporated under vacuum for 5 hours until a viscous oil is obtained. Subsequently, said oil is dissolved in dichloromethane and washed with deionized water and dried with sodium sulphate. This process is repeated 3 times. Finally, the DAP-F127 is precipitated with and excess of diethylether at low temperature. The obtained precipitate is allowed to dry under vacuum for a day.

1.5. Preparation of the irreversible gelation hydrogel

The base of this irreversible gelation Covergel is distilled water with a 20% of the thermosensible tensioactive Pluronic F127 modified with the addition of acrylate groups (Sigma-Aldrich, ICN2), a 2% of Methylcellulose (Sigma-Aldrich) and a 1% of Hyaluronic acid (TCI Europe).

First, the desired quantity of Di-acrylate Pluronic-F127 was placed on a clean vial and the needed volume of distilled water was added; the vial was set to agitation at 500 rpm until complete dissolution. Then, Methylcellulose was added to the vial and it was put back in agitation at 500rpm until complete dissolution. Finally, Hyaluronic Acid was added following the same agitation conditions. This preparation was carried out at 4°C to avoid the effect of temperature which would slower the process.

1.6. Preparation of the photo-initiator

In a 5 mL vial, 154 mg of the photo-initiator Irgacure 2959 (Sigma-Aldrich) are added on 700 μL of ethanol and 300 μL of deionized water. This mixture is left stirring at 500 rpm for 10 minutes. The photo-initiator concentration is 1.15% compared to the amount of DAP-F127 in the hydrogel. The photo-initiator dissolution must be protected from light with aluminum foil.

1.7. Gelation assay

This assay was carried out to determine the behavior of Covergel with ultraviolet light and with different temperatures. The following scenarios were tested:

- 1mL of Covergel and 15 μL of photo-initiator solution were mixed and placed on a petri dish. Covergel was heated at 37°C for 30 min and gelation was tested. Next, Covergel was cooled.
- 1 mL of Covergel and 15 μL of photo-initiator solution were mixed and placed on a petri dish. The dish was placed under ultraviolet light

2000 mV/cm² for 3 minutes (AnalytikJeta UVP Crosslinker) keeping the temperature below 20°C. Covergel was heated at 37°C for 30 min and gelation was tested. Next, Covergel was cooled.

- 1mL of Covergel was placed on a petri dish. Covergel was heated at 37°C for 30 min and gelation was tested. Next, Covergel was cooled.
- 1 mL of Covergel was placed on a petri dish. The dish was placed under ultraviolet light 2000 mV/cm² for 3 minutes (AnalytikJeta UVP Crosslinker) keeping the temperature below 20°C. Covergel was heated at 37°C for 30 min and gelation was tested. Next, Covergel was cooled.

1.8. Degradation assay

We aimed to know the degradation rate of Covergel under different conditions that would try to mimic the different conditions found in the gastrointestinal tract.

For this, 1 mL of Covergel was irreversibly gelified and then, submerge in 10 mL of one of the following solutions:

- PBS pH=7
- PBS pH=3
- PBS pH=9
- PBS pH=11
- Rat feces bacteria culture on Luria-Bertani (LB) Broth at a starting range of 10^5 CFU/mL*.

The piece of Covergel was weighed before the submersion (Wo) and then on set date points until complete dissolution of the hydrogel or until one month under the conditions was reached. Each time point the medium was also changed when the weighting took place.

*On a previous experiment, a calibration curve for the Optical Density/Colony Formation Units (CFU) was performed by reconstituting 1g of rat feces on 10 mL of LB and then performing a series of dilutions from -1 to -11. These dilutions were both, cultured on LB Agar petri dishes to account the number of CFUs and measured with a spectrophotometer at 600nm for the Optical Density evaluation. Later, the curve equation was obtained: $y=7.452\times10^{-7}x-0.002385$. $R^2=0.9988$. Data not shown.

1.9. Drug release/absorbance study

We were interested in studying the capacity of Covergel to both release and absorb molecules of different molecular weight, in order to further study the capability of Covergel to act as a drug-delivery platform.

For these experiments, we worked with two molecules:

- Trypan blue, which is a dye used in Biology as a vital stain to selectively color dead tissues or cells blue. Its chemical formula is $C_{34}H_{24}N_6Na_4O_{14}S_4$ and has a molar mass of approximately 960 Daltons

- Bovine serum albumin (BSA) which has a molecular weight of 66.5 kDa.

For the trypan blue experiments, first, a calibration curve was prepared by measuring the absorbance of different concentrations of trypan blue diluted in water with a spectrophotometer (Varioskan Flash, Thermo) with the excitation wave measuring 450nm. SkanIt Software 2.4.1 was used to analyze results. Then, the curve equation was obtained: $y=6234.9x+0.1008$. $R^2 = 0.99349$. Data not shown.

Absorbance and release of BSA was evaluated with the Bicinchoninic acid (BCA) Protein Assay Kit (Pierce™, Thermo Scientific).

The BCA Protein Assay Kit is a colorimetric detection and quantification

method of total protein. It is based on the reduction of Cu^{+2} to Cu^{+1} by proteins in an alkaline medium (Biuret reaction) with the detection of cuprous cation (Cu^{+1}) using BCA. The purple-colored reaction product of this assay is formed by the chelation of two molecules of BCA with one cuprous ion. Plates are then read at 562nm using a spectrophotometer (Varioskan Flash, Thermo). SkanIt Software 2.4.1 was used to analyze results.

To incorporate substances inside Covergel, 0.25 mL of gelated Covergel were submerged in 5 mL of 0.0005 mg/mL trypan blue or 2 mg/mL BSA. Covergel incorporated the solution at room temperature for 48 hours. To calculate the amount of substance incorporated into the matrix of Covergel, the following equation was used:

$$\text{Incorporating efficiency (\%)} = \frac{(V_1 C_1 - V_2 C_2)}{V_1 C_1} \text{ X } 100$$

Where:

- V_1: original volume of substance solution (mL).
- V_2: remaining volume of substance solution after 48h (mL).
- C_1: initial concentration of substance (μg/mL).
- C_2: remaining concentration of substance (μg/mL).

Covergel was withdrawn from the solution and placed in release medium (PBS). At specific time points, amount of substance released into the medium was evaluated as mentioned before.

The kinetics of drug release from Covergel was studied using several mathematical models which describe the kinetic behavior of drug release in diffusion system without a membrane[111].

Three different models were analyzed, to asses which one fitted best with the release data from our experiments. The three different models were:

$$\text{Higuchi release model: } M_t = K_h t^{1/2}$$

$$\text{Zero-order release model: } M_t = K_0 t$$

$$\text{First-order release model: } M_t = 1 - e^{-K_1 t}$$

Where M_t is the fraction of drug released at each time point (t) and K_h, K_0 and K_1 are the Higuchi release kinetic constant, the zero-order release kinetic constant and the first-order release kinetic constant respectively.

Lastly, the drug release mechanism was analyzed using the Korsmeyer-Peppas model. This is a semi-empirical model used when the exact mechanism is not known or in the case that more than one mechanism is involved in the drug release[111].

$$\text{Korsmeyer-Peppas model: } F = (M_t/M) = K_m t^n$$

Where F is the fraction of drug released at time (t), M_t is the amount of drug released at time (t), M is the total amount of drug in the hydrogel, K_m is a kinetic constant and n is the release exponent, indicative of the drug release mechanism. n is estimated from linear regression of log (M_t/M) versus log t; when determining the n exponent, only portions of the release curve $\leq 60\%$ should be used.

1.10. Biocompatibility

1.10.1. Co-culture with cells. Cell Viability

To study the possible cytotoxicity induced by Covergel we carried out a co-culture of a cell line with different conditions involving Covergel. The cell line chosen for these experiments was Caco-2 (ATCC® HTB-37™) a human colorectal adenocarcinoma cell line.

For cell viability evaluation, 3×10^4 cells/cm² cells were cultured in 24-well cell plates under the following conditions:

- Normal culture medium (DMEM medium supplemented with 10% Fetal Bovine serum, 1% L-Glutamine and 1%

Penicilyn/Streptomicyn) as a positive control.

- Normal culture medium supplemented with 10% Dimethyl sulfoxide (DMSO) as a negative control

- Normal culture medium supplemented with 1%-2%-5%-10%-15% of Covergel v/v.

Cells were cultured at 37ºC and 5% CO_2 for 24, 48, 72 and 96 hours. At specific time points cell viability was evaluated using Resazurin Sodium Salt (Sigma-Aldrich).

Briefly, Resazurin sodium salt (7-Hydroxy-3H-phenoxazin-3-one-10-oxide sodium salt) is a blue dye weakly fluorescent until it is irreversibly reduced by living organism (bacteria, fungi, mammalian cells…) to Resofurin, a highly red fluorescent. The reduction of Resazurin Sodium Salt correlates with the number of living cells. Samples are exposed to Resazurin Sodium Salts for 4 hours and then absorbance at 570 nm is analyzed using a spectrophotometer (Varioskan Flash, Thermo).

1.10.2. Hemolysis test

Two mL of gelified Covergel were placed in 20 mL of sterile saline and incubated for 72 h at 37ºC. After, the solution was collected and filtered with a 0.22 µm membrane. Two mL blood samples were freshly collected from six male Sprague Dawley rats into an anticoagulant tube and gently mixed, blood was then diluted with 2.5 mL of saline.

For the hemolysis test 10 mL of the Covergel extraction, distilled water, and saline were poured in 50 mL test tubes and placed at 37ºC for 30 min. After that, 0.2 mL of diluted blood were added to each test tube with gently shaking and the solution was placed at 37ºC for 1 hour (Figure 15). The absorbance of the samples after 1 hour was evaluated with a spectrophotometer (Varioskan Flash, Thermo) at 545 nm. SkanIt Software 2.4.1 was used to analyze results. This protocol was adapted from Li *et al* [112].

Hemolisys ratio was calculated with the following formula:

$$\text{Hemolysis ratio } (\%)= \frac{\text{A hydrogel extraction-A saline solution}}{\text{A distilled water-A saline solution}} \times 100$$
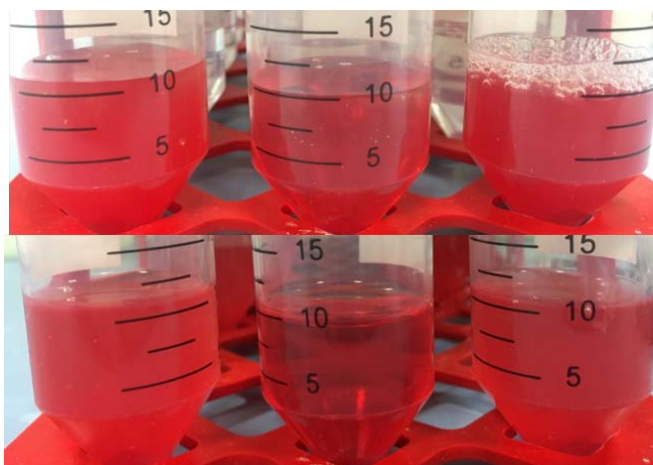

Figure 15. Hemolysis test, at beginning (top) and after one hour (bottom). Positive control (saline) is on the left, negative control (distilled water) on the middle, and sample testes on the right.

1.10.3. Acute toxicity test. Histopathological study

Nine male Sprague Dawley rats, 7 months of age (400-550 g) were used to evaluate acute toxicity induced by Covergel. All experiments were approved by the ethics committee of the animal facility of Germans Trias I Pujol Research Institute. Animals were divided in three groups: two subjects and a control group. Rats from the subject groups were injected with 10 mL/kg of Covergel into the abdominal cavity and rats from the control group were injected with 10 mL/kg saline into the abdominal cavity. Animals were observed daily after administration, evaluation of general conditions (activity, hair, feces, behavior and other clinical signs), body weight and mortality were done. Animals were euthanized at 3, and 7 days with anesthetic overdose and major organs (heart, liver, spleen, lung and kidney) were extracted, evaluated, and fixed in 10% formaldehyde solution. Organs were then stained with hematoxylin-eosin (H/E) for histopathological evaluation. Blood was also

extracted, and hematological and biochemistry analysis were performed. This protocol was adapted from Li *et al* [112].

1.10.4. Subcutaneous placement of hydrogel in rats. Histopathological study

Six male Sprague Dawley rats, 7 months of age (420-500 g) were used to evaluate the effect of subcutaneous implantation of Covergel. Rats maintained the subcutaneous implantation for 10 days. Under anesthesia, a 2 cm incision was done on the dorsal back of the rat and 0.5 g of gelified Covergel were introduced subcutaneously. The incision was then sutured and rats were allowed to recover with food and water *ad libitum.*

After 10 days, rats were euthanized and Covergel was extracted and cut in two. One piece was placed in Carnoy solution (60% ethanol, 30% chloroform and 10% glacial acetic acid) for histological evaluation and the other piece was lyophilized (Christ Loc-1m, B.Braun) and evaluated using Scanning Electron Microscopy (SEM).

1.10.5. Adherence to mucosa

Two mL of Covergel with sodium barium (Barilux, Iberoinvesa pharma) was endoscopically administered in rats to study the time of adherence of Covergel to the mucosa. Rats underwent X Ray scan at 3 different time points, before application, after application and 36 h after application.

1.11. Statistical analysis

All values are expressed in median ± range unless otherwise stated. Comparison of groups was done using 2 way ANOVA and Tuckey's multiple comparison test as a posthoc. Release kinetics was studied using mean values of 6 different experiments and a nonlinear regression fit to each different model equation. Graphpad Prism 6.0 software was used to perform analysis.

2. Implementation of our hydrogel on the endoscopic technique

This study was aimed to analyze the capacity of our hydrogel to be implemented in normal endoscopic techniques such as EMR or ESD. We wanted to evaluate its capacity to act as a submucosal injection solution and the possible benefit on mucosal healing after endoscopic resection techniques, in order to avoid possible adverse events. For this part of the study, we decided to supplement Covergel with Rifaximin, an antibiotic which presents really low absorption when taken orally and rather shows a local effect in the GI tract. Covergel with rifaximin will be referred to as Covergel-Bibio from now on.

2.1. Submucosal Injection Solution

2.1.1. *Ex vivo* model of porcine stomach

Fresh porcine stomachs were used to analyze properties of different submucosal injection solutions. Measurements were performed in fundus in all cases. Two mL of each solution were injected using a 22G needle. For the measurement of cushion decrease and trans-epithelial resistance stomach portions of 8x5 cm were used. Stomach pieces were maintained at 37°C during tests. EMR resection was performed after prior submucosal injection with a standard polypectomy snare (Olympus Medical System, Tokyo, Japan) with blended current on full stomachs for the measurement of EMR time and Muscular Tª. To standardize the force applied in all procedures to the polypectomy snare, the snare was placed in Laboratory Syringe Pump (Advance Infusion Pump Series 1200, Parkland Scientific, USA) with a linear force of 22 lbs.

2.1.2. Solutions

The following solutions were tested: 0.9% Saline (S), Platelet-rich plasma (PRP), Glyceol®, (GC), Hyaluronic acid 2% (HA), Pluronic-F127 20% (PL), Glucosated serum 10% (GS), Gelaspan (GP), Covergel-Bibio (BB) and PRP

with BB (PRP+BB).

S, GS and GP were acquired from the hospital pharmacy service. GC was manufactured in our laboratory (10% glycerol, 5% fructose, 0.9% sodium chloride). PRP was obtained by extraction of blood with a syringe containing 1/10 total blood volume of 10% sodium citrate. Then, blood was centrifuged at 160 G for 10 minutes at room temperature; this resulted in a 2 phases tube, the top one containing plasma. Plasma was recollected and transferred to a new centrifuge tube, and further centrifuged at 400 G for 15 minutes. The result of this was platelet-poor plasma (2/3 of total volume) and PRP (the bottom 1/3 of the total volume). PRP was activated by addition of 0,05 mL/mL PRP of 10% calcium chloride. BB (Covergel-Bibio) was prepared as before mentioned for Covergel alone, plus the addition of 1% w/v Rifaximin.

2.1.3. Resistivity, EMR time, Temperature and Cushion decrease measurements

Resistivity (R) was evaluated using a multimeter SK-7707 with conventional electrodes; one electrode was positioned at the apical surface of the cushion (gastric mucosa) and the other one on the basal surface of the cushion (serosa layer), to evaluate the trans-epithelial resistivity that the stomach wall had with the submucosal solution injected. Measurements were done at 0, 15, 30, 45 and 60 minutes after submucosal injection (Figure 16). Electrodes were also placed in each substance alone, once cm in distance, to evaluate resistivity of substances.

Temperature (Tª) analysis was carried out using a Thermometer K/J type thermocouple with the sensor located at muscular layer to check the risk of deep thermal injury (Figure 17). Measurement started after submucosal injection and finished after EMR was completed. Moreover, time needed to perform EMR was registered with each solution.
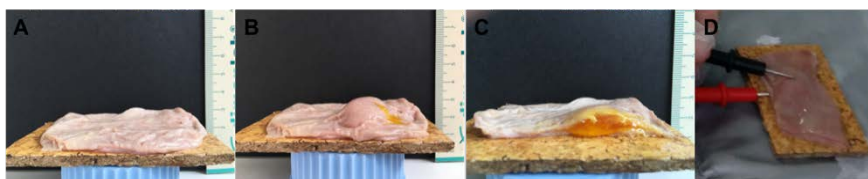
Figure 16. Evaluations on stomach samples. Stomach pieces of 8x5cm were used to evaluate cushion decrease and trans-epithelial resistivity of substances. A; Stomach piece. B; stomach piece after submucosal injection. C; stomach piece cut to visualize submucosal cushion. D; evaluation of transepithelial resistivity with a multimeter.

Figure 17. Evaluations on full stomachs. Full stomachs were used to evaluate muscular Ta after EMR and time to perform EMR. A; submucosal injection on fundus region of porcine stomach. B; standardized mucosal elevation to perform EMR. C; evaluation of Ta with one thermometer on the apical face of the stomach and the other (black arrow) on the serosa layer.

Submucosal cushion height was studied considering three different aspects: 1) differences of height at time 0 after injection, 2) differences of height at time 60 after injection and 3) the percentage of decrease for each substance. We evaluated this by taking standardized pictures at time: 0, 15, 30, 45 and 60 minutes. Images were evaluated using ImageJ software. Decrease of the cushion is shown as % of the original height of each solution. All these determinations were performed by triplicate for statistical evaluation. Osmolarity and viscosity of each solution were obtained from each manufacturer.

2.1.4. Statistical analysis

A descriptive analysis was carried out for each experiment. ANOVA tests were performed to compare groups. Tuckey tests were done as post-hoc analysis. SPSS software, 15.0 version was used. A nonparametric Spearman correlation

study was carried out between all the characteristics evaluated using SPSS software, 15.0 version software.

2.2. Endoscopic Shielding Technique

Twenty-four male Sprague Daley rats and eight female pigs (Specipig, Barcelona, Spain) were used in this study. Colonoscopies were carried out with the same endoscope: Olympus FQ260Z (Olympus, Tokyo, Japan), with an outer diameter of 9.5 mm, working channel diameter of 2.8 mm. Room air was used for insufflation during the endoscopy. To carry out endoscopic shielding technique, agents were applied over mucosal lesions as a coverage shield, with a catheter through the endoscope channel, positioning the tip of the catheter over the ulcer. An amount of 1 mL in rats and 5 mL in pigs was applied in each animal (Figure 18), approximately 0.5–2 mL per cm^2 of mucosal lesion.
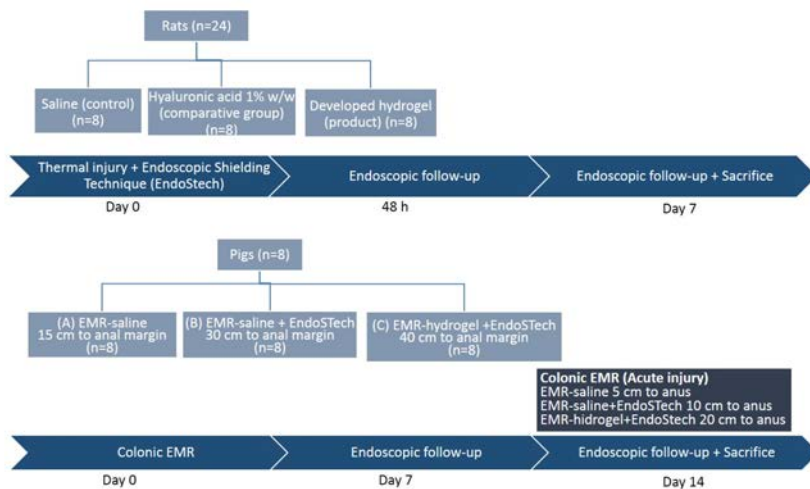
Figure 18. Experimental layout for the Endoscopic Shielding Technique study.

2.2.1. Covergel-Bibio resistance to bacterial degradation

To test the ability of Covergel-Bibio to resist bacterial degradation three conditions were tested. In Columbia agar + 5% sheep blood, 100 μL of a 10^6

CFU/mL feces culture were seeded. Then 1 mL of Covergel or Covergel-Bibio was poured on the plate and placed at 37°C to allow Covergel to gelify. Pictures were taken at 0, 24 and 72 h in order to check bacterial growth. Covergel-Bibio was also poured in a plate without feces culture as a control.

2.2.2. Induction of lesions in rats

Rats were anesthetized by isoflurane inhalation and placed in a supine position. Remaining feces were flushed away by injecting water enema. A drop of lubricating jelly (Aquagel; Ecolab, Leeds, UK) was applied on the anal sphincter to facilitate insertion of the endoscope. The endoscope was then gently passed through the anus and further introduced under endoscopic vision. Water was injected through the endoscope's working channel to visualize the lumen of the colon. Occasionally, the colon was inflated with air for better visualization of the lumen. Conventional EMR technique with prior submucosal injection was not able to be done as a result of wall thickness. Lesions were created in the left colon, 6 cm to the anal margin, by Coagrasper Hemostatic Forceps (Olympus), with a power setting of forced coagulation 40 W during 4 s [113]. This technique induces deep thermal damage in the acute phase (48 h), with development of CS and large mucosal defects in the late phase, 1 week after the injury. Animals were randomly divided into three groups (n = 8) for endoscopic shielding technique with saline (control, Group A), hyaluronic acid sodium salt 1% w/v (comparative example, Group B) and Covergel-Bibio (Group C) (Figure 19). Rats underwent endoscopic follow up at 48 h and 7 days and were euthanatized by anesthetic overdose. After death, the colon was retrieved and opened longitudinally to examine colonic mucosa. Full-thickness samples of approximately 4 cm were taken from the proximal left colon surrounding endoscopic lesions (Figure 18).
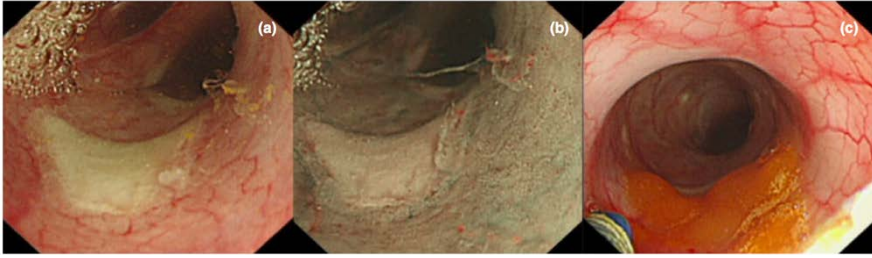
Figure 19. Endoscopic shielding technique with the hydrogel applied on colonic induced lesions in the rat model. (a) Endoscopic view with high-resolution white-light imaging and (b) the corresponding narrow-band image. (c) Hydrogel was applied onto the lesion.

2.2.3. Induction of lesions in pigs

In the porcine model, food was retrieved 12 h prior to the procedure. Preparation for colonoscopy was done with saline irrigation. Colonoscopy was carried out under sedation with propofol. Three ulcer sites were prepared in each pig: Mucosal elevation by submucosal injection of saline was created at 15 cm to the anal margin, then EMR with snare polypectomy and forced coagulation was carried out (Group D; EMR-saline; Figure 20), EMR-saline plus endoscopic shielding technique with Covergel-Bibio at 30 cm to anus (Group E; EMR-saline-P; Figure 21), and EMR with prior injection of Covergel-Bibio plus endoscopic shielding technique with Covergel-Bibio at 40 cm to anal verge (Group F; EMR-P-P; Figure 22). At the end of the 14-day study, new lesions (EMR-saline; EMR-saline-P and EMR-P-P) were created in healthy colonic mucosa to assess the basal injury of the different approaches, at 5, 10 and 20 cm to anal margin; respectively. These new lesions were not used to assess mucosal healing. Animals underwent endoscopic follow up at 7 and 14 days after EMR. After this time, pigs were euthanatized and necropsied to obtain colonic samples as described above (Figure 18).
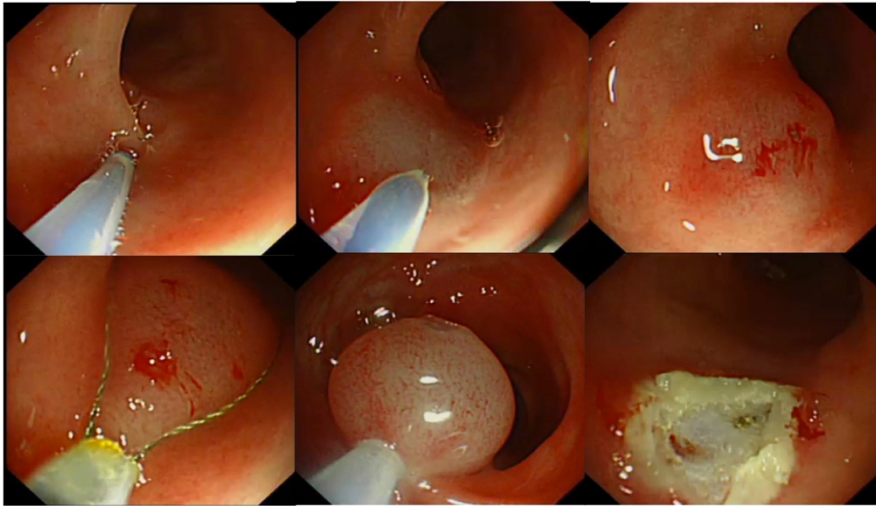
Figure 20. Mucosal elevation by submucosal injection of saline was created at 15 cm to the anal margin in the porcine model. Endoscopic mucosal resection was carried out with snare polypectomy with blended current.
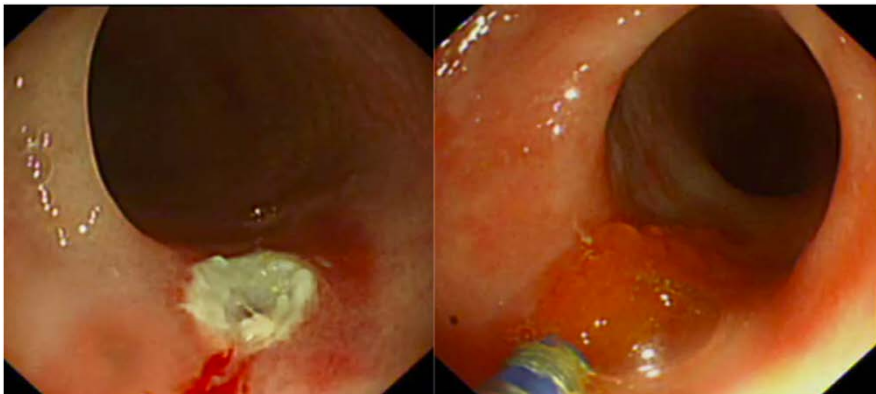

Figure 21. Endoscopic mucosal resection-induced lesion in the porcine model with prior saline injection was created at 30 cm to the anus. Endoscopic shielding technique with hydrogel was applied onto the lesion.
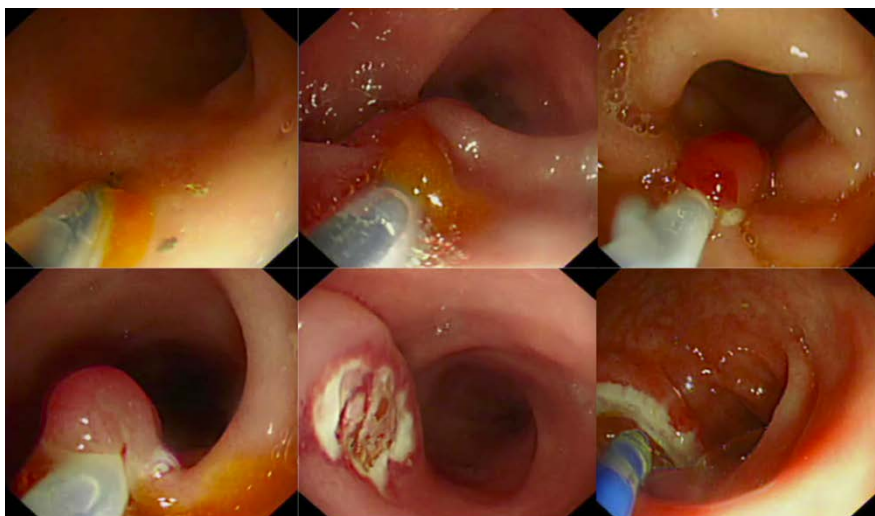
Figure 22. Endoscopic mucosal resection-induced lesion with prior hydrogel submucosal injection was performed at 40 cm to the anus. Endoscopic shielding technique with hydrogel was applied onto the lesion.

2.2.4. Assessments

Mucosal healing was evaluated as mean ulcerated area after 48 h and 7 days in rats, and after 7 and 14 days in pigs. Mucosal healing rate was defined as percentage of mucosal restoration. Measurement of mucosal lesion was carried out as comparison with opened forceps (5 mm) or by direct measurement with the specimen. We calculated the mean ulcerated and mucosal healing rate by the use of ImageJ public software. Physiological or fibrotic healing, as absence or presence of fibrosis, was evaluated with histological study of the specimen. Thermal injury was evaluated with a 1–4 scale: (1) mucosal necrosis; (2) submucosal necrosis; (3) transmural necrosis; and (4) peritonitis and/or microperforation, in H/E histological sections.

2.2.5. Statistical study

Statistical analysis results are expressed as mean ± SEM or proportions as required. Comparison of means among groups was done using the one-way ANOVA or its corresponding non-parametric (Kruskal-Wallis) test. Post-hoc

comparisons, to identify pairs of groups significantly different at the 0.05 level, were made with the Duncan test or the Mann–Whitney U-test. Comparisons of proportions among groups were made with the v2 -test. Statistical analyses were carried out with SPSS for Windows version 14.0 (SPSS Inc., Chicago, IL, USA).

3. Hydrogel as a drug-delivery platform for intestinal diseases. CRC and experimental colitis animal models

The third study was focused on the ability of our hydrogel to act as a drug eluting platform for the endoscopic treatment of different mucosal lesions associated to typical colorectal pathologies. For this, we worked with three different animal models: acute experimental colitis (EC), chronic experimental colitis and colorectal cancer. In this study, Covergel was loaded with mAb's to act as a drug-delivery platform, thus, we will refer to it as Covergel-Tribio.

3.1. CRC animal study

3.1.1. Layout

Twenty male Sprague Dawley rats (Harlan Laboratories Models SL, Barcelona, Spain) weighting 100-125 g were included in this study. The experimental CRC animal model was performed by the subcutaneous administration, once a week for two weeks, of 15 mg/kg of Azoxymethane (AOM); induction phase. After this, animals were kept in the animal facility during the progression phase. From weeks 30 to 35 of the progression phase, endoscopic follow up was done to check for the development of tumors. When CRC presence was confirmed, animals were randomized into one of the 5 treatment groups (Figure 23):

- Covergel-Tribio with Irinotecan (I) (3.5 mg/mL) and Aflibercept (A) (2 mg/mL) (Chemotherapy + mab anti Vascular endothelial growth factor receptor (VEGFR)).

- Covergel-Tribio with Irinotecan (3.5 mg/mL) and Bevacizumab (B) (5 mg/mL) (Chemotherapy + mab anti Vascular endothelial growth factor receptor).

- Covergel-Tribio with Irinotecan (3.5 mg/mL) and Panitumumab (P) (6 mg/mL) (Chemotherapy + mab anti epithelial growth factor receptor)

- Covergel-Tribio with Irinotecan (3.5 mg/mL) and Cetuximab (C) (16 mg/mL) (Chemotherapy + mab anti epithelial growth factor receptor)
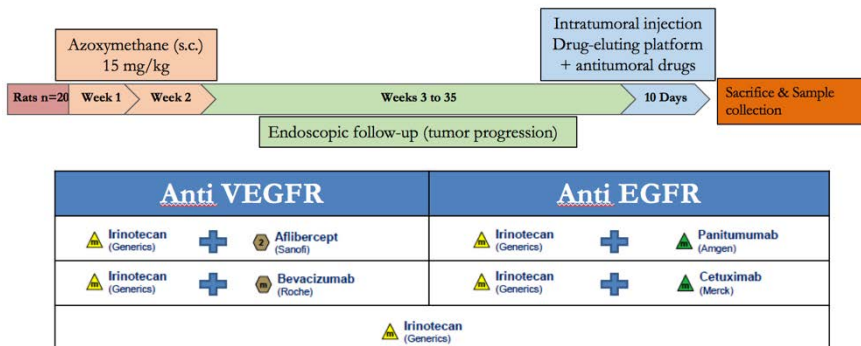
- Covergel-Tribio with Irinotecan (3.5 mg/mL).

Figure 23. Experimental layout of the CRC animal study.

3.1.2. Assessments

10 days after treatment application, animals were euthanized, colon was extracted, and tumors were evaluated macroscopically, fixed in 10% formaldehyde and stained in H/E for histopathological evaluation. A blinded-histopathological evaluation was done by a pathologist from the Germans Trias i Pujol Hospital.

Tumor size was evaluated with endoscopic pictures taken at the day of treatment and the day of euthanasia, analyzed with ImageJ software.

3.1.3. Statistical analysis

Values are expressed as median ± range. Comparison of means among groups was done using the two-way ANOVA or its corresponding non-parametric (Kruskal-Wallis) test. Post-hoc comparisons, to identify pairs of groups significantly different at the 0.05 level, were made with the Tuckey's multiple comparison test or the Mann–Whitney U-test.

3.2. Acute EC animal study

3.2.1. Layout

Forty male Sprague Dawley rats (Harlan Laboratories Models SL, Barcelona, Spain) weighting 250-300 g were included in this study. The experimental colitis animal model was performed by the rectal administration of 0.6 mL of a 3.5% TNBS solution in 50% ethanol (Day 0). The peak of colitis was stablished 3 days post administration (Day 3) and animals were examined to evaluate the affection and apply treatments. Finally, four days after treatment (Day 7) animal were euthanatized and evaluations were done (Figure 24).

Animals were randomized in 5 groups:

- Sham group: Healthy animals with no administration of TNBS. Instead, animals were administered a 0.6 mL saline solution on day 0. Animals went through all the same tests as the other groups.
- Control Group: Animals with experimental colitis which, on day 3, did not receive any treatment. Instead, 1 mL of saline was applied through the endoscope on the day of treatment.
- Platform group: Animals with experimental colitis and treated on day 3 with Covergel-TriBio with no active substance.
- Platform + IFX group: Animals with experimental colitis and treated on day 3 with Covergel-TriBio with Infliximab (1 mg/mL).

- Platform + VDZ group: Animals with experimental colitis and treated on day 3 with Covergel-TriBio with Vedolizumab (1 mg/mL).
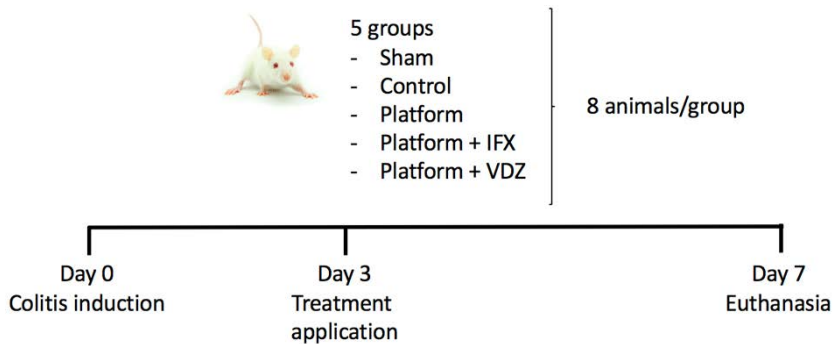

Figure 24. Experimental layout of the acute EC animal study

Exclusion criteria were fixed at day 3. Animals had had to lose at least 8% of the original weight (Day 0) and endoscopy at day 3 had to show, at least in some part of the colon, a circumferentially affected area.

3.2.2. Assessments

Animals were weighted on days 0, 3 and 7. Endoscopic procedures were carried out on the same days and images of the colonic mucosa were taken. Blood was extracted on the same days by a small cut on the tail, and serum from the three time points was kept frozen for future evaluations.

On day 7, animals were euthanized by an anesthetic overdose. First, a piece of liver was retrieved under sterile conditions and placed in saline until further analysis. Then, the colon was extracted, cleaned, measured and weighted. Pictures were taken, and then, the ulcer site was cut and placed in 10% formaldehyde for H/E staining and histopathological evaluation.

A blinded-histopathological evaluation was done by a pathologist from the Germans Trias i Pujol Hospital. The scoring system (Table 9) followed was extracted from Erben et al[114].

Table 9. Scoring scheme for chemically-induced colonic inflammation

Inflammatory cell infiltrate:			Intestinal architecture:		
Severity	Extent	Score 1	Epithelial changes	Mucosal architecture	Score 2
Mild	Mucosa	1	Focal erosions		1
Moderate	Mucosa and submucosa	2	Erosion	± Focal ulcerations	2
Marked	Transmural	3		Extended ulcerations ± granulation tissue ± pseudopolyps	3
Sum of scores 1 and 2:					0-6

Liver was retrieved, and 0.5 g were placed in 1mL of saline and homogenized. Then, 0.1 mL of the homogenate were cultured on a LB Agar petri dish at 37ºC for 24 hours. The appearance of CFU was evaluated as a way to stablish bacterial translocation to the liver, a marker of a weak intestinal wall due to inflammation.

3.3. Chronic EC animal study

3.3.1. Layout

Twelve male Sprague Dawley rats (Harlan Laboratories Models SL, Barcelona, Spain) weighting 250-300 g were included in this study. The experimental colitis animal model was performed by the rectal administration of 0.6 mL of a 3.5% TNBS solution in 50% ethanol. In order to reproduce a chronic EC, 4 rounds of TNBS were applied following the same time line as for acute EC (Colitis induction – Treatment application – Evaluation of treatment and 2nd round of colitis induction). Four days after the fourth treatment application, animals were euthanized, and evaluations were done (Figure 25).

Animals were randomized in two groups:

- Infliximab s.c. group: Animals with EC treated with 5 mg/kg of IFX subcutaneously on days 3, 10, 17 and 24.

- Platform + Infliximab group: Animals with EC and treated on days 3, 10, 17 and 24 with Covergel-TriBio with IFX (1 mg/mL).
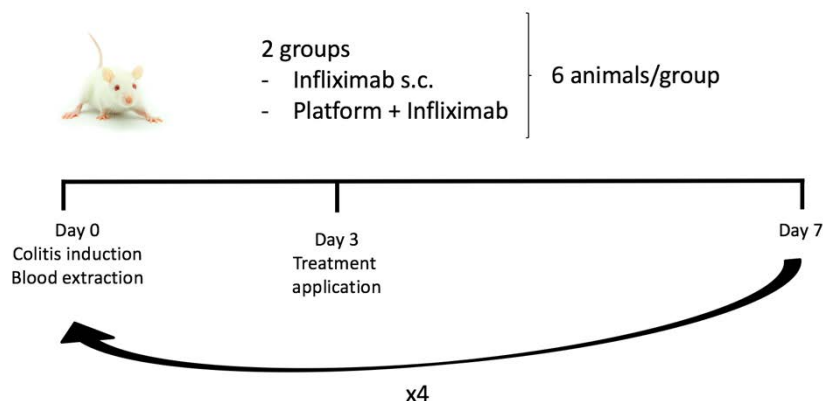

Figure 25. Experimental layout of the chronic EC animal study.

All assessments were carried out the same way as in the acute EC study.

3.3.2. Immunodetection of antibodies to Infliximab.

Serum samples from all the treatment days (3, 10, 17, 24) and the day of euthanasia (day 28) were tested for ATIs.

Briefly, to separate ATIs from IFX as the might be found on blood, a protein G column and acidic buffer treatment were used. 600 µL of a 1:10 dilution of serum was applied onto the protein G column (Ab Spin trap; GE Healthcare) and washed. Trapped ATIs were eluted with 400 µL of elution buffer (0.1 M Glycine-HCl pH 2.7) which releases proteins trapped in the protein G column and at the same time, dissociates ATI's-IFX complexes. Samples were eluted into neutralizing buffer (1 M Tris-HCl pH 9) containing an IgG concentration of 20 µg/mL to prevent the re-formation of immune complexes.

Then, with the samples obtained from the protein G column, a 96-well plate was coated with 200 µL/well O/N at 4ºC or for 1 hour at 37 ºC. Plates were washed with washing buffer (PBS 0.1% Triton) and 200 µL/well Horseradish peroxidase conjugated-Infliximab (HRP conjugation Kit, abcam) (0.2 µg/mL IFX-HRP) were added for 30 minutes at room temperature, protecting the plate from direct light. The plate was further washed and finally, a substrate solution (3,3',5,5'-Tetramethylbenzidine/H_2O_2 50% vol/vol) was added to the microplate. The enzyme reaction yields a blue product that turns yellow when stop solution (2 M sulfuric acid) is added. The intensity of the color measured is in proportion of the quantity of ATIs bound in the initial step; this intensity is measured by determining the optical density of each well using a microplate reader at 450 nm with a wavelength correction set to 540 nm using a spectophotometer (Varioskan Flash, Thermo). SkanIt Software 2.4.1 was used to analyze results. This protocol was extracted from Imaeda *et al*[115].

RESULTS

1. Development and characterization of the new hydrogel

1.1. Rheological and structural study

Rheological tests were carried out on the first four combinations of hydrogels, and thus, adhesion and viscosity properties were evaluated. Both characteristics were influenced by temperature.

Adhesion was measured in mN/s, the lower the value the higher the adhesion of the gel to the surface. All hydrogels showed a similar adhesion force at 22ºC, but when temperature was raised, adhesion force of only CD2 was highly increased, from -25 to -3993 mN/s (Table 10).

Table 10. Adhesion force test.

Sample	Adhesion (mN/s) 22ºC	SD	Adhesion (mN/s) 37ºC	SD
CD1	-21.68	4.24	-41.25	5.47
CD2 (Covergel)	-24.48	5.34	-3992.93	536.21
CD3	-21.12	6.22	-11.75	6.48
CD4	-30.98	7.27	-15.17	13.48

Viscosity (η) of all samples was similar at 22°C, but as in adhesion test, when temperature was increased to 37°C, viscosity of Covergel was increased from<1 Pa·s at 22 ºC to 1500 Pa·s at 37 ºC. Figure 26 shows the evolution of viscosity of the hydrogels depending on the shear rate at two different temperatures.

Based on adhesion and viscosity properties, we chose Covergel (CD2) due to its capacity to increase these two major properties when body temperature was reached (Figure 27). The final composition of Covergel was 20% pluronic F-127, 2% methylcellulose and 1% hyaluronic acid in distilled water.
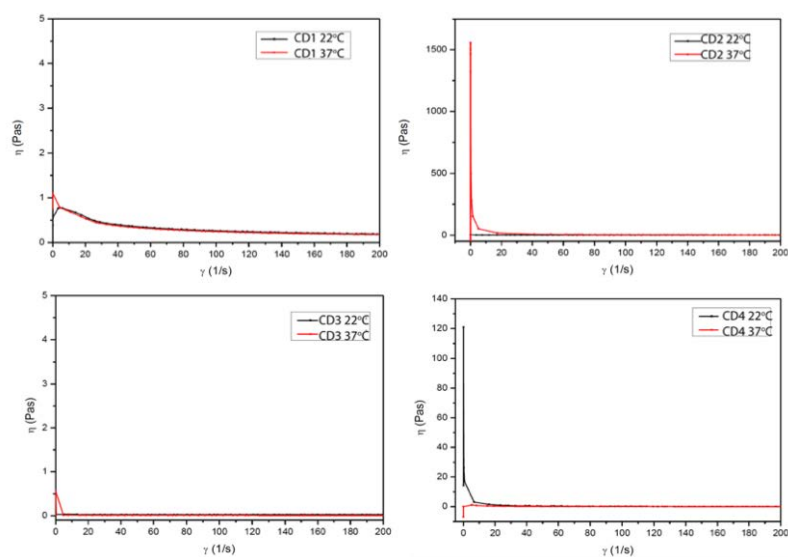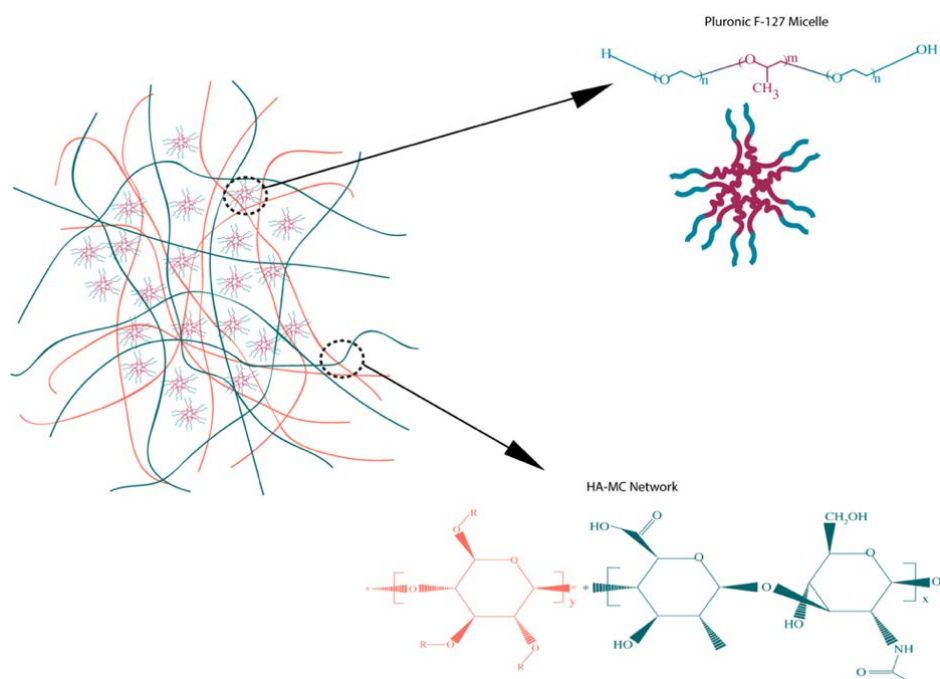
Figure 26. Viscosity test.

Figure 27. Original Covergel structure.

Covergel was able to gellify with an increase in temperature, but since only physical interactions held Covergel together, when submerge in medium it would dissolve, making it impossible to continue with the characterization experiments we wanted to carry out. This is why, a modification on one of the original components of Covergel was proposed in order to achieve an irreversible gelation if desired (Figure 28). For this, acrylate groups were added to Pluronic-F127. This allowed the chemical crosslinking of Covergel using a photoinitiator and UV light exposure (Figure 29), as well as the temperature induced physical crosslinking of the original Covergel.
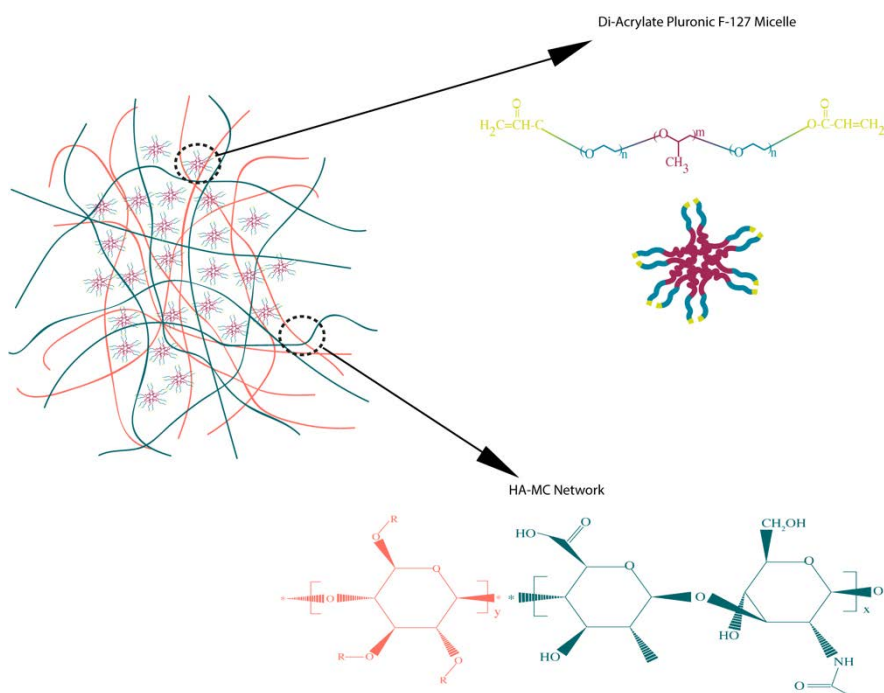
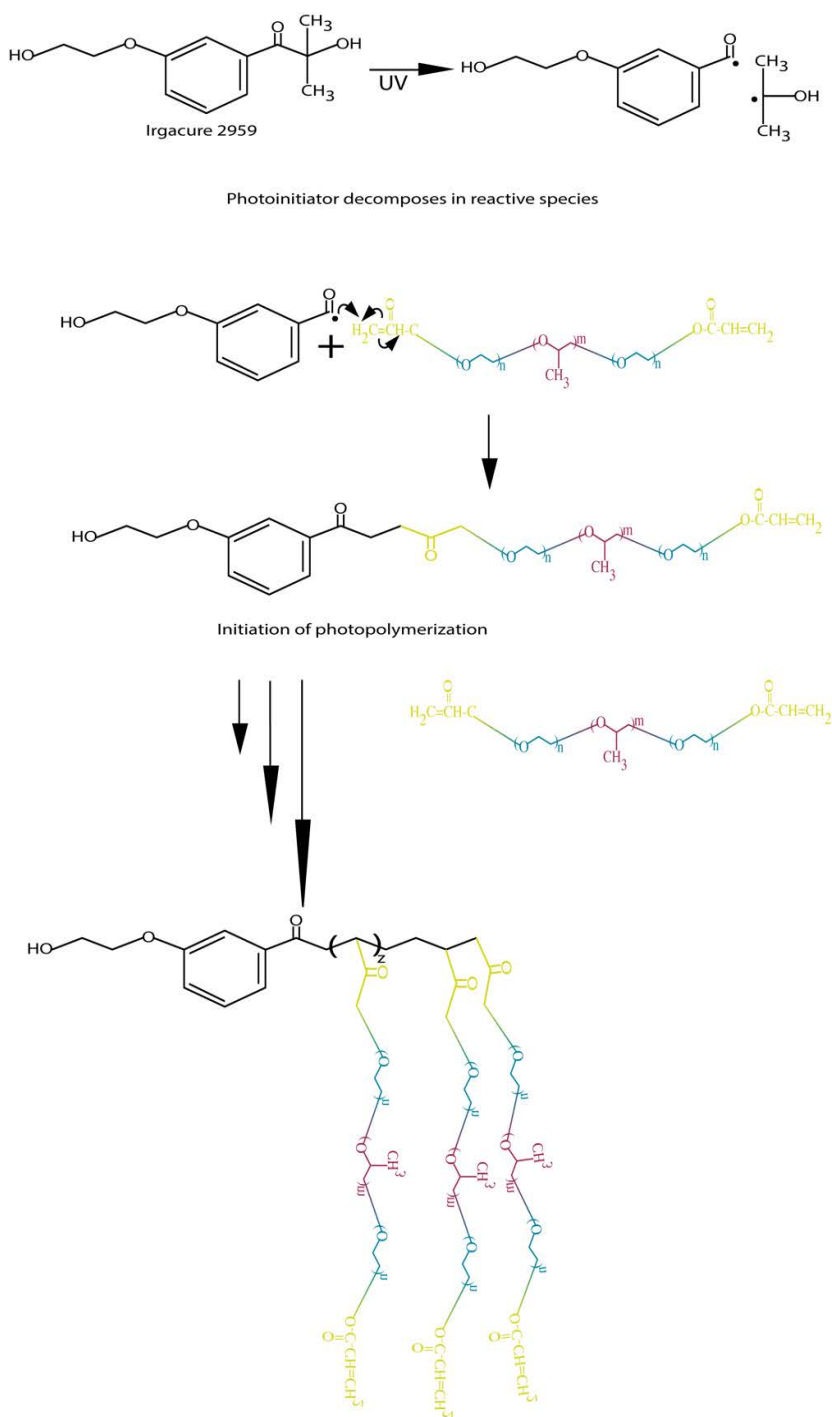Figure 28. Modified Covergel without exposure to UV light.

Figure 29. Photopolymerization of Covergel.

Once Covergel is exposed to UV light and temperature reaches an adequate value, an irreversible gelation is induced, characterized by a network formed between the DAP-F127 micelles that will not dissolve when temperature decreases, thus maintaining the gelation state (Figure 30).
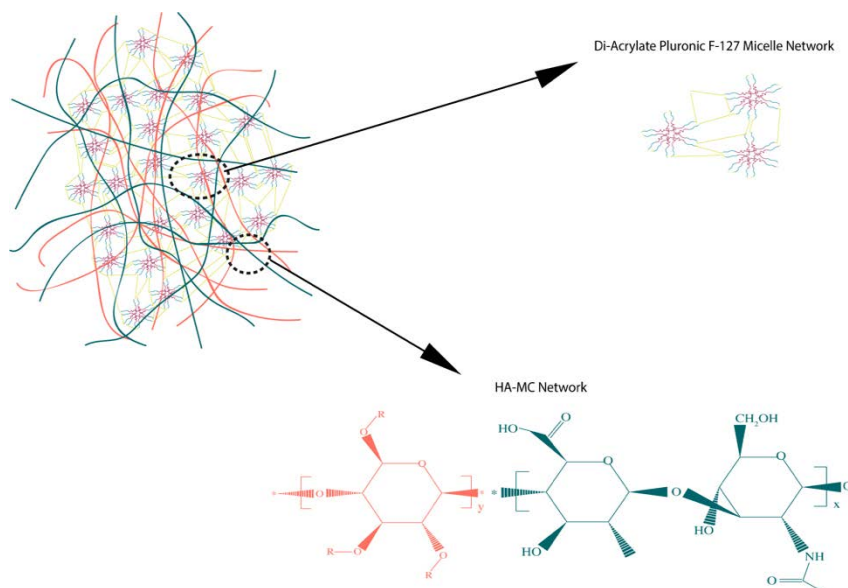

Figure 30. Modified Covergel with exposure to UV light.

Table 11 shows the different conditions tested to ensure the correct gelation of Covergel. Irreversible gelation was only achieved when photoinitiator was added to the hydrogel in a 1.15% with respect of the total amount of DAP-F127, Covergel was placed under UV light and 37ºC were reached.

Table 11. Gelation study.

Test	Vol. Gel	Photoinitiator	UV radiation	37 ºC	22 ºC	Irreversible Gelation
1	1 mL	Yes, 15 μL	No	Gel	Liquid	No
2	1 mL	Yes, 15 μL	Yes	Gel	Gel	Yes
3	1 mL	No	No	Gel	Liquid	No
4	1 mL	No	Yes	Gel	Liquid	No

The capability of administering Covergel though the endoscope was also

checked, and we stablished that this composition can be given smoothly through a catheter (diameter 2.0–2.2 mm) by applying a force of 370 mmHg (0.48 atmospheres) (data not shown).

One mL of Covergel, and different compositions of similar hydrogels were gelified and lyophilized in order to obtain SEM images to evaluate the structure and porosity of the inner network. Figure 31 shows three different combinations of materials (PA: Di-acrylate Pluronic-F127, HA: Hyaluronic acid, ALG: Alginate, MC: Methylcellulose). SEM images show that these combinations do not present a structured network and pores are not well defined.

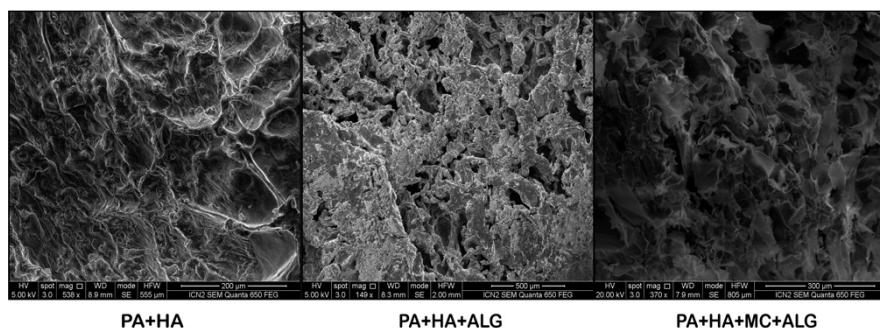**PA+HA**   **PA+HA+ALG**   **PA+HA+MC+ALG**

Figure 31. SEM images of hydrogels with variations on the composition from our hydrogel.

On the contrary, Figure 32 shows three SEM pictures of Covergel. A well-defined network can be observed, pores present a variety of sizes ranging from 50-300 μm diameter.

Swelling and degradation rates were studied in different conditions for one month. pH=7 as a physiological medium, pH=3 imitating the acidity found in the stomach, pH=9 and bacterial culture as a medium similar to the colon environment, and pH=11 as an extreme situation. Results are shown in Figure 33.
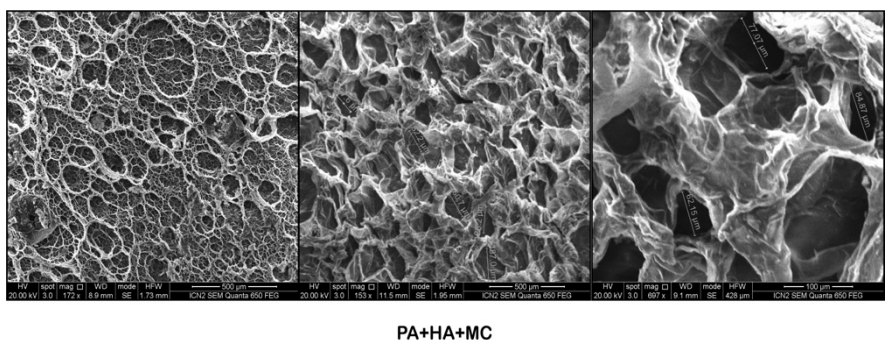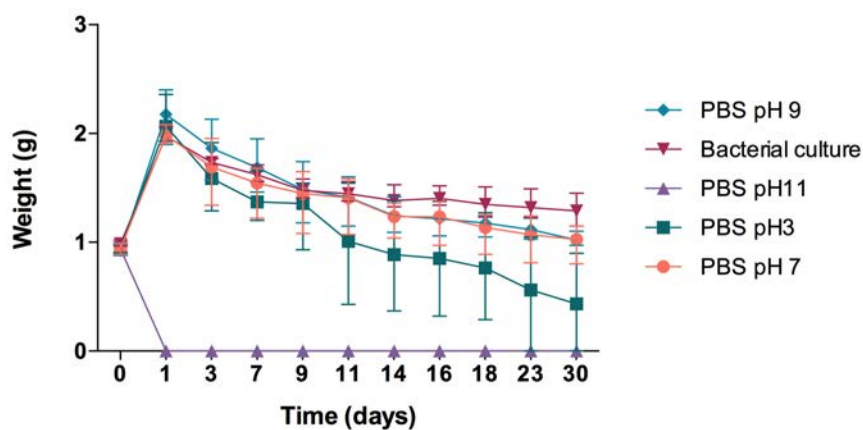
PA+HA+MC

Figure 32. SEM images of Covergel.

Figure 33. Degradation of the Covergel in different situations.

At an extreme condition such as a highly basic medium (pH 11) Covergel quickly disintegrates. Interestingly, at high acidic conditions like the ones found in the stomach, Covergel was able to last for 30 days although the structure was not as well maintained. Water intake was higher than in other conditions, but weight was lower, indicating that the majority of the weight is from water inside Covergel, but the overall structure is starting to dismiss. Degradation in other situations (pH 7, 9 and bacterial culture) showed a similar fashion, being able to last for at least 30 days under these conditions.

1.2. Drug Release Study

First, we analyzed the incorporating efficacy of drug inside Covergel. For Trypan Blue, the incorporating efficacy was $58.96 \pm 2.8\%$ and for BSA $24.09 \pm 4.34\%$ (mean $\pm$ SD). Then, experimental data was used to study the release kinetics model that better fitted out results, as well as the release mechanism that better explained the release kinetics from Covergel. Figure 34 shows the representative curve of the different kinetic models and the Korsmeyer-Peppas mechanism model. Correlation coefficient of the different equations are shown in Table 12.
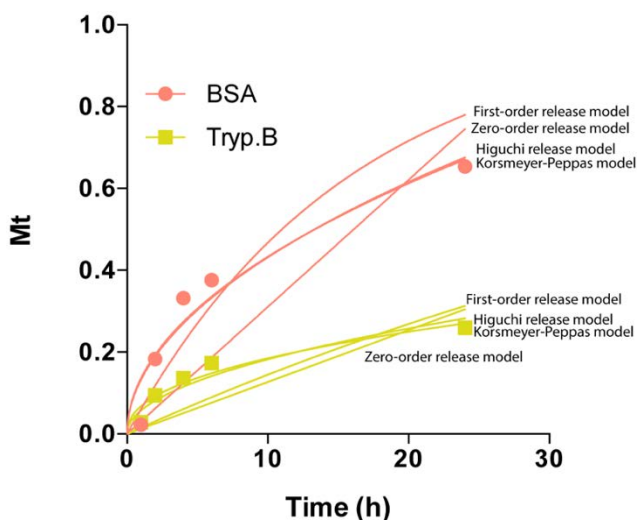
Figure 34. Release profiles of different drugs from Covergel and several kinetic models.

Table 12. Correlation coefficient (R^2) between release profiles and several kinetic models and Korsmeyer-Peppas model.

Sample	0-order R^2	1st-order R^2	Higuchi R^2	Korsmeyer-Peppas
Tryp. B	0.2022	0.3361	0.8986	0.9169
BSA	0.5393	0.8324	0.9167	0.9171

The release kinetics model that best fits our results is the Higuchi release model, being the final equation obtained for our results:

For Trypan Blue $\quad\quad$ $Mt=0.05760t^{1/2}$ $\quad\quad$ $R^2=0.8986$

For BSA $\quad\quad$ $Mt=0.1369t^{1/2}$ $\quad\quad$ $R^2=0.9167$

Korsmeyer-Peppas model equation for our release profiles were:

For Trypan Blue $\quad\quad$ $Mt=0.06803t^{0.4338}$ $\quad\quad$ $R^2=0.9169$

For BSA $\quad\quad$ $Mt=0.1329t^{0.5116}$ $\quad\quad$ $R^2=0.9171$

The release exponents (n) were 0.4338 for Trypan Blue and 0.5116 for BSA. The release exponent (n) gives us information about the diffusion mechanism by which drugs diffuses from dosage form. When n is less than 0.45 it follows a quasi fickian diffusion, n=0.45 fickian diffusion, 0.45<n<0.89 anomalous diffusion or nonfickian diffusion. 0.89<n<1 Zero order, case-2 relaxation or non fickian case 2, >1 Non fickian super case 2.

1.3. Biocompatibility Study

In order to characterize the biocompatibility of Covergel, we first evaluated its effect on cell viability *in vitro* by culturing Caco-2 cells in conditioned medium with 1%, 2%, 5% 10% and 15% of Covergel v/v.

Figure 35 shows the results after 96 hours of culture. Values are expressed in Relative Fluorescence Units (RFU). Cell viability was not compromised by any of the percentages of Covergel in culture medium. On the contrary, all percentages of Covergel diluted in culture mediumd improved cell viability compared to positive control, reaching a top at 10%. This results were expected as for the trophic effect of HA on cells.
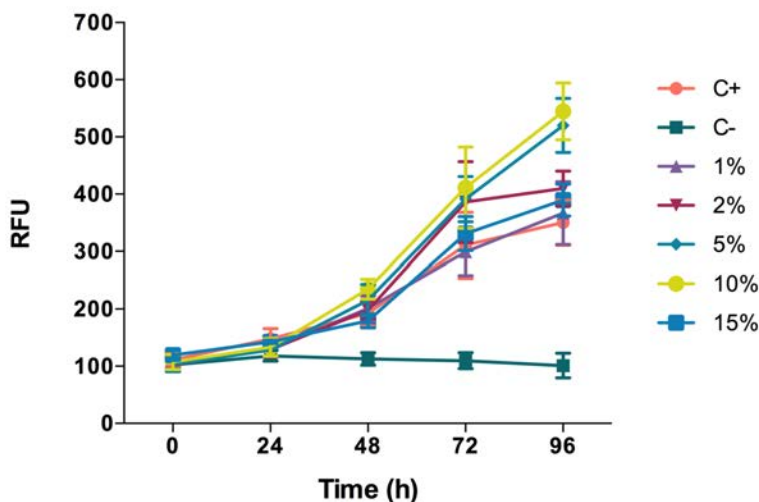
Figure 35. Cell viability of Caco-2 cells in medium with our hydrogels.

We also analyzed the biocompatibility of Covergel *in vivo*. To do so, blood from rats that underwent the intraperitoneal injection of Covergel was analyzed for traces of toxicity. Results are shown in Table 13.

Table 13. Blood tests results.

	Reference values	Control	3 days post injection	7 days post injection
Hemoglobin (g/100mL)	14-20	14.46 ± 0.32	13.69 ± 1.77	14.27 ± 1.41
Hematocrit (vol.%)	36-48	43.75 ± 1.56	40.83 ± 6.65	42.85 ± 2.83
RBC ($x10^{12}$/L)	5.4-8.5	8.43 ± 0.29	7.65 ± 0.85	8.32 ± 0.85
Leucocytes ($x10^9$/L)	6-17	6.29 ± 1.27	2.14 ± 0.35	1.99 ± 1.49
Platelets ($x10^9$/L)	450-885	806.89 ± 52.09	640.14 ± 30.41	692.15 ± 231.49
Neutrophils (%)	18-36	15.61 ± 7.6	20.87 ± 1.70	24.92 ± 12.18
Eosinophils (%)	1-4	2.53 ± 0.55	2.12 ± 0.5	2.16 ± 2.52
Lymphocytes (%)	62-75	80.27 ± 7.28	72.39 ± 4.31	67.87 ± 20.86
Monocytes (%)	1-6	0.25 ± 0.2	0.25 ± 0.3	0.12 ± 0.09
Basophils (%)	0-0.3	0	0	0
AST (U/L)	39-92	81.91 ± 19.63	70.75 ± 8.49	78.46 ± 3.54
ALT (U/L)	17-50	44.84 ± 5.93	38.02 ± 5.23	38.68 ± 13.58

Results show normal values for blood evaluations except a slight leucopenia. Liver parameters are also normal meaning no hepatic toxicity. Hemolysis rate caused by Covergel on blood from three different rats was $2.829 \pm 1.135\%$.

No mortality was observed during this study; rats showed normal levels of energy, behavior, movement and kept a shining hair. There were no signs of inflammation on skin, no salivation or vomit and no mouth, nose nor eye secretion. Body weights were normal and increased in a similar fashion as rats fed *ad libitum* do.

Macroscopic evaluation of major organs didn't show any signs of abnormalities, and organs weight with respect of total body mass did not present any significant differences. Results are shown in Figure 36.
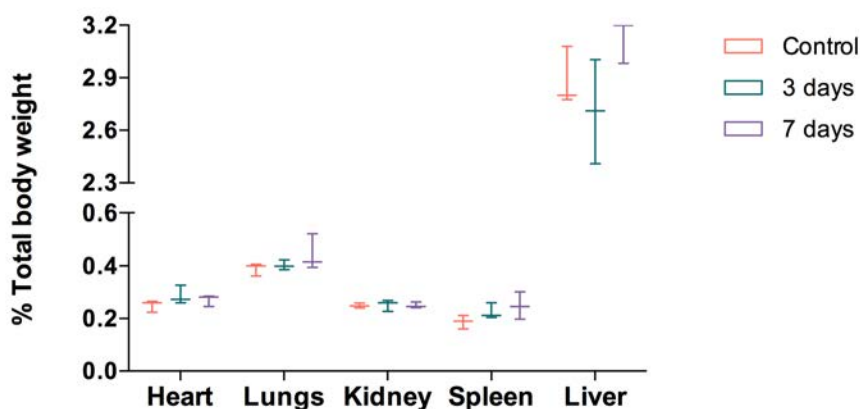

Figure 36. Organ's weight.

After macroscopic evaluation, organs were fixed in 10% formaldehyde and stained with H/E for histological evaluation. Figure 37 shows representative pictures of 5 major organs: Heart, Lungs, Liver, Kidney and Spleen from control rats and from 3 and 7 days post intraperitoneal injection of 10 mg/kg of Covergel.

The heart tissue didn't show signs of toxicity, cardiac myocytes maintain a good arrangement, and no hemorrhage, inflammation nor necrosis is observed. In the liver, no hepatocellular degeneration occurs, and there isn't

an abnormal neutrophil, lymphocyte or macrophage infiltrate in the tissue. Tissue structure from spleen, kidneys and lungs is maintained as well. These results confirm that Covergel was non-toxic in major organs after 7 days post intraperitoneal injection.
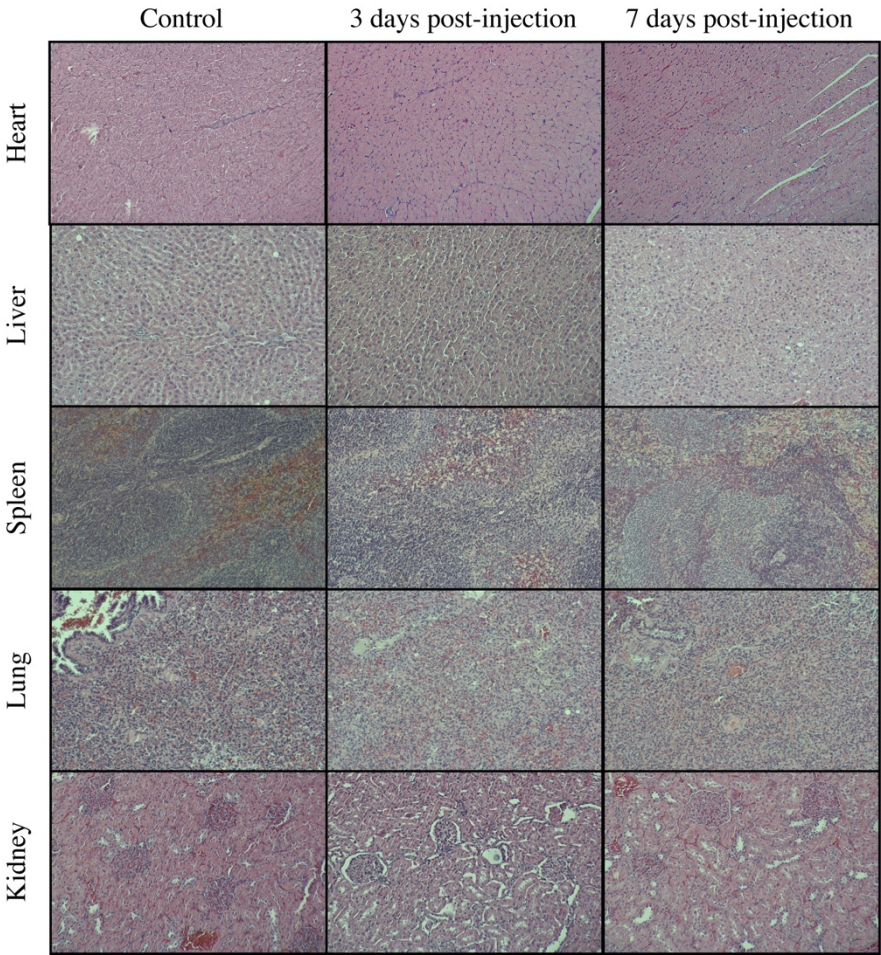

Figure 37. Organ's histology.

To evaluate the effect of gelified Covergel inside the body, we performed a subcutaneous (s.c). placement of 0.5g of Covergel.

The tissue surrounding Covergel at the time of euthanasia was fixed, stained in H/E and evaluated by a pathologist. Figure 38 shows a synovial metaplasia,

a capsular surface covered by fibrohistiocytic cells that are grouped forming pseudovilli. No toxicity or inflammation was seen in the surrounding tissue, meaning that the body responded by encapsulating the hydrogel as it would do with a foreign body, but no rejection response was triggered.

At the time of placement, Covergel samples weighted 0.5 g; when extracted, the weight was 0.95 ± 0.06 g.
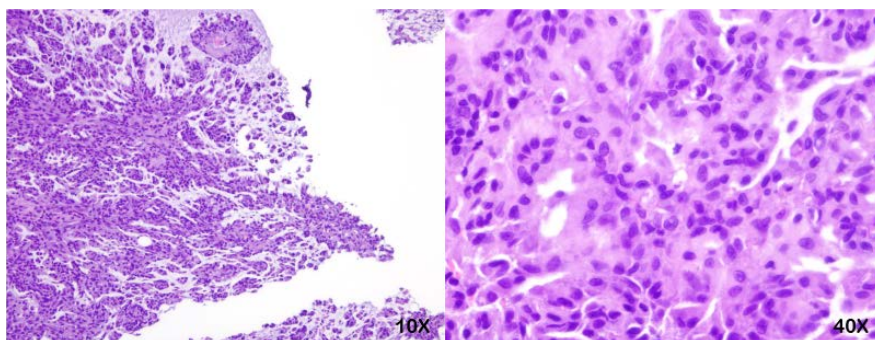

Figure 38. Histological findings on the surrounding tissue of the implanted hydrogels on rats.

Covergel samples were also evaluated with Scanning Electron Microscopy to study the maintenance of the inner network when it was placed inside the body.

Figure 39 shows SEM images of Covergel 10 days after placement; porosity and inner network are maintained, and no major variabilities are observed. No cell invasion was detected in Covergel 10 days after s.c. placement.

Finally, time of adhesion of Covergel to the mucosae was studied. Figure 40 shows X ray images of the same rat before Covergel application (A) after Covergel application (B) and 36 hours after Covergel application (C). Results indicate that Covergel is able to stay adhered to the mucosae for at least 36 hours *in vivo.*
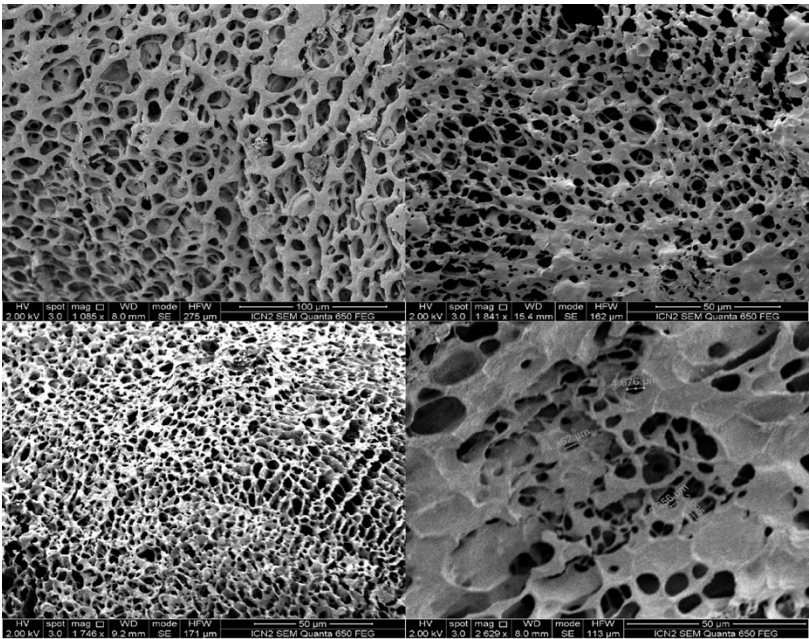
Figure 39. SEM images of the implanted Covergel in rats.

Figure 40. X ray images of the same rat at (A) before Covergel application, (B) at the time of application and (C) 36 h after application.

2. Implementation of our hydrogel on the endoscopic technique

2.1. Submucosal Injection Solution

Trans-epithelial R was measured at times 0, 15, 30, 45 and 60 min after substance injection on the submucosal layer. Electrical resistivity of porcine stomach without submucosal injection was 5×10^4 Ω. Solutions showed a wide variability of trans-epithelial R after submucosal injection (Time 0: GP 20×10^4 Ω, BB 20×10^4 Ω, GC 16×10^4 Ω, GS 13×10^4 Ω, HA 9×10^4 Ω, PL 8×10^4 Ω, PRP 6×10^4 Ω, S 6×10^4 Ω, and PRP+BB 6×10^4 Ω) (Table 14). Next measurements at 15, 30 and 45 minutes showed a trend to decrease R in all solutions except HA, PL, PRP and PRP+BB that maintained stable values.

Table 14: Electrical and rheological properties of different solutions to perform submucosal injection. Values represent the mean of three separate experiments for each substance

Solutions	Resistivity (10^4 Ω)	Musc. T^a (ºC)	Heigh t=0 (cm)	Heigh t=60 (cm)	Cushion decrease (%)	Time (sec)	Osmolarity (mOsm/L)	Viscosity (Pa)
Saline	6	198.4	1.68	1.22	27.46%	33.4	286	0.0043
PRP	6.5	110.4	2.14	1.67	22.12%	20.3	278	0.01
Gliceol®	16	82.4	2.12	1.53	28.74%	17.6	288	0.009
HA	9	56.6	2.41	1.76	27.06%	28	282	0.04
PL	8	47.6	2.37	1.93	18.63%	34.6	300	0.9
GS 10%	13	82.9	2.33	1.15	50.84%	23.5	556	0.008
Gelaspan	20	133.6	2.45	1.73	30.51%	30.7	284	0.009
BB	20	55	2.63	2.32	11.74%	51.7	300	0.9
PRP+BB	6	80.1	2.60	1.65	36.55%	33	280	0.045

The substances that were able to maintain a higher R after 60min post-injection were BB (7×10^4 Ω), HA (7×10^4 Ω) and PL (7×10^4 Ω) (Figure 41).
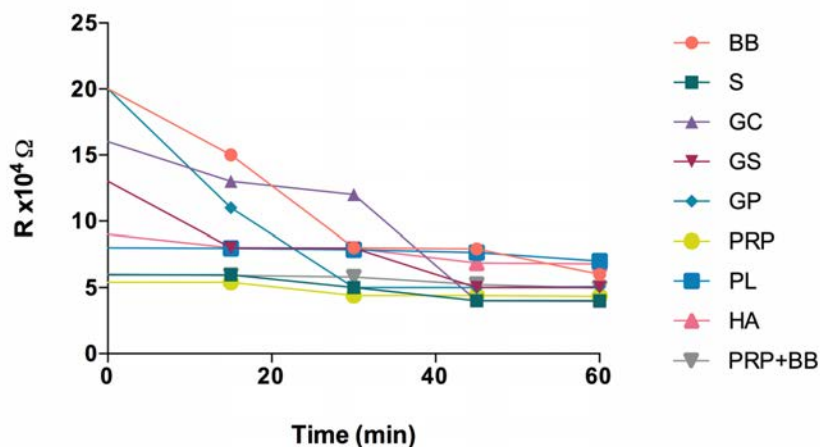
Figure 41. Trans-epithelial R of different solutions in fresh porcine stomach at baseline, 15, 30, 45 and 60 minutes after submucosal injection.

EMR without any substance used to create a cushion resulted in muscular layer Tª of 79.48ºC and a total time for resection of 31 seconds (basal determinations). Solutions showed very different patterns in Tª increase during EMR at muscular layer (Figure 42). High risk of deep thermal injury (Tª higher than 60ºC) was observed with S (198.4ºC), GP (133.55ºC), PRP (110.4ºC), GS (82.85ºC), GC (82.4ºC) and PRP+BB (80.1ºC). By contrast, protective solutions were PL (47.6ºC), BB (55ºC) and HA (56.63ºC).
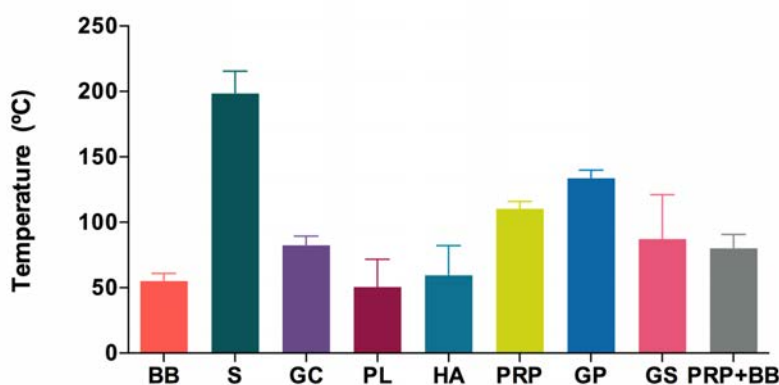

Figure 42. Temperature after EMR reached at muscular layer.

Time to perform EMR was comparable or higher than basal with HA (28"),

GP (30.73"), PRP+BB (33"), S (33.41"), PL (34.64") and BB (51.67"). Solutions able to shorten this time were GC (17.66"), PRP (20.3") and GS (23.45") (Figure 43).
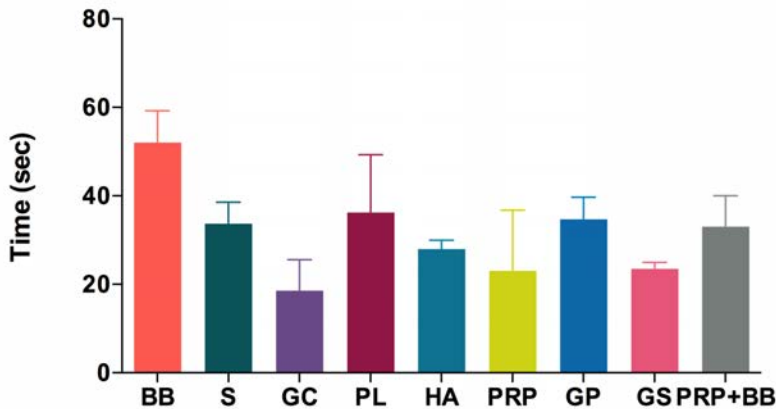

Figure 43. Time to perform EMR with different substances using a standard polypectomy snare.

Submucosal cushion height with the different solutions at time 0 and 60 minutes after injection is shown in Table 14. The substances capable of maintaining at least a 75% of the original height after one hour were (cushion decrease <25%): BB (11.74%), PL (18.63%) and PRP (22.12%) (Figure 44).

A nonparametric Spearman correlation study was done for all the characteristics evaluated and results are shown in Table 15. Correlation quantifies the degree to which two variables are related. Correlation tests compute a correlation coefficient (r) that indicates how much one variable tends to change when the other one does. When r is 0.0, there is no relationship. When r is positive, there is a trend that one variable goes up as the other one goes up. When r is negative, there is a trend that one variable goes up as the other one goes down.

The only significant correlations were: muscular T vs resistivity (-0.7851) muscular T vs osmolarity (-0.8740) and EMR time vs resistivity (0.6938). These results indicate that as resistivity and viscosity of a substance increase,

the muscular temperature reached decreases, so solutions with higher resistivity and viscosity will be more efficient for thermal protection. Also, time to perform EMR is increased when resistivity of a solution is increased, as we have seen in our results.
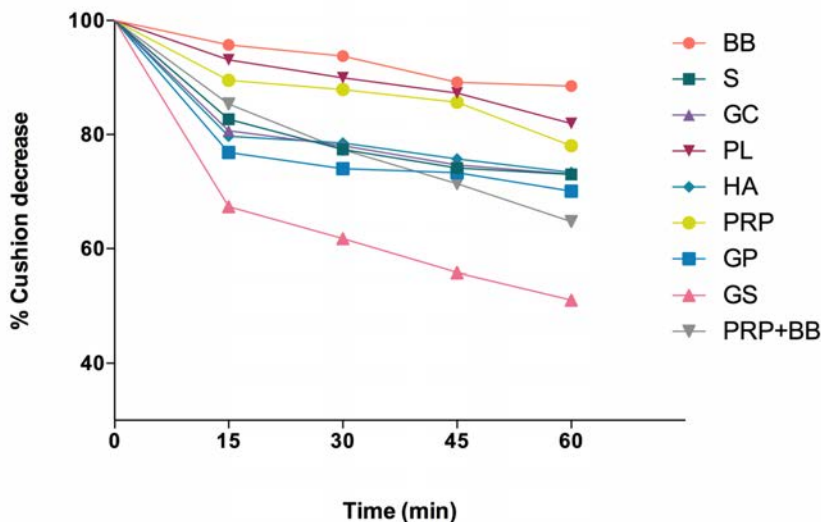
Figure 44. Percentage of submucosal cushion decrease of the height acquired by each substance at time 0.

Table 15. Nonparametric Spearman correlation for all characteristics evaluated.

	Resistivity	Viscosity	Osmolarity	Muscular T^a	EMR time	Cushion decrease
Resistivity	---	0.635	0.357	-0.785 **	0.693*	-0.529
Viscosity	0.635	---	-0.337	-0.874**	0.495	-0.605
Osmolarity	0.357	-0.337	---	0.025	0.390	0.075
Muscular T^a	-0.785 **	-0.874**	0.025	---	-0.383	0.483
EMR time	0.693*	0.495	0.390	-0.383	---	-0.450
Cushion decrease	-0.529	-0.605	0.075	0.483	-0.450	---

* p-value <0.05. ** p-value <0.01.

118

The rest of correlations studied, although not statistically significant, show a clear trend towards interesting results. For example, as viscosity of a solution is higher, cushion decrease is lower, meaning that more viscous solutions will last longer on the submucosal layer. Higher viscosity of a solution also means higher resistivity, lower osmolarity, and longer time to perform EMR.

2.2. Endoscopic Shielding Technique

As seen in Figure 45, Covergel-Bibio was capable of maintaining an inhibition zone on the petri dish 72 h after seeding. On the contrary, Covergel did not inhibit bacterial growth, but the state of Covergel itself was not checked as we had previously seen that it was resistant to bacteria for at least 30 days. Control test shows dehydrated Covergel-Bibio.
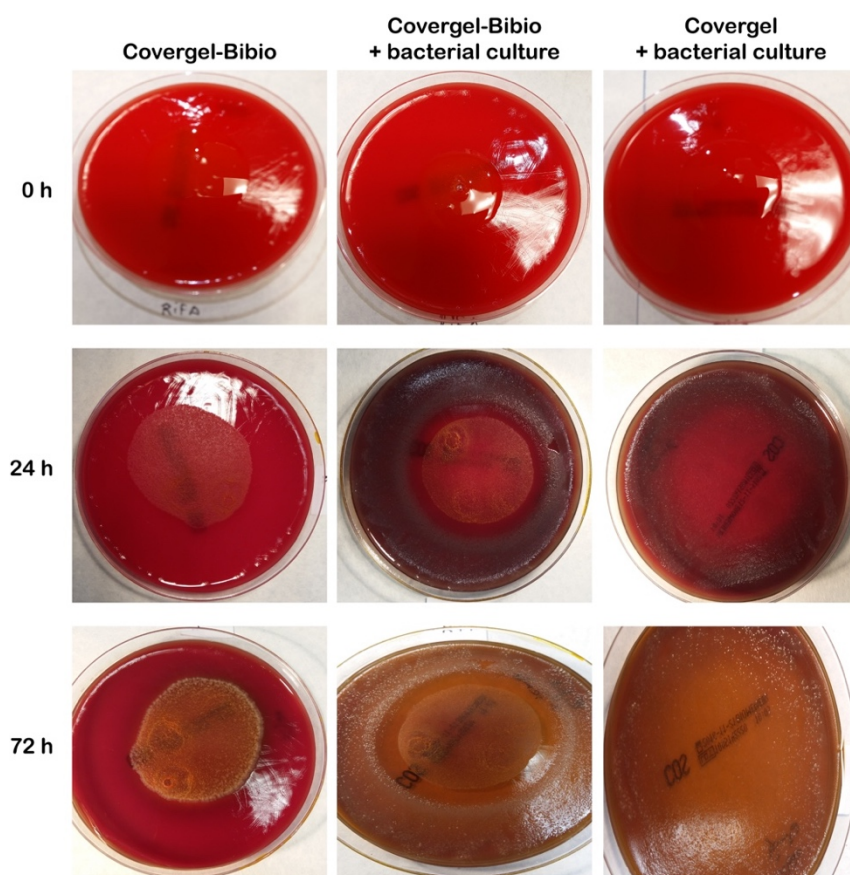

Figure 45. Covergel-Bibio test of bacterial inhibition.

2.2.1. Thermal injury

Endoscopic Shielding Technique with Covergel-Bibio induced a marked trend towards a less deep thermal injury on the pathological specimen in both animal models (Figure 46). In rats, treatment with Covergel-Bibio showed the best results in comparison with control and comparative groups, avoiding mortality (0% vs 50% and 25%; $P = 0.038$), and avoiding the risk of perforation at 7 days (0% vs 100% and 33.3%; $P = 0.02$) (Table 16). Mortality in rats happened during the first 48 h after the procedure. Perforation in dead rats was detected during necropsy. In those rats, only macroscopic assessments were done. In the surviving animals, delayed perforation was evaluated in histological studies. Although we didn't observe statistical significance between groups, because of the number of animals, non-treated animals showed higher deep thermal injury (1.45 ± 0.88 vs 2.25 ± 1.38 and 1.50 ± 1.19).
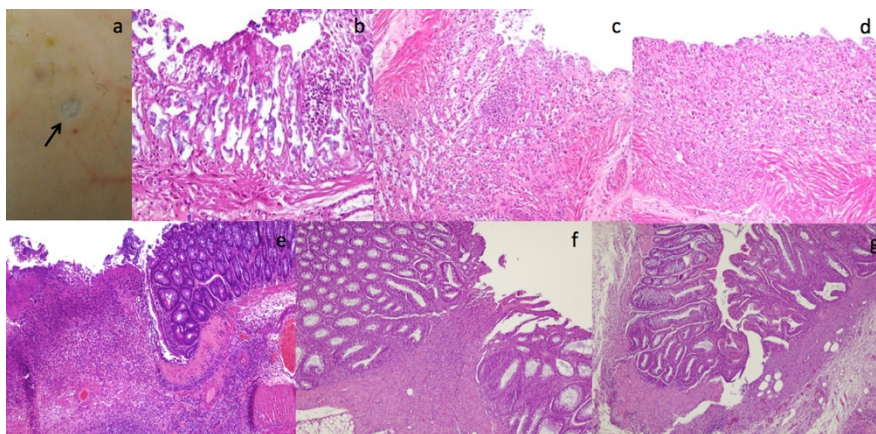
Figure 46. Histological evaluation of rat model (a-d) and porcine model (e-g).

Figure 46 shows relevant histopathological findings on both animal models. Picture a shows an open perforation on rat's colon found when necropsy was done. Picture b shows transmural necrosis on an animal from group A, and pictures c and d show the absence of deep thermal injury in rats from groups B and C. Pictures e-g show necrosis, or absence of it, of the muscularis propria

in porcine model that underwent EMR from groups D (picture e) E (picture f) and F (picture g).

In the porcine model, no mortality was observed. Submucosal injection of Covergel-Bibio induced a marked trend towards a less deep thermal injury in acute lesions induced at the end of the 14-day study (Group F = 2.25 ± 0.46 vs D and E= 2.75 ± 0.46; P = 0.127) (Table 17).

2.2.2. Mucosal healing

In rats (Table 16), ulcers at 48 h were similar in all treatment groups (Group A: 0.56 ± 0.10 cm²; Group B:0.55 ± 0.01 cm²; Group C:0.57 ± 0.34 cm²; P value n.s.). Mean ulcerated area after 7 days was significantly smaller with Covergel-Bibio than with saline and comparative (Group C: 0.17 ± 0.07 cm²; Group A: 0.39 ± 0.04 cm²; Group B: 0.29 ± 0.01 cm²; P value < 0.01). Mucosal healing rate (percentage of mucosal restoration) at 7 days was significantly higher with Covergel-Bibio (Group C: 70.3%; Group A: 47.2%; Group B: 30.3%; P value = 0.003). Physiological healing (absence of submucosal fibrosis) was significantly higher with Covergel-Bibio (6 of 8 animals, 75%) than in saline (0 of 4 animals, 0%) and comparative example (4 of 6 animals, 66.6%) (P value = 0.02).

Table 16. Thermal injury and mucosal healing in rat model.

	Group A	Group B	Group C
Mortality n (%)	4/8 (50)	2/8 (25)	0/8 (0)
Delayed perforation n (%)	4/4 (100)	2/6 (33.3)	0/8 (0)
Mean ulcerated area at 48 h (cm²)	0.56 ± 0.10	0.55 ± 0.01	0.57 ± 0.34
Mean ulcerated area at 1 week (cm²)	0.39 ± 0.04	0.29 ± 0.01	0.17 ± 0.07
Mucosal healing rate (%)	30.3	47.2	70.3
Physiological healing n (%)	0/4 (0)	4/6 (66.6)	6/8 (75)
Fibrotic healing n (%)	4/4 (100)	2/6 (33.3)	2/8 (25)
Thermal injury	2.25 ± 1.38	1.50 ± 1.19	1.45 ± 0.88

In the porcine model (Table 17), basal mean ulcerated area induced by EMR was comparable in the three groups (Group D: 2.12 ± 1.45 cm², Group E: 2.57

± 1.53 cm², Group F: 2.66 ± 1.64 cm²; P value n.s.). Mucosal healing rate at week 2 (percentage of mucosal restoration) was significantly higher in animals treated with Covergel-Bibio (Group E: 90.2 ± 3.9%, Group F: 91.3 ± 5.5%; Group D: 73.1 ± 12.6%; P = 0.002), as can be observed during endoscopic follow up (Figure 47).

Table 17. Mucosal healing and thermal injury in porcine model.

	Group D (n=8)	Group E (n=8)	Group F (n=8)
Basal ulcer (cm²)	2.12 ± 1.45	2.57 ± 1.53	2.66 ± 1.64
Mucosal healing rate (%)	73.1 ± 12.6	90.2 ± 3.9	91.3 ± 5.5
Thermal injury	2.75 ± 0.46	2.75 ± 0.46	2.25 ± 0.46

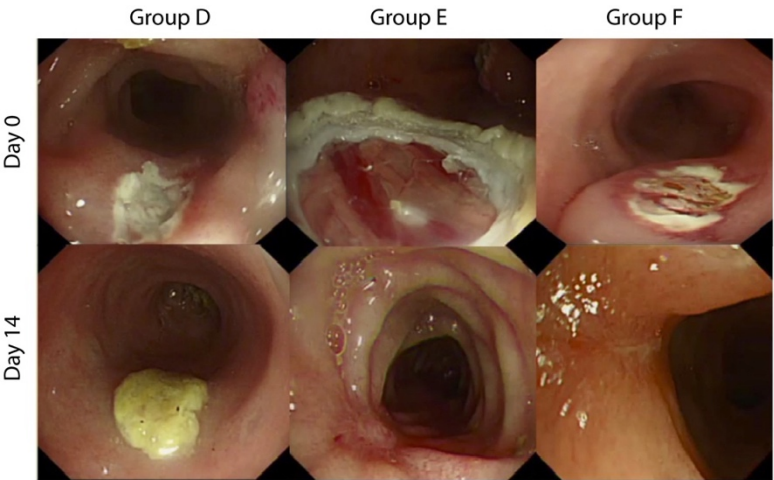Figure 47. Endoscopic follow-up in porcine model.

3. Hydrogel as a drug-delivery platform for intestinal diseases. CRC and experimental colitis animal models

3.1. CRC animal model

Animals underwent endoscopic follow-up from week 30 after AOM application to week 35, which is the estimated time for tumors to appear. Once a tumor was seen, intratumoral application with selected treatment was done

and 10 days after animals were euthanized. Features of obtained tumors in this animal study are reviewed in Table 18. Figure 48 shows representative pictures of each group. Endoscopic pictures from treatment application day and macroscopic, and histological pictures after euthanasia are shown.

Table 18. Feature results of the animal model.

Features	
Tumor incidence	100% of animals
Tumor multiplicity	1.25 (15 rats 1 tumor, 5 rats 2 tumors)
Tumor location	20 tumors distal, 5 tumors proximal
Tumor size average (mm)	7.2 mm
Tumor histology	100% adenocarcinomas

The only case where intratumoral injection seemed to have a clear necrotizing effect was in rats treated with Aflibercept + Irinotecan, where a clear necrosis can be seen both macroscopically and histologically.

These results are in line with results from the histopathological study where, the only treatment that produced a significant tumor size reduction and tumor necrosis was Aflibercept + Irinotecan. Results are shown in Figure 49.

3.1. Acute experimental colitis model

All animals included in this protocol underwent an endoscopic follow-up at day of induction (day 0), day of treatment (day 3) and day of euthanasia (day 7). Furthermore, when animals were euthanized, colon was extracted and evaluated macroscopically, pictures were taken.

At day 0 no differences were seen on the aspect of the colonic wall, with absence of any ulcers or inflammation and normal vascular pattern throughout the colon (data not shown). At day 3, all animals presented, at least in some part, an entire circumferential affectation of the wall, moreover, a minimum of 8% of weight loss was require for animals to be included in the study. Figure 50 shows endoscopic and macroscopic images of representative animals from each group.
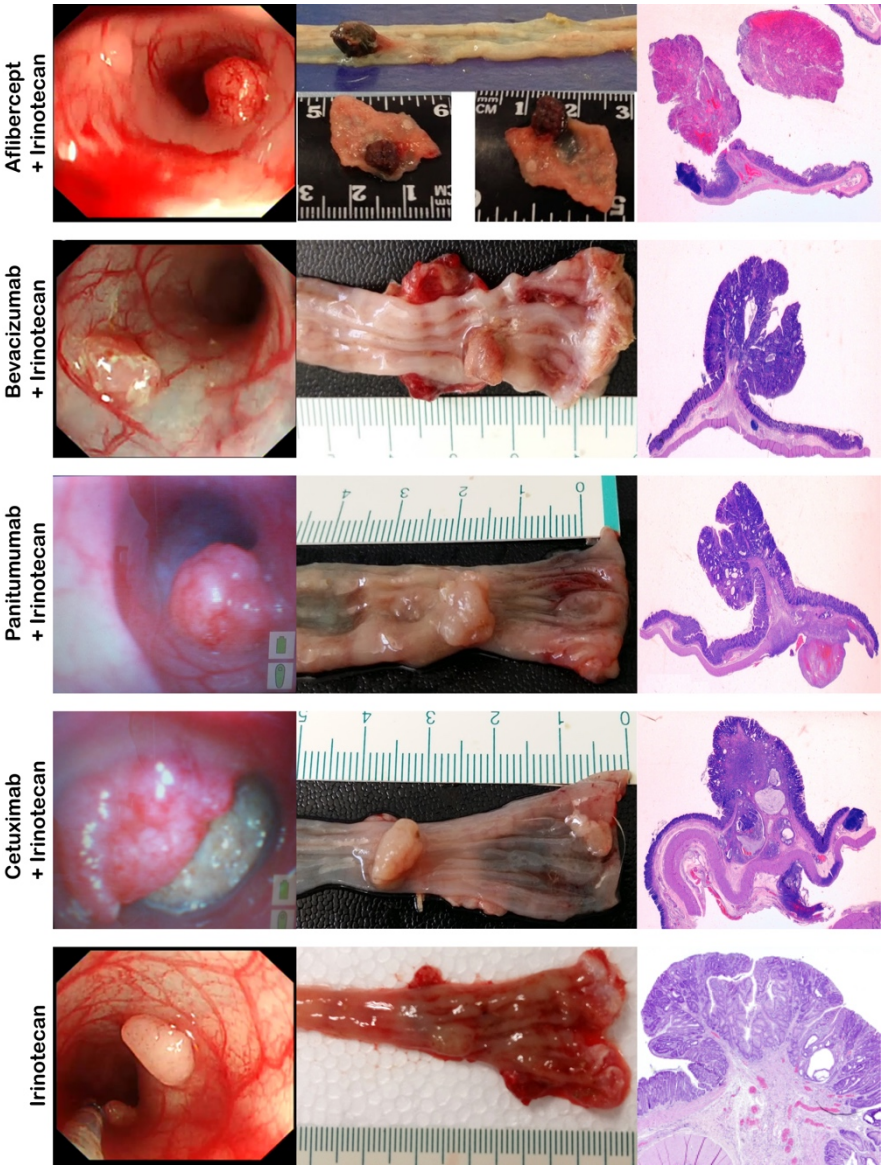
Figure 48. Endoscopic, macroscopic and histological pictures of CRC animal model.
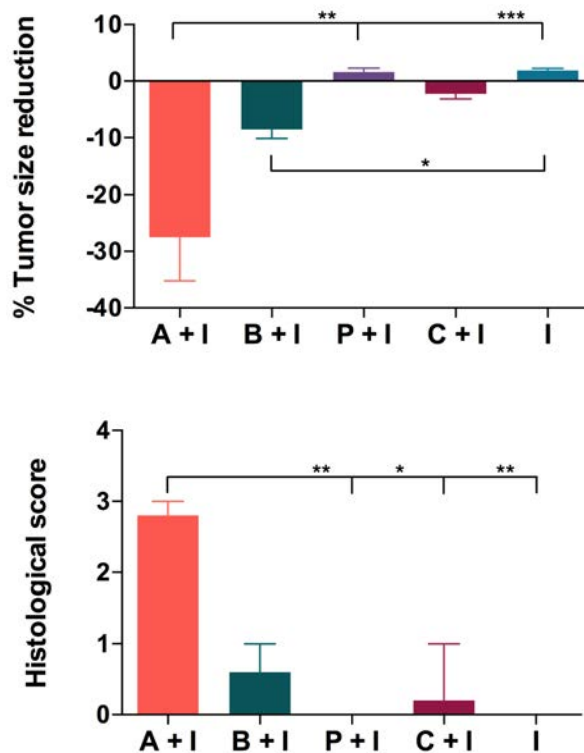
Figure 49. Tumor size reduction and histological score for necrosis after treatment.

Mucosal restoration on treated groups was easily seen both by endoscopy and during necropsy. Vascular pattern was recovered, and signs of ulceration or friability were diminished. Samples were later analyzed histologically.

Ponderal evolution was studied as variation (Δ) of original weight at day 0 for each rat. At day 3, variations of original weights expressed in median (range) were: Sham +11 (4) g, Control -49 (34) g, Platform -40 (23) g, Platform + IFX -39 (26) g and Platform + VDZ -35 (31) g. All groups that underwent colitis induction had lost >8% of original weight. At day 7, variations of original weights expressed in median (range) were: Sham 23 (14) g, Control -55 (33) g, Platform -36 (51) g, Platform + IFX -17 (56) g and Platform + VDZ -20 (34) g (Figure 51).
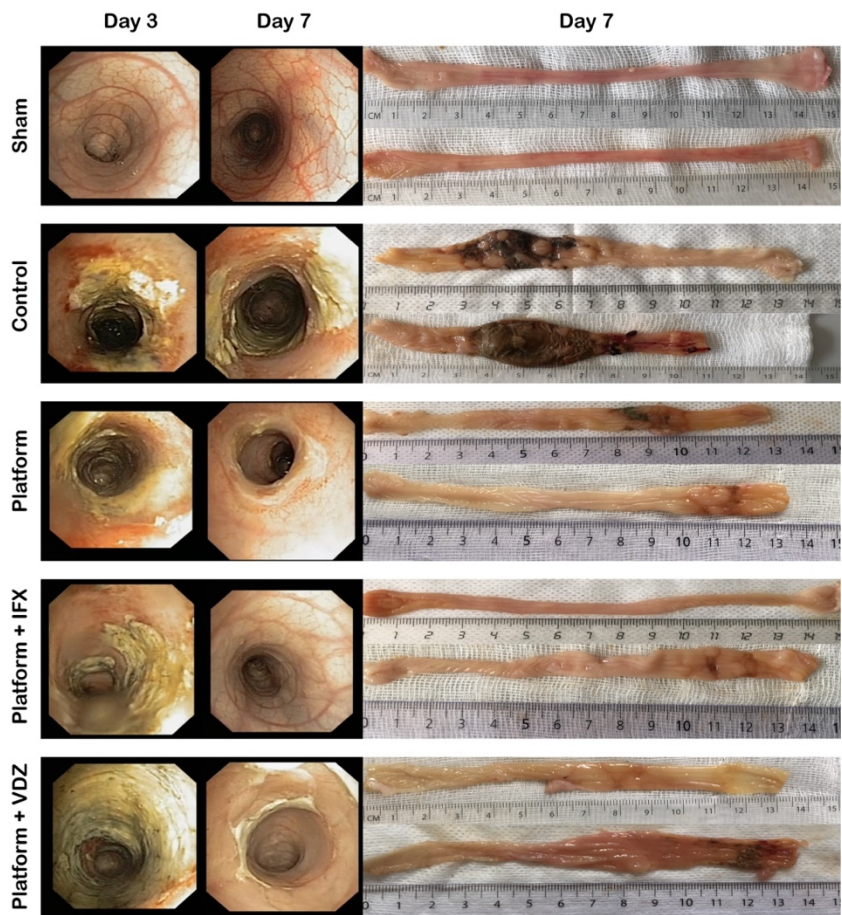
Figure 50. Endoscopic and macroscopic images of colitis induction and resolution 4 days after.
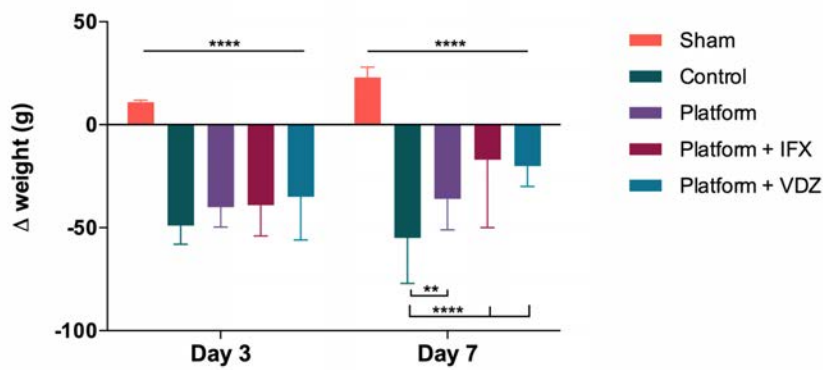
Figure 51. Ponderal evolution.

The ratio between colon's length and weight is a simple indicator of edema and inflammation in the tissue. Colon weight/length ratio for animals at day 7 expressed in Median (Range) was: Sham 0.09758 (0.0407) g/cm, Control 0.3157 (0.244) g/cm, Platform 0.2063 (0.1012) g/cm, Platform + IFX 0.1854 (0.1527) g/cm and Platform + VDZ 0.1914 (0.0545) g/cm (Figure 52).

Another sign of a weak intestinal barrier is bacterial translocation to liver, which happens when the permeability of the barrier is hindered due to inflammation or edema. Cases and percentages of bacterial translocation to liver at day 7 were: Sham (0/6; 0%) Control (8/8; 100%) Platform (5/8; 62.5%) Platform + IFX (1/7; 14.3%) and Platform + VDZ (1/6, 16.6%).

Figure 52. Colon weight/length ratio

Histological study evaluated the maintenance of the intestinal architecture and the inflammatory cell infiltrate in a 0-3 scale for both characteristics and a final 0-6 scale. Histological score for groups as mean ± SD is: Sham 1 ± 0, Control 5.87 ± 0.35, Platform 5.24 ± 0.76, Platform + IFX 5.34 ± 0.98 and Platform + VDZ 5.28 ± 0.82. Representative images of each group are shown in Figure 53.
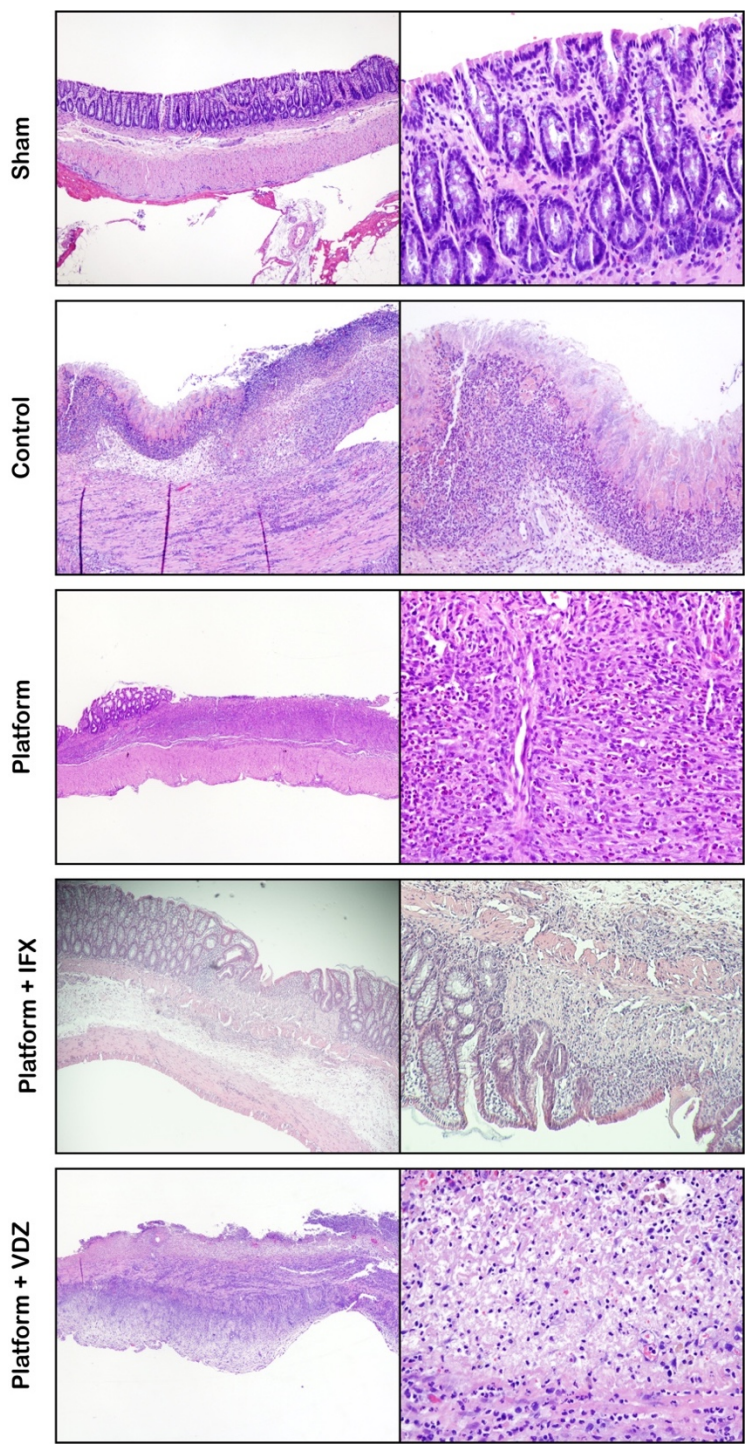
Figure 53. Histological images of the Acute experimental colitis study.

3.2. Chronic experimental colitis model

All animals included in this protocol underwent 4 rounds of TNBS colitis induction in the same fashion as the acute model, thus, induction was done on days 0, 7, 14 and 21, treatments were given on days 3, 10, 17 and 24 and euthanasia was performed on day 28. Animals underwent endoscopic follow-up at days of induction, days of treatment and day of euthanasia. Furthermore, when animals were euthanized, colon was extracted and evaluated macroscopically, pictures were taken.

At Day 0 no differences were seen on the aspect of the colonic wall, with absence of any ulcers or inflammation and normal vascular pattern throughout the colon (data not shown). All animals decreased at least an 8% of weight on the first colitis induction at day 3, nevertheless, no exclusion criteria were set on this study as the main aim was to evaluate the final concentration of ATIs after 4 rounds of treatment application. There was variation in both groups in the degree of colitis induction throughout the 4 TNBS applications. Figure 54 shows representative images of both groups at day 3 (first treatment application), day 7 (second TNBS induction), day 21(fourth TNBS induction), day 24 (fourth treatment application) and day 28 (euthanasia).

Ponderal evolution was studied as percentage (%) of original weight at day 0 for each group (Figure 55), values are expressed in median (range). No statistically significant differences were observed at any day of the study.

Bacterial translocation to liver in both groups had the same values, two animals out of six (33.3%).

Colon weight/length ratio for animals at day 28 expressed in median (range) are shown in Figure 56. This ratio was significantly lower in the IFX subcutaneous treated group compared to the group treated with our platform and IFX (0.213 (0.124) vs 0.3497 (0.129), p value 0.0087).
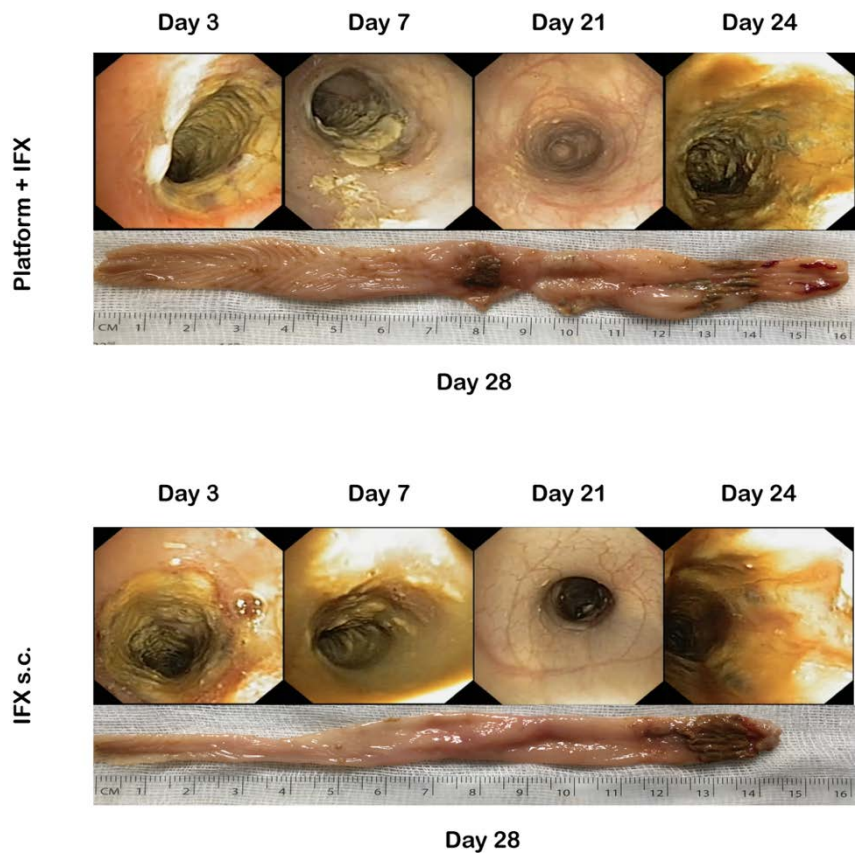
Figure 54. Endoscopic and macroscopic images of chronic experimental colitis model.
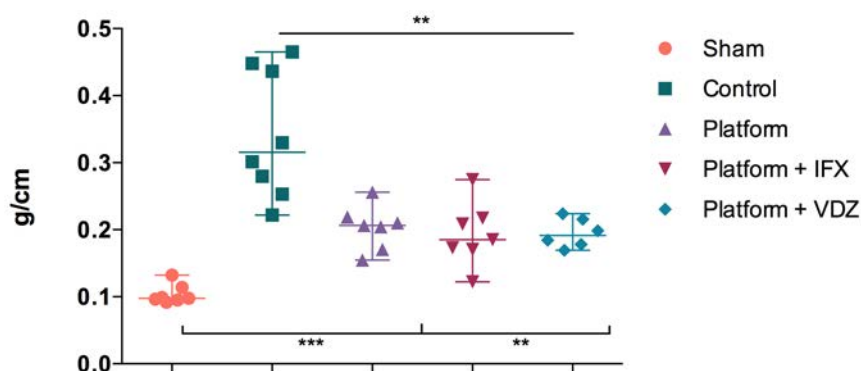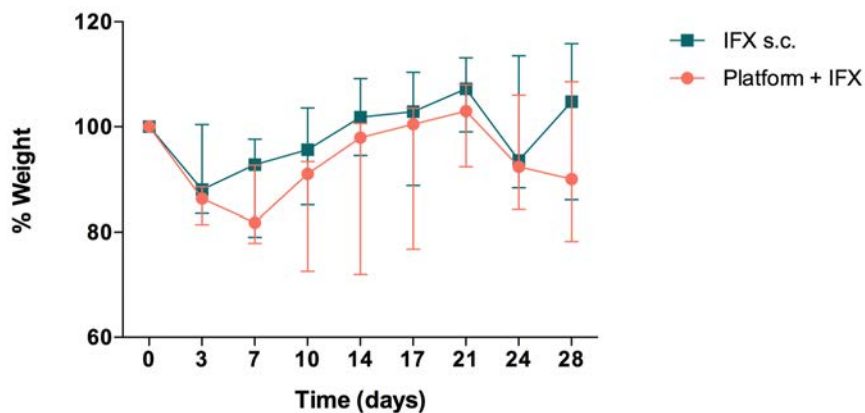

Figure 55. Ponderal evolution
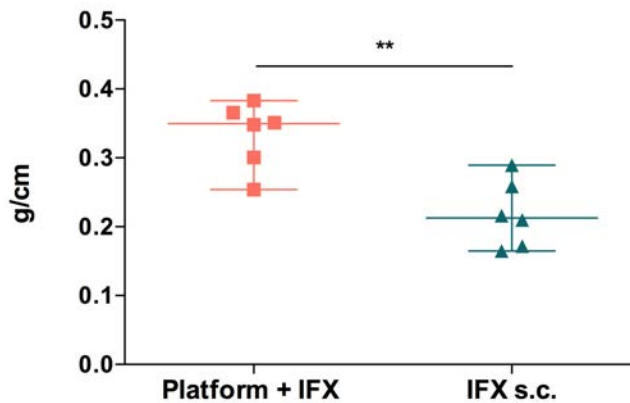
Figure 56. Colon weight/length ratio

Histological study evaluated the maintenance of the intestinal architecture and the inflammatory cell infiltrate in a 0-3 scale for both characteristics and a final 0-6 scale. Histological score for groups as mean ± SD is: Platform + IFX 5.48 ± 0.55 and IFX s.c. 4.96 ± 0.71. Representative images of each group are shown in Figure 57.

Finally, concentration of ATIs after four treatment applications was evaluated. The evolution of levels of ATIs for each group is shown in Figure 58, values are represented in mean (± SEM) of μg/mL-calibrated (μg/mL-c) where values have been compared to a polyclonal rabbit α-IgG standard. At day of euthanasia, levels of ATIs were significantly lower in rats treated with our platform + IFX compared to rats treated with IFX subcutaneously (0.90 ± 0.06 μg/mL-c vs 1.97 ± 0.66 μg/mL-c, p value 0.0025).
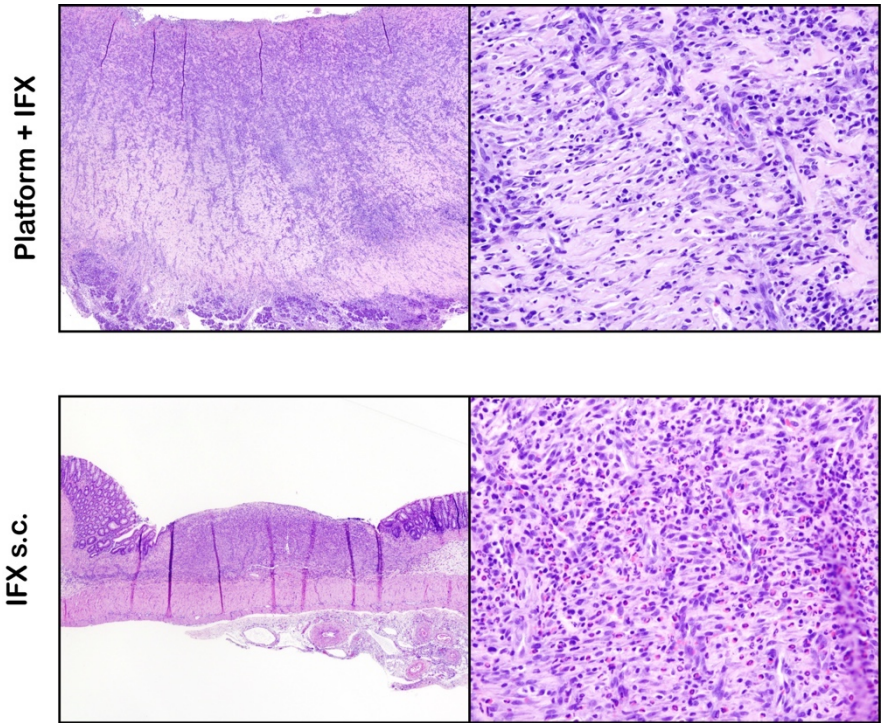
Figure 57. Histological images of the Chronic experimental colitis study
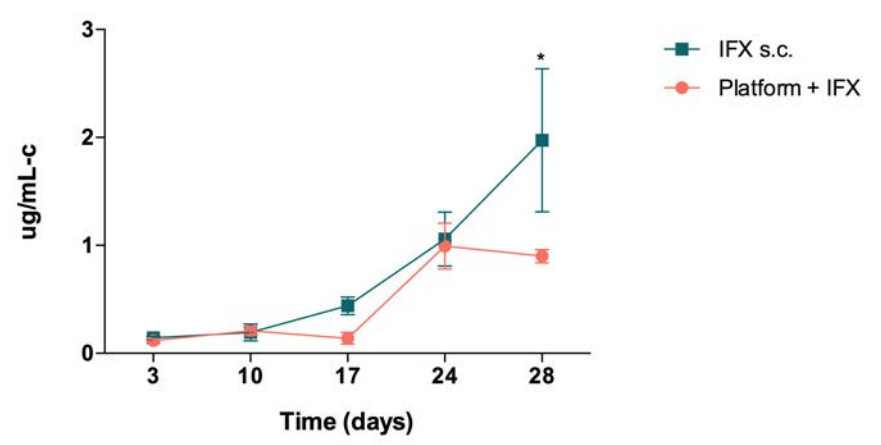
Figure 58. ATIs evolution.

DISCUSSION

Endoscopy has become a day-to-day basis medical procedure not only for its importance as a diagnostic tool in gastrointestinal pathologies or as a surveillance tool for colorectal cancer. It also offers many benefits as a therapeutic tool, permitting a less invasive way to solve mucosal and mechanical problems of the gastrointestinal tract. Nevertheless, as all medical interventions, adverse events are present and hinder the use of endoscopy in some scenarios, making the patient go through a much more invasive procedure such as surgery. In this work we have tried to give a solution to some of the unmet needs of endoscopy, as well as to provide new therapeutic tools for endoscopy.

We have developed a new hydrogel, which we named Covergel, based on Poloxamer Pluronic-F127, Hyaluronic acid and Methylcellulose which presents biocompatible, bioadhesive and bioactive properties. Alone, these three components of which our hydrogel is composed have proven their biocompatibility among other beneficial characteristics[108,109,116–118].

Rheological studies on Covergel showed a reverse thermosensible capacity of gelation, characteristic given by P-F127. Gelation was accompanied by a greater adhesion of Covergel. Adhesion force greatly increased when temperature increased from 22 to 37°C *in vitro*. This characteristic is especially interesting for mucoadhesion of Covergel. When Covergel contacts the mucosal layer at a physiological temperature, is gellifies permitting the adhesion to the mucosae[119]. We have proven that Covergel is able to stay adhered to the mucosae for at least 36 hours. Irreversible gelation was accomplished by the addition of acrylate groups to P-F127 and the exposure of Covergel with a photoinitiator to UV light. Since temperature increase is still necessary for Covergel to gelate with modified P-F217, rheological properties of both the initial and final mixture of Covergel are maintained, but this chemical gelation gives Covergelmuch more resistance in aqueous mediums. Modified P-F127 thus, results in a higher union force of the

hydrogel matrix, making it less vulnerable to matrix transformations due to osmotic pressure or tissue extrusion, which is an advantage for a controlled drug release of Covergel[120]. Rheological studies in Covergel confirmed that it is a non-Newtonian fluid, meaning that its viscosity varies with temperature. This kind of fluids don't have a constant and well-defined value of viscosity.

Morphologically, Covergel presents a large microporosity with an interconnected network that can be the matrix for cell ingrowth as well as nutrients and waste flow, essential characteristics for cell survival within the hydrogel. Ganji *et al*[121] classified hydrogels according to the extent of porosity and the type of porous structure. According to this description, Covergel would fall in the super-porous type. This type presents a "High porosity with interconnected open-cell structure" and is particularly interesting for "Drug delivery systems, especially in the gastrointestinal tract, and for tissue engineering"[121]. Furthermore, this microporous structure could provide a pathway to nutrients and oxygen flow to encapsulated cells, support cell proliferation and differentiation and offer a way of waste product retrieval[122].

Molecules were incorporated in Covergel by the swelling method. It was expected that the incorporating efficacy will be limited to the swelling capacity of Covergel. We also found that the size of the molecule might have a say on this efficacy. Incorporating efficacy for Trypan Blue was more than twice higher than for BSA. Another explanation for this different efficacy could be the concentration of each substances in the liquid that Covergel was submerged in. BSA concentration was 4000 times higher than Trypan Blue (2mg/mL vs 0.0005 mg/mL). This means that incorporating efficacy for trypan blue could have been hindered by swelling capacity, but it was sufficient water absorption to reach an osmotic pressure equilibrium inside and outside the hydrogel. Whereas for BSA, the swelling capacity of the hydrogel was not enough to reach this osmotic pressure equilibrium, due to the high original concentration.

Different kinetic models were studied with the results obtained from the drug release experiments. The kinetic model that best fitted our results was the Higuchi release model. This model is explained by Fick´s law, in which diffusion of a molecule is related to its concentration. The diffusion flux goes from a higher concentrated area to a lesser concentrated one. The magnitude of the diffusion flux will be proportional to the concentration gradient. These results and kinetic model were confirmed when mechanistic of drug release from Covergel were studied by the Korsmeyer-Peppas model. In this model, the value of the release coefficient (n) gives information about the mechanism of drug release. When we fitted the Korsmeyer-Peppas model to our data, the release coefficient obtained was 0.43. If the value of n is <0.45 means that the diffusion coefficient follows a Fickian diffusion, thus, following Fick´s laws.

Hydrogel degradation is a process that transforms the microstructure of the hydrogel matrix, thus having an impact on other important aspects such as drug release[120]. As stated before, hydrogel degradation is a three stage process: swelling, swelling-induced degradation and bulk degradation[95]. Previous reports on P-F127 hydrogels showed that this kind of hydrogels swelled rapidly on the first hours in aqueous medium, accelerating bulk degradation process that was reached in approximately 1 week[118]. Temperature also affected P-F127 hydrogels swelling due to its thermo-sensitive properties, decreasing the swelling ratio when temperature was increased[118]. As seen in our results, Covergel reached a swelling equilibrium within the first 24 hours, as previously reported for other P-F127 based hydrogels[118]. Nevertheless, bulk degradation was not reached 30 days after Covergel submersion in normal conditions. Degradation-induced swelling was the main process occurring as Covergel continuously lost weight, but overall shape was maintained, and Covergel did not shred to pieces in this time. Only in extreme conditions (pH=11 and pH=3) degradation was accelerated and bulk degradation occurred. A possible explanation for this prolonged resistance in aqueous medium is the modifications Covergel presents. Modifications such as acetyl

groups have been proposed to increase hydrophobicity of the hydrogel affecting water penetrability inside[108]. The mixture of P-F127 with additives such as polymers, or modifications like UV curing have also been proven to increase the mechanical force of hydrogels, making them more suitable for clinical applications like sustained drug release[123–125]. Although a fast degradation profile is beneficious for a fast delivery of cells or drugs, it is inconvenient for other tissue engineering applications where a longer-lasting and with higher mechanical strength material is needed[118].

Cellular viability of cells co-cultured with Covergel at different percentages was evaluated. Covergel showed the capacity to improve cellular viability in a dose-dependent manner at least until a 10%. The highest percentage tested was 15%, in which case cell viability decreased but still was maintained the same as the positive control of the experiment. We believe that this increase in cell viability is due to the trophic action of HA. The ability of HA to promote cell growth is understood to be via both the CD44 receptor and the IL6 pathway, and it has also been seen in tumor cells[126–128]. Despite this, HA hydrogels loaded with antitumoral drugs have been very useful in inducing cancer cell death[129]. Covergel can support cell proliferation *in vitro*, demonstrating a good potential to become a cell carrier.

Hemolysis test represent and easy and accurate method to evaluate blood compatibility to material *in vitro*. This test is recommended by the FDA for many substances applied intravenously such as drug excipients[130]. Materials can be classified depending on the hemolysis they cause as: hemolytic for materials causing >5% hemolysis, slightly hemolytic for materials causing between 5-2% hemolysis and non-hemolytic for materials causing >2% hemolysis[131]. According to this, Covergel should be placed in the low rank of slightly hemolytic materials since our hemolysis rate was 2.83%.

Intraperitoneal injection of Covergel was performed to evaluate possible acute toxicity produced. Rats were monitored throughout the whole experiment and

no affectation to their overall health state was seen. They presented normal behavior, well taken-care of hair, mobility and no nose or eye secretion. Furthermore, when organs were extracted and evaluated they didn't present any major abnormalities not macroscopically neither histologically. These results allow us to state that Covergel did not cause an acute toxicity reaction on animals three or seven days post intraperitoneal injection.

Subcutaneous placement of 0.5 g of Covergel in rats was done to evaluate *in vivo* behavior and biodegradability of our hydrogel. Original weight of Covergel implants was 0.5g and when extracted, weight was 0.95 ± 0.06g. This result means that Covergel, as it did *in vitro*, underwent a swelling process once placed in an aqueous medium like the body. Since only one time point, 10 days, was checked, we cannot state whether it was in a swelling-induced degradation state yet or not. Upon extraction, they Covergel piece had a yellowish color and was intact in one piece. Covergel had been encapsulated by fibrohistiocytic cells grouped forming pseudovilli, but no inflammation or adverse reaction was seen. Covergel samples were evaluated by SEM and we confirmed that the inner structure was maintained 10 days after s.c. placement. Nevertheless, no cell invasion was observed inside Covergel. We believe that this might be due to the way the Covergel implant was placed inside the body. Subcutaneous placement was carried out by performing an incision and the suturing it, however well done the procedure it is still a highly invasive procedure, that probably led to the encapsulation of the foreign body. Possibly a subcutaneous injection of Covergel will improve its ability to accept different cell types and study their behavior inside and with the hydrogel.

We can safely say that we have developed a new hydrogel based on pluronic-F127, methylcellulose and hyaluronic acid. Covergel present thermosensitive characteristics, has a well define microporous structure and we have the possibility to either reversibly or irreversibly gelate it as more convenient. Drug release studies have proven that Covergel is able to diffuse substances for a

prolonged period of time. The durability of Covergel has been proved *in vitro* in physiologically-like situations for at least 30 days. No cell damage or toxicity has been observed in the biocompatibility studies performed with Covergel. All of these results help us conclude that Covergel is a good candidate to be used in the digestive system and implement it in endoscopic techniques in order to cover some unmet needs of the field. Although *in vitro* and *in vivo* results are really promising, further experiments on *in vivo* drug release kinetics and degradation need to be performed, as these characteristics have previously been reported to vary from *in vitro* analysis to *in vivo*, due to inflammatory cell response[122,132,133].

EMR and ESD have been stablished as safe and feasible techniques for the removal of large lesions throughout the gastrointestinal tract. Avoiding the main complications associated, bleeding and perforation, is of interest to the endoscopy field and for this, many improvements in the ressection techniques have been developed. Submucosal injection, as the introduction of a substance in the submucosal layer of the gastrointestinal wall to elevate the mucosal layer thus protecting the muscular layer, has been proved effective to prevent this complications and to improve the clinical outcome of the procedure.

The search for the most appropiate solution to perfom this submucosal injection is still a matter of debate, studies have been more focused on the capacity of the solution to elevate the mucosa and to maintain this elevation, ignoring some other important aspects of this solutions that may have and important role on the outcome of the procedure. Endoscopic resections are carried out using a ESU which applies an electrical current to perform the coagulation or cutting desired on the procedure; thus, studying the electrical related properties of the solutions is of great interest, and essential to prevent not only perforation but also the cautery effect on the intestinal wall, as electrical conductivity may vary according to the type of solution injected[59,62,64,67].

We have tested both comercial and non-comercial solutions to performe submucosal injection and we have tried to relate the electrical resistivity, viscosity and osmolarity of the solutions with clinical aspects that will have a impact of the clinical outcome, such as height and lasting of the elevation, time to perform EMR or temperature reached after EMR.

Resistivity is a property of a material that quatifies the opposition of said material to the flow of an electric current. Osmolarity is a value indicative of the osmotic pressure of a solution, with will determine how this solution will diffuse across a sempipermeable membrane (osmosis). Viscosity is often referred to as the thickness of a fluid, at a molecular level is a result of the interactionn betweenn the different molecules in a fluid and it will determine the energy needed to make a fluid flow. Previous studies related the electrical resistivity of blood to its viscosity, affected by the quantitiy of fibrinogen[60,61].

Our results showed a wide variability of trans-epithelial R after submucosal injection. Substances with high viscosity were associated with higher and maintained stable values of R (BB, PL and HA). These solutions have also higher protective effect against deep thermal injury and less cushion decrease. By contrast, solutions able to perform EMR at shorter time were GC, PRP and GS.

Statistical correlation study only showed a significant correlation between: resistivity of the solutions and the muscular temperature reached after EMR (-0.7851 p value 0.002, negative correlation, the higher the resistivity, the lower the temperature reached), resistivity of the solutions and the time to perform EMR (0.6938 p-value 0.042, positive correlation, the higher the resistivity, the longer to perfomr EMR) and between viscosity and the muscular temperature reached after EMR (-0.8740 p-value 0.003, negative correlation, the higher the viscosity the lower the temperature reached). The rest of correlations, altough not statistically significative, show a clear trend. For example, the risk of

thermal injury seems to be higher with higher osmolarity, and EMR time is higher with higher resistivity, viscosity annd osmolarity of the substance.

Our study was an attemp to explore electrical and rheological properties of different solutions used in EMR. An *ex vivo* model to study any organ phisiology has some drawbacks such as absence of perfusion and active absorption that in this case can mean a longer time for the submucosal fluid to resolve; anyway we tried to minimize this problem by using porcine stomachs within the first hour from the animal's death, which avoids significan tissue changes[134].

For this study we have tried to standarized all procedures as much as possible by using the same part of the stomach for each substance, creating a 2 mL submucosal cushion, appliying the same force at the polypectomy snare by using an automatic injector set and cutting the same ammount of stomach mucosal layer. These small-sized mucosal resections we performed do not usually require a submucosal injection clinically as lessions smaller than 2cm do not require submucosal injection for the EMR or if it is done, the solution used doesn't have much impact on the final outcome[67]. Anyway we prioritize the standarization of the lessions and the EMR technique for the better comparision of the results.

We also assume our small size sample and the lack of *in vivo* data as this is only a proof of concept research work in which we wanted to see a possible correlation or trend between the characteristics studied and thus, open the door for a future study more clinically representative.

Taking together all results comparing different submucosal injection solutions tested, we can say that HA, PL and BB were the best solutions with long-term protective effects (trans-epithelial R, lower thermal injury and less cushion descrease). Solutions with quicker resection time were GC, PRP and GS.

We have also shown that the use of endoscopic shielding technique with Covergel-Bibio, applied directly onto endoscopic induced mucosal lesions in the colon, is able to reduce the depth of thermal injury in two experimental models. In addition, endoscopic shielding technique with Covergel-Bibio has a protective effect for the appearance of delayed perforation and CS in rats. Previous reports in clinical practice have demonstrated that clipping closure[135] or sealing bowel defects with tissue adhesives[77] have achieved promising results in the prevention of delayed perforation by maintaining high mechanical strength; despite this, the use of clips sometimes is complex or is limited to lesions smaller than 40 mm^2 [135]. Tissue shielding method also has the disadvantage of being time consuming[76,77]. In this sense, sealing mucosal lesions with endoscopic applied chitosan hydrogel containing epidermal growth factor induced both, a significant reduction in mucosal resection-induced gastric ulcers in rabbits and pigs, and the appearance of deep scar formation and fibrotic submucosa in untreated lesions[136]. More recently, our group has assessed the utility of platelet-rich plasma applied onto colonic-induced lesions, showing strong healing properties in preclinical studies[137]. Our study suggests that carrying out endoscopic shielding technique with Covergel-Bibio, which is able to gellify over induced lesions after therapeutic endoscopy, is a quick (<5 min) and safe method to prevent complications secondary to deep thermal injuries. Covergel-Bibio has also proven effective in facilitating physiological healing of the wound. This characteristic is most likely given by two of the components, MC and HA. Both substances have antioxidant properties[138] and HA has a well-known antioxidant benefit that has been proven both *in vitro* and *in vivo*[139–142]. Besides this antioxidant properties, low-weight HA has also been linked to angiogenesis[143], increasing its wound healing properties. The duration of the adhesion to the affected area has not been calculated in this study, but it has proven to be sufficient to improve mucosal healing, promoting physiological tissue repair, and avoid perforation. The addition of a bioadhesive substance such as methylcellulose

has demonstrated its trophic and protective effect toward the mucosal layer of the intestine, preventing bacterial translocation in different experimental models, as we have demonstrated in previous work[144]. Finally, rifaximin is a low-absorbance, wide-spectrum antibiotic that has been used in several pathologies to clean the intestine. Giving rifaximin would ensure a lower rate of infection of the wounded area, reducing local inflammation and bacterial translocation, thereby facilitating the healing process in a faster way.

CS is a condition characterized by the development of fever, abnormal levels of inflammatory markers, and abdominal pain, with or without symptoms of peritoneal irritation, as has been described with the use of hot forceps biopsy in the right colon[145,146]. The incidence of CS ranges from 0.07% to 1.0% in patients submitted for polypectomy, being higher in ESD, where more frequent and repetitive electrocoagulation is needed, reaching an incidence of 7.1% in gastric lesions[146].

In our study, the application of Covergel-Bibio had a positive influence by reducing the depth of the thermal injury and preventing mortality and peritonitis. As a consequence of its biological and adhesion properties, it also improves mucosal restoration and the physiological healing process, avoiding mechanical damage and providing a safe and wet environment surrounding the affected area. Delayed perforation was observed in non-treated rats. Delayed bleeding was not observed in any case, and thus was not reported in the present study.

In the prevention of CS it is important to avoid high thermal load of the intestinal wall, optimizing the impedances of the tissue. In this sense, clinically injected solutions have high significant differences of specific impedances[59]. Furthermore, submucosal injection of Covergel-Bibio reduced thermal damage in the porcine model by maintaining a good elevation of the area to be resect.

Although endoscopic resection techniques are still improving, they are established techniques that have given endoscopy a therapeutic role. Nevertheless, endoscopy is still evolving, and new therapeutic tools need to be pursued.

Drug delivery directly to the colon is an option thanks to oral dosage formulations that are designed to achieve a controlled drug release. However, this controlled release has mainly been achieved with small molecules but not for macromolecules, such as mAb's[147]. Direct release in the colon is beneficial to prevent early absorption of the drug, thus increasing the quantity of drug reaching the target tissue and at the same time decreasing systemic exposure and associated side-effect[148]. A specific form of control drug release is polymer-based drug delivery. Polymers offer a wide range of possibilities useful for colonic delivery. This polymers can be triggered to start releasing drug by physiological characteristics of the healthy colon, as well as in different disease situations[147]. Hydrogels for drug delivery have also been studied for their capacity of mucoadhesion and controlled delivery.

In therapeutic endoscopy, first reports of hydrogels being used were focused on the treatment of ulcers after endoscopic resection. The most common options to treat ulcers and prevent bleeding are epinephrine injection, thermal coagulation, argon plasma coagulation or mechanical induction of coagulation using clips[149]. Later on, Maeng et al[136] reported a EGF-coating chitosan hydrogel capable of mucoadhesion that had a therapeutic efficacy for the treatment of GI ulcers. This hydrogel could be applied endoscopically and hemostatically treat ulcers, accelerating healing rate and preventing rebleeding.

This hydrogel went on to become EGF-endospray, a highly absorptive polysaccharide that can be applied to GI bleeding foci via an endoscope. When in contact with blood/gastric fluids, the EGF-endospray absorbs moisture and forms a bioadhesive hydrogel which acts as a mechanical barrier and

precipitates ulcer-healing. This was specially though to be used in ulcers on the upper GI due to their difficulty to be treated[150].

In this work, we have used Covergel to act as a drug delivery platform loaded with monoclonal antibodies, Covergel-Tribio, to treat two main colonic affectations, IBD and CRC.

Covergel-Tribio with IFX and VDZ were studied using an acute EC animal model. TNBS induces colitis has been proven as a valid method to elucidate different mechanisms underlying the mechanism of the disease[151]. Furthermore, and besides its limitations mimicking all different aspects of this complex disease, which are still unknown, this model is a great tool to study the immunopathogenesis of the disease and the potential benefit of different therapies[151].

Our results show that the simple application of Covergel-Tribio as a dressing on the inflamed tissue by means of endoscopic shielding technique improves the overall outcome and restoration of the mucosal layer. But when Covergel-Tribio is loaded with drugs that have proven efficacy treating this disease, the effect is even more pronounced. Endoscopically, mucosal improvement was obvious 4 days after treatment in all treatment groups. This was accompanied by different clinical aspects such as body weight loss, colon weight/length ratio or bacterial translocation to the liver, all features improved in the groups treated with Covergel alone or Covergel-Tribio, in combination with drugs.

Histologically, no differences were seen between treated groups and control group. This might be due to the scoring system which might not be the most appropriate one to use in this model, and because 4 days after treatment, improvements might be clear endoscopically but now at a histological level.

Zhang et al[152] reported a similar approach to treat IBD. They described an inflammation-targeting hydrogel based on ascorbyl palmitate loaded with Dexamethasone, which was applied as an enema and had the ability to adhere

to mucosa, specially inflamed mucosa. Their results were promising as histological score of overall mean colitis score, and other aspects such as colon weight or TNFα levels also improved in animals treated with the hydrogel loaded with dexamethasone[152]. Nevertheless, significant differences arise between his work and the work we present here. First of all, Covergel-Tribio was thought to be applied though endoscopy, in order to leverage the endoscopic procedures which IBD patients already have to undergo, instead of applying it as an enema with the associated welfare affectation. Furthermore, we believe that an endoscopic administration can be even more localized, focusing extensively on the inflamed mucosal sites, instead of affecting all colonic tissue. Zhang et al[152] study plan was as well slightly different as they used two different animal models (DSS and a genetically engineered model) none of them our animal model, they administered 2 rounds of treatment on days 1 and 3 and euthanasia was performed at day 5 after first treatment application. However, this study showed promising results, and they looked into important aspects such as mucosal adherence time, *in vivo* drug release and overall systemic drug affectation. These important features when studying a hydrogel were not all the way evaluated on our project, and further experiments need to be performed.

Moreover, another goal of our project was to improve one of the main problems associated with mAb's, which is the patient developing resistance to this kind of treatment. This resistance is caused by the formation of ADA's, as a response of the body to these exogenous complex proteins. The kind of mAb's most used in IBD, no matter their nature, cause to a greater or lesser degree ADA's formation[42]. Since new drug development is a complex and long-lasting effort, new therapeutic approaches are needed to reduce this risk, and allow patients to continue on a successful therapy longer.

The direct drug administration with Covergel-Tribio was able to significantly improve the disease outcome in an animal model using a much lower dose

than the intravenously applied dose. Because of this, we wanted to evaluate if the formation of ADA's specific to IFX was also reduced, compared with the traditional way of treatment application. In this case, we evaluated the formation of ATI's from a subcutaneous injection of 5mg/kg IFX vs Covergel-Tribio loaded with IFX 1mg/mL in an experimental model of chronic EC. We decided to use this model in order to mimic for a longer period of time the disease state, and thus be able to apply therapy four times instead of one. Our results showed that there were no significant differences on the outcome of the diseases between both ways of treatment application, except on colon weight/length ratio which was smaller on the s.c. treatment group. Apart from this, meaning that a lower dose is as effective when applied locally as the higher is in a systemic way in resolving the disease, the levels of ATI's were also evaluated. Here we did see a significant difference, being these levels lower on the group treated with Covergel-Tribio. These results confirmed our theory that a locally applied therapy at a lower dose is able to obtain a good clinical result and at the same time reduce adverse events and complications associated with the systemic application of a drug.

The formation of ADA's is a serious clinical event that leads to a loss of response in patients. This loss of response is thought to be by one of two mechanisms: increased clearance of mAb's or direct neutralization[42]. Different approaches have already been studied to reduce the levels of ADA's. Shormon *et al*[53] accompanied IFX therapy with a immunomodulator and found that patients with loss of response to IFX due to the creation of ATI's recovered effective drug levels because of the elimination of ATI's. This approach is an interesting result, but it means that patients must be treated with more drugs, increasing the risk of different adverse events and with a modulation of the immune system, with the risk associated to it.

Our approach, although preliminary and preclinical, could mean an improvement on the quality of life of patients. Taking advantage of the endoscopic procedures these patients undergo routinely to apply therapy at a

lower dose would shorten the time patients spend at the hospital and decrease the risk of toxicity and adverse event of drugs. Nevertheless, this is a very preclinical study, and further research needs to be pursued, both preclinical and of course, clinical, in order to safely evaluate and introduce this technique as a standard treatment and increase the pool of therapeutic interventions to treat IBD patients.

Following the same purpose of administering local therapy and reducing adverse events of systemic drug exposure, we addressed another typical disease already treated with endoscopy, colorectal cancer. We evaluated the feasibility of intratumoral injection of Covergel-Tribio loaded with different drugs as a technique to administer drugs.

For this we used the AOM animal model of CRC. We tested intratumoral injection of Covergel-Tribio with five different drug combinations. Two anti-VEGFR (Aflibercept and Bevacizumab), two anti-EGFR (Panitumumab and Cetuximab) all in combination with a chemotherapeutic agent, Irinotecan, and also the latter alone. Out of these five combinations, only one clearly acquired tumor size reduction and necrosis, the combination of Aflibercept with Irinotecan. This finds an explanation if we look into the study design. Since we were testing just a new way to apply therapy, we decided to try therapies that had proven successful treating CRC, and we choose these combinations with the help of an oncologist. Irinotecan is a topoisomerase I inhibitor which normally is administered intravenously, where it reaches the blood and arrives to the liver, place where it is metabolized into its active form, SN-38. We can guess then, that local administration of Irinotecan with our hydrogel, alone or in combination of other anticancer drugs like mAb's, is not effective since the amount of irinotecan that will arrive to the liver to be metabolized seems really low, and not enough for it to affect the tumor.

Anti-EGFR treatments have proven effective when administered alone or in combination with chemotherapy in treating advance CRC. However, only

about 10% of patients seems to respond to this kind of therapy. This is explained because mutations in the KRAS gene are associated with resistance to anti-EGFR drugs[154]. Interestingly, one of the most common characteristics in the AOM induced CRC animal model are mutations in the KRAS gene, which evolve into aberrant crypt foci and later on, adenocarcinoma[155]. This is a simple explanation of the failure of these two treatments on our study.

Anti-VEGFR treatments tested produced both necrosis and tumor size reduction, although aflibercept was clearly more efficient than bevacizumab. Aflibercept binds to different molecules activating VEGFR (VEGF-A, -B and placental growth factor) whereas bevacizumab only binds to VEGF-A. Aflibercept has proven more efficient than bevacizumab before, in patient derived xenograft models of CRC[156].

We have confirmed the feasibility of intratumoral injection of Covergel-Tribio loaded with antitumoral drugs as an efficient way to produce tumor size reduction and necrosis. This opens the possibility to administer drugs during endoscopic procedures, reduce the systemic exposure to these harmful drugs and improve patient's quality of life. Nevertheless, this technique needs to be further studied and improved before being able to be done in humans. This study as a proof of concept has proven successful but clear limitations such as animal model, drugs used, and low number of animals are present and need to be addressed.

CONCLUSIONS

1. Covergel is a novel biocompatible and bioadhesive hydrogel capable of being administered endoscopically throughout the digestive system, that presents the following properties:
    - A well-defined microstructure of a super-porous type hydrogel, showing the ability to absorb and liberate molecules.
    - Suitable viscosity and thermoreversible properties permitting mucoadhesion when in contact with tissue.
    - Irreversible gelation can be acquired with the addition of a photoinitiator and the exposure to UV light.
    - Resistance to colonic bacterial degradation and broad pH values.

2. Covergel-Bibio is able to prevent deep thermal injury when resection techniques are performed.
    - Endoscopic shielding technique with Covergel-Bibio is effective promoting physiological wound healing of eschars after endoscopic resection techniques and prevent adverse events (perforation and bleeding).
    - Covergel-Bibio when used as a submucosal injection solution shows long-term protective effects such as high trans-epithelial resistivity, high thermal protection and low cushion decrease.

3. Covergel-Tribio as a drug-delivery platform shows clinical efficacy in CRC and EC animal models.
    - Intratumoral injection of Covergel-Tribio with Aflibercept is a feasible technique to treat colorectal cancer lesions in a preclinical model of Azoxymethane induced colorectal cancer.
    - Endoscopic shielding technique using Covergel-Tribio with Infliximab or Vedolizumab is able to improve the outcome of colonic inflammation in an animal model of experimental colitis.

- The lower dose of drugs used in Covergel-Tribio is useful in reducing the formation of anti-drug antibodies while resolving the disease in a similar fashion as the standard way of treatment.

4. Covergel, with all its possible modifications, has proven effective in solving some of the unmet needs of endoscopy, while also providing some new therapeutic tools such as direct drug administration.

FUTURE PERSPECTIVES

Our results have open and stablished a new research strategy within the endoscopy unit in the Health Research Institute Germans Trias i Pujol.

Having obtained promising results in the improvement of resection techniques when using Covergel-Bibio, we aim to start clinical studies with Covergel-Bibio as a submucosal injection solution and as a coverage agent in endoscopic shielding technique after routine EMR. Two patents have been developed out of this project: PCT/EP2016/053928 (Covergel-Bibio) which has entered national phases in 08/2017 and PCT/EP2017/068876 (Covergerl-Tribio) which has entered national phases in 01/2019.

There are still some complications endoscopy fails to address, such as strictures. This is why we also aim to apply for another Spanish government project to continue with this research strategy, prototyping stents produced with our hydrogel by irreversible gelation, or recovered on it, in order to treat malignant stenosis produced in the colon. The introduction of living cells inside our hydrogel is also another goal for us to increase mucosal healing in large mucosal defects. Being able to apply cell therapy though endoscopy and better address mucosal defects could increase the limited size lesion manageable nowadays.

This project also offers us great opportunities in collaboration with other research facilities. Covergel project was awarded with the 1st prize in the FIPSE-MIT Innovation Program 2018 and CaixaImpulse 2018. This great recognition will give us the access to work with international groups leading the field of medical devices and hydrogels.

BIBLIOGRAPHY

1.   Kevin T Patton, G. T. *Anatomy & Physiology.* (2003).

2.   Fiser, S. M. *The ABSITE Review.* (2004).

3.   Annemarie Brüel, Erik Ilsø Christensen, Jørgen Tranum-Jensen, K. Q. & Geneser, F. *Histología.* (2015).

4.   Humphries, A. & Wright, N. A. Colonic crypt organization and tumorigenesis. *Nat. Rev. Cancer* **8,** 415–424 (2008).

5.   Lindstrom, C. G., Rosengren, J. & Fork, F. COLON OF THE RAT An anatomic , histologic and radiographic investigation. **20,** 523–536 (1974).

6.   Bartolí, R., Boix, J., Òdena, G., Ossa, N. D. De & Vega, V. M. De. Colonoscopy in rats : An endoscopic , histological and tomographic study. **5,** 226–230 (2013).

7.   Pomerri, F. *et al.* Microradiographic Anatomy of the Explanted Rat Colon. **1851,** 210–214 (2010).

8.   Robert, M. E. *et al.* Morphology of isolated colonic crypts. *Cells Tissues Organs* **168,** 246–251 (2001).

9.   Ponder, B. A. et al. Derivation of mouse intestinal crypts from single progenitor cells. *Nature* **313,** 689–691 (1985).

10.   Medema, J. P. & Vermeulen, L. Microenvironmental regulation of stem cells in intestinal homeostasis and cancer. *Nature* **474,** 318–326 (2011).

11.   Kosinski, C. *et al.* Gene expression patterns of human colon tops and basal crypts BMP antagonists as intestinal stem cell niche factors. *PNAS* **104,** 15418–15423 (2007).

12.   van der Wath, R. C., Gardiner, B. S., Burgess, A. W. & Smith, D. W. Cell Organisation in the Colonic Crypt: A Theoretical Comparison of the Pedigree and Niche Concepts. *PLoS One* **8,** (2013).

13.   Karrasch, T. & Jobin, C. Wound healing responses at the gastrointestinal epithelium: A close look at novel regulatory factors and investigative approaches. *Z. Gastroenterol.* **47,** 1221–1229 (2009).

14.   Turner, J. R. Intestinal mucosal barrier function in health and disease. *Nat. Rev. Immunol.* **9,** 799–809 (2009).

15.   Rieder, F., Brenmoehl, J., Leeb, S., Schölmerich, J. & Rogler, G. Wound healing and fibrosis in intestinal disease. *Gut* **56,** 130–139 (2007).

16.   Wallace, H. A. & Bhimji, S. S. Wound Healing Phases. *StatPearls publishing* (2018).

17.   Florholmen, J. Mucosal healing in the era of biologic agents in

treatment of inflammatory bowel disease. *Scand. J. Gastroenterol.* **50,** 43–52 (2015).

18. *Colorectal cancer Source: Globocan 2018 Number of new cases in 2018, both sexes, all ages.* (2018).

19. Brenner, H., Kloor, M. & Pox, C. P. Colorectal cancer. *Lancet* **383,** 1490–1502 (2014).

20. American Cancer Society. *Colorectal Cancer. Facts & Figures 2017-2019.* (2017).

21. Malvezzi, M. *et al.* European cancer mortality predictions for the year 2018 with focus on colorectal cancer. *Ann. Oncol.* **29,** 1016–1022 (2018).

22. Cox, Adrienne D, Der, C. J. Ras history. The saga continues. *Small GTPases* **1,** 2–27 (2010).

23. Sobin LH, Gospodarowicz M, W. C. *TNM classification of malignant tumours.* (NEw York; Wiley-Blackwell., 2009).

24. Al-Sohaily, S., Biankin, A., Leong, R., Kohonen-Corish, M. & Warusavitarne, J. Molecular pathways in colorectal cancer. *J. Gastroenterol. Hepatol.* **27,** 1423–1431 (2012).

25. Colussi, D., Brandi, G., Bazzoli, F. & Ricciardiello, L. Molecular pathways involved in colorectal cancer: implications for disease behavior and prevention. *Int. J. Mol. Sci.* **14,** 16365–85 (2013).

26. Mundade, R., Imperiale, T. F., Prabhu, L., Loehrer, P. J. & Lu, T. Genetic pathways, prevention, and treatment of sporadic colorectal cancer. *Oncoscience* **1,** 400 (2014).

27. Golovko, D., Kedrin, D., Yilmaz, O. H. & Roper, J. Review: US Spelling Colorectal cancer models for novel drug discovery HHS Public Access. *Expert Opin Drug Discov* **10,** 1217–1229 (2015).

28. Clarke, K. & Chintanaboina, J. Allergic and Immunologic Perspectives of Inflammatory Bowel Disease. *Clin. Rev. Allergy Immunol.* (2018). doi:10.1007/s12016-018-8690-3

29. Clark, C. & Turner, J. Diagnostic Modalities for Inflammatory Bowel Disease. Serologic Markers and Endoscopy. *Surg. Clin. North Am.* **95,** 1123–1141 (2015).

30. Dignass, A. *et al.* Second European evidence-based consensus on the diagnosis and management of ulcerative colitis Part 1: Definitions and diagnosis. *J. Crohn's Colitis* **6,** 965–990 (2012).

31. Baumgart, D. C. & Sandborn, W. J. Crohn's disease. *Lancet* **380,** 1590–1605 (2012).

32.   Cabré, E. *et al.* Phenotypic concordance in familial inflammatory bowel disease (IBD). Results of a nationwide IBD Spanish database. *J. Crohn's Colitis* **8,** 654–661 (2014).

33.   DeRoche, T. C., Xiao, S.-Y. & Liu, X. Histological evaluation in ulcerative colitis. *Gastroenterol. Rep.* **2,** 178–192 (2014).

34.   Ungaro, R., Mehandru, S., Allen, P. B., Peyrin-Biroulet, L. & Colombel, J. F. Ulcerative colitis. *Lancet* **389,** 1756–1770 (2017).

35.   Xavier, R. J. & Podolsky, D. K. Unravelling the pathogenesis of inflammatory bowel disease. *Nature* **448,** 427–434 (2007).

36.   Strober, W., Kitani, A., Fuss, I., Asano, N. & Watanabe, T. The molecular basis of NOD2 susceptibility mutations in Crohn's disease. *Mucosal Immunol.* **1 Suppl 1,** S5-9 (2008).

37.   Coskun, M. Intestinal epithelium in inflammatory bowel disease. *Front. Med.* **1,** 24 (2014).

38.   Baumgart, D. C. & Carding, S. R. Inflammatory bowel disease: cause and immunobiology. *Lancet* **369,** 1627–1640 (2007).

39.   Baumgart, D. C. & Sandborn, W. J. Inflammatory bowel disease: clinical aspects and established and evolving therapies. *Lancet* **369,** 1641–1657 (2007).

40.   Rousseaux, C. *et al.* Intestinal antiinflammatory effect of 5-aminosalicylic acid is dependent on peroxisome proliferator–activated receptor-γ. *J. Exp. Med.* **201,** 1205–1215 (2005).

41.   Rawla, P., Sunkara, T. & Raj, J. P. Role of biologics and biosimilars in inflammatory bowel disease: Current trends and future perspectives. *J. Inflamm. Res.* **11,** 215–226 (2018).

42.   Vermeire, S., Gils, A., Accossato, P., Lula, S. & Marren, A. Immunogenicity of biologics in inflammatory bowel disease. *Therap. Adv. Gastroenterol.* **11,** 1756283X1775035 (2018).

43.   Vande Casteele, N. *et al.* The relationship between infliximab concentrations, antibodies to infliximab and disease activity in Crohn's disease. *Gut* **64,** 1539–1545 (2015).

44.   Mizoguchi, A. Animal Models of Inflammatory Bowel Disease. in 263–320 (2012). doi:10.1016/B978-0-12-394596-9.00009-3

45.   Kolios, G. Animal models of inflammatory bowel disease: how usefull are they really? *Curr. Opin. Gastroenterol.* **32,** 251–257 (2016).

46.   Schmidt, A., Meier, B. & Caca, K. Endoscopic full-thickness resection: Current status. *World J. Gastroenterol.* **21,** 9273–9285 (2015).

47.   Paper, W. ASGE/SAGES working group on Natural Orifice

Translumenal Endoscopic Surgery: White Paper October 2005. *Gastrointest. Endosc.* **63,** 199–203 (2006).

48. Fisher, D. A. *et al.* Complications of colonoscopy. *Gastrointest. Endosc.* **74,** 745–752 (2011).

49. Tutticci, N. & Bourke, M. J. Advanced endoscopic resection in the colon: recent innovations, current limitations and future directions. *Expert Rev. Gastroenterol. Hepatol.* **8,** 161–177 (2014).

50. Inoue, H. *et al.* Endoscopic mucosal resection, endoscopic submucosal dissection, and beyond: Full-layer resection for gastric cancer with nonexposure technique (CLEAN-NET). *Surg. Oncol. Clin. N. Am.* **21,** 129–140 (2012).

51. Tanaka, S. *et al.* JGES guidelines for colorectal endoscopic submucosal dissection/endoscopic mucosal resection. *Dig. Endosc.* **27,** 417–434 (2015).

52. Dekker, E. & Rex, D. K. Advances in CRC Prevention: Screening and Surveillance. *Gastroenterology* **154,** 1970–1984 (2018).

53. Kim, H. S. *et al.* Risk factors for immediate postpolypectomy bleeding of the colon: A multicenter study. *Am. J. Gastroenterol.* **101,** 1333–1341 (2006).

54. Burgess, N. G. *et al.* Risk Factors for Intraprocedural and Clinically Significant Delayed Bleeding After Wide-field Endoscopic Mucosal Resection of Large Colonic Lesions. *Clin. Gastroenterol. Hepatol.* **12,** 651–661.e3 (2014).

55. Panteris, V., Haringsma, J. & Kuipers, E. J. Colonoscopy perforation rate, mechanisms and outcome: From diagnostic to therapeutic colonoscopy. *Endoscopy* **41,** 941–951 (2009).

56. Shioji, K. *et al.* Prophylactic clip application does not decrease delayed bleeding after colonoscopic polypectomy. *Gastrointest. Endosc.* **57,** 691–694 (2003).

57. Kingo Hirasawa, Chiko Sato, Makomo Makazu, Hiroaki Kaneko, Ryosuke Kobayashi, Atsushi Kowaka, S. M. Coagulation syndrome: Delayed perforation after colorectal endoscopic treatments. *World J. Gastroenterol.* **7,** 1055–1061 (2015).

58. Polymeros, D. *et al.* Comparative performance of novel solutions for submucosal injection in porcine stomachs: An ex vivo study. *Dig. Liver Dis.* **42,** 226–229 (2010).

59. Park, S. *et al.* Electrical characteristics of various submucosal injection fluids for endoscopic mucosal resection. *Dig. Dis. Sci.* **53,** 1678–1682 (2008).

60. Pop GA, de Backer TL, de Jong M, Struijk PC, Moraru L, Chang Z, Goovaerts HG, Slager CJ, B. A. On-Line Electrical Impedance Measurement for Monitoring Blood Viscosity during On-Pump Heart Surgery. *Eur Surg Res* **36,** 259–265 (2004).

61. Zhao, T. X. & Jacobson, B. Quantitative correlations among fibrinogen concentration, sedimentation rate and electrical impedance of blood. *Med. Biol. Eng. Comput.* **35,** 181–185 (1997).

62. Huai, Z. Y., Feng Xian, W., Chang Jiang, L. & Xi Chen, W. Submucosal Injection Solution for Endoscopic Resection in Gastrointestinal Tract: A Traditional and Network Meta-Analysis. *Gastroenterol. Res. Pract.* **2015,** (2015).

63. Uraoka, T., Saito, Y., Yamamoto, K. & Fujii, T. Submucosal injection solution for gastrointestinal tract endoscopic mucosal resection and endoscopic submucosal dissection. *Drug Des. Devel. Ther.* 131–138 (2008). doi:10.2147/DDDT.S3219

64. Fujishiro, M. *et al.* Tissue damage of different submucosal injection solutions for EMR. *Gastrointest. Endosc.* **62,** 933–942 (2005).

65. Ferreira, A., Moleiro, J., Torres, J. & Dinis-Ribeiro, M. Solutions for submucosal injection in endoscopic resection: a systematic review and meta-analysis. *Endosc. Int. Open* **04,** E1–E16 (2015).

66. Jung, Y. S. & Park, D. Il. Submucosal injection solutions for endoscopic mucosal resection and endoscopic submucosal dissection of gastrointestinal neoplasms. *Gastrointest. Interv.* **2,** 73–77 (2013).

67. Yandrapu, H. *et al.* Normal saline solution versus other viscous solutions for submucosal injection during endoscopic mucosal resection: a systematic review and meta-analysis. *Gastrointest. Endosc.* **85,** 693–699 (2017).

68. Uraoka, T. *et al.* Effectiveness of glycerol as a submucosal injection for EMR. *Gastrointest. Endosc.* **61,** 736–40 (2005).

69. Lee, S.-H. *et al.* A new method of EMR: submucosal injection of a fibrinogen mixture. *Gastrointest. Endosc.* **59,** 220–4 (2004).

70. Lee, S.-H. *et al.* Clinical efficacy of EMR with submucosal injection of a fibrinogen mixture: a prospective randomized trial. *Gastrointest. Endosc.* **64,** 691–6 (2006).

71. Hyun, J. J. *et al.* Comparison of the characteristics of submucosal injection solutions used in endoscopic mucosal resection. *Scand. J. Gastroenterol.* **41,** 488–92 (2006).

72. Fujishiro, M. *et al.* Comparison of various submucosal injection solutions for maintaining mucosal elevation during endoscopic mucosal resection. *Endoscopy* **36,** 579–83 (2004).

73. Burns, J. W., Colt, M. J., Burgees, L. S. & Skinner, K. C. Preclinical evaluation of Seprafilm bioresorbable membrane. *Eur. J. Surg. Suppl.* 40–8 (1997).

74. Bon, I., Bartoli, R. & Lorenzo-Zúniga, V. Endoscopic shielding technique, a new method in therapeutic endoscopy. *World J. Gastroenterol.* **23,** 3761–3764 (2017).

75. Maeng, J. H. *et al.* Endoscopic application of EGF-chitosan hydrogel for precipitated healing of GI peptic ulcers and mucosectomy-induced ulcers. *J. Mater. Sci. Mater. Med.* **25,** 573–582 (2014).

76. Takimoto, K., Toyonaga, T. & Matsuyama, K. Endoscopic tissue shielding to prevent delayed perforation associated with endoscopic submucosal dissection for duodenal neoplasms. *Endoscopy* **44,** E414–E415 (2012).

77. Tsuji, Y. *et al.* Endoscopic tissue shielding method with polyglycolic acid sheets and fibrin glue to cover wounds after colorectal endoscopic submucosal dissection (with video). *Gastrointest. Endosc.* **79,** 151–5 (2014).

78. Hiroyuki, T. *et al.* A basic study of the effect of the shielding method with polyglycolic acid fabric and fibrin glue after endoscopic submucosal dissection. *Endosc. Int. open* **4,** E1298–E1304 (2016).

79. Takao, T. *et al.* Tissue shielding with polyglycolic acid sheets and fibrin glue on ulcers induced by endoscopic submucosal dissection in a porcine model. *Endosc. Int. open* **3,** E146-51 (2015).

80. Fisher, D. A. *et al.* Role of endoscopy in the staging and management of colorectal cancer. *Gastrointest. Endosc.* **78,** 8–12 (2013).

81. Brooker, J. C. *et al.* Treatment with argon plasma coagulation reduces recurrence after piecemeal resection of large sessile colonic polyps: a randomized trial and recommendations. *Gastrointest. Endosc.* **55,** 371–5 (2002).

82. Jacob, B. J., Moineddin, R., Sutradhar, R., Baxter, N. N. & Urbach, D. R. Effect of colonoscopy on colorectal cancer incidence and mortality: an instrumental variable analysis. (2012). doi:10.1016/j.gie.2012.03.247

83. Shergill, A. K. *et al.* The role of endoscopy in inflammatory bowel disease. *Gastrointest. Endosc.* **81,** 1101–1121.e13 (2015).

84. Terheggen, G. *et al.* Safety, feasibility, and tolerability of ileocolonoscopy in inflammatory bowel disease. *Endoscopy* **40,** 656–663 (2008).

85. Cellier, C. *et al.* Correlations between clinical activity, endoscopic severity, and biological parameters in colonic or ileocolonic Crohn's disease. A prospective multicentre study of 121 cases. The Groupe

d'Etudes Therapeutiques des Affections Inflammatoires Digestives. *Gut* **35,** 231–235 (1994).

86. Eliakim, R. & Magro, F. Imaging techniques in IBD and their role in follow-up and surveillance. *Nat. Rev. Gastroenterol. Hepatol.* **11,** 722–736 (2014).

87. Dionisio, P. M. *et al.* Capsule endoscopy has a significantly higher diagnostic yield in patients with suspected and established small-bowel crohn's disease: A meta-analysis. *Am. J. Gastroenterol.* **105,** 1240–1248 (2010).

88. Annese, V. *et al.* European evidence based consensus for endoscopy in inflammatory bowel disease. *J. Crohn's Colitis* **7,** 982–1018 (2013).

89. Leighton, J. A. *et al.* ASGE guideline: Endoscopy in the diagnosis and treatment of inflammatory bowel disease. *Gastrointest. Endosc.* **63,** 558–565 (2006).

90. Tharian, B., George, N. & Navaneethan, U. Endoscopy in the diagnosis and management of complications of inflammatory bowel disease. *Inflamm. Bowel Dis.* **22,** 1184–1197 (2016).

91. Ferreira, J. *et al.* Prevalence and lifetime risk of endoscopy-related complications among patients with inflammatory bowel disease. *Clin. Gastroenterol. Hepatol.* **11,** 1288–1293 (2013).

92. Mazzuoli, S. *et al.* Definition and evaluation of mucosal healing in clinical practice. *Dig. Liver Dis.* **45,** 969–977 (2013).

93. Samuel, S. *et al.* Validation of the Ulcerative Colitis Colonoscopic Index of Severity and Its Correlation With Disease Activity Measures. *Clin. Gastroenterol. Hepatol.* **11,** 49–54.e1 (2013).

94. Mary, J. Y. & Modigliani, R. Development and validation of an endoscopic index of the severity for Crohn's disease: a prospective multicentre study. Groupe d'Etudes Thérapeutiques des Affections Inflammatoires du Tube Digestif (GETAID). *Gut* **30,** 983–9 (1989).

95. Hoffman, A. S. Hydrogels for biomedical applications ✩. *Adv. Drug Deliv. Rev.* **64,** 18–23 (2012).

96. Buwalda, S. J. *et al.* Hydrogels in a historical perspective : From simple networks to smart materials. *J. Control. Release* **190,** 254–273 (2014).

97. Ahmed, E. M. Hydrogel : Preparation , characterization , and applications : A review. *J. Adv. Res.* **6,** 105–121 (2015).

98. Varaprasad, K., Malegowd, G., Jayaramudu, T., Mohan, M. & Sadiku, R. A mini review on hydrogels classi fi cation and recent developments in miscellaneous applications. *Mater. Sci. Eng. C* **79,** 958–971 (2017).

99. Bemmelen, J. M. Van. Der Hydrogel und das kristallinische Hydrat des Kupferoxydes. *Z. Anorg. Chem* **5,** 466 (1894).

100. O. Wichterle, D. L. Hydrophilic gels for biological use. *Nature* **185,** 117–118 (1960).

101. Kamata, H., Li, X., Chung, U. & Sakai, T. Design of Hydrogels for Biomedical Applications. 2360–2374 (2015). doi:10.1002/adhm.201500076

102. Pal, K. & Paulson, A. T. *Delivery Systems.* (2009). doi:10.1016/B978-0-12-374195-0.00016-1

103. Almond, A. Hyaluronan. *Cell. Mol. Life Sci.* **64,** 1591–1596 (2007).

104. Neuman, M. G., Nanau, R. M., Oruña-Sanchez, L. & Coto, G. Hyaluronic acid and wound healing. *J. Pharm. Pharm. Sci.* **18,** 53–60 (2015).

105. Jooybar, E. *et al.* An injectable platelet lysate-hyaluronic acid hydrogel supports cellular activities and induces chondrogenesis of encapsulated mesenchymal stem cells. *Acta Biomater.* (2018). doi:10.1016/j.actbio.2018.10.031

106. Silva Garcia, J. M., Panitch, A. & Calve, S. Functionalization of hyaluronic acid hydrogels with ECM-derived peptides to control myoblast behavior. *Acta Biomater.* (2018). doi:10.1016/j.actbio.2018.11.030

107. Tabasum, S. *et al.* Glycoproteins functionalized natural and synthetic polymers for prospective biomedical applications: A review. *Int. J. Biol. Macromol.* **98,** 748–776 (2017).

108. Gupta, D., Tator, C. H. & Shoichet, M. S. Fast-gelling injectable blend of hyaluronan and methylcellulose for intrathecal, localized delivery to the injured spinal cord. *Biomaterials* **27,** 2370–2379 (2006).

109. Caicco, M. J. *et al.* Characterization of hyaluronan-methylcellulose hydrogels for cell delivery to the injured spinal cord. *J. Biomed. Mater. Res. - Part A* **101 A,** 1472–1477 (2013).

110. Moore, T., Croy, S., Mallapragada, S. & Pandit, N. Experimental investigation and mathematical modeling of Pluronic(®) F127 gel dissolution: Drug release in stirred systems. *J. Control. Release* **67,** 191–202 (2000).

111. DASH, S., MURTHY, P. N., NATH, L. & CHOWDHURY, P. KINETIC MODELING ON DRUG RELEASE FROM CONTROLLED DRUG DELIVERY SYSTEMS. *Acta Pol. Pharm. ñ Drug Res.* **67,** 217–223 (2010).

112. Li, X. *et al.* Cytotoxicity and biocompatibility evaluation of N,O-

carboxymethyl chitosan/oxidized alginate hydrogel for drug delivery application. *Int. J. Biol. Macromol.* **50,** 1299–1305 (2012).

113.   Lorenzo-Zúñiga, V. *et al.* Microperforation of the colon: animal model in rats to reproduce mucosal thermal damage. *J. Surg. Res.* **188,** 415–418 (2014).

114.   Erben, U. *et al.* A guide to histomorphological evaluation of intestinal inflammation in mouse models. *Int. J. Clin. Exp. Pathol.* **7,** 4557–4576 (2014).

115.   Imaeda, H., Andoh, A. & Fujiyama, Y. Development of a new immunoassay for the accurate determination of anti-infliximab antibodies in inflammatory bowel disease. *J. Gastroenterol.* **47,** 136–43 (2012).

116.   Tam, R. Y., Cooke, M. J. & Shoichet, M. S. A covalently modified hydrogel blend of hyaluronan-methyl cellulose with peptides and growth factors influences neural stem/progenitor cell fate. *J. Mater. Chem.* **22,** 19402–19411 (2012).

117.   Law, N. *et al.* Characterisation of hyaluronic acid methylcellulose hydrogels for 3D bioprinting. *J. Mech. Behav. Biomed. Mater.* **77,** 389–399 (2018).

118.   Diniz, I. M. A. *et al.* Pluronic F-127 hydrogel as a promising scaffold for encapsulation of dental-derived mesenchymal stem cells. *J. Mater. Sci. Mater. Med.* **26,** 153 (2015).

119.   Khutoryanskiy, V. V. Advances in Mucoadhesion and Mucoadhesive Polymers. *Macromol. Biosci.* **11,** 748–764 (2011).

120.   Jiang, G., Sun, J. & Ding, F. PEG-g-chitosan thermosensitive hydrogel for implant drug delivery: cytotoxicity, *in vivo* degradation and drug release. *J. Biomater. Sci. Polym. Ed.* **25,** 241–256 (2014).

121.   Ganji, Samira Fariba; Vasheghani-Farahani, S. E. & Vasheghani-Farahani. Theoretical Description of Hydrogel Swelling: A Review. *Iran. Polym. J.* **19,** 75–398 (2010).

122.   Jin, R. *et al.* Injectable chitosan-based hydrogels for cartilage tissue engineering. *Biomaterials* **30,** 2544–2551 (2009).

123.   Oh, S. H., Kim, T. H. & Lee, J. H. Creating growth factor gradients in three dimensional porous matrix by centrifugation and surface immobilization. *Biomaterials* **32,** 8254–60 (2011).

124.   Cohn, D., Sosnik, A. & Levy, A. Improved reverse thermo-responsive polymeric systems. *Biomaterials* **24,** 3707–14 (2003).

125.   Sosnik, A. & Cohn, D. Ethoxysilane-capped PEO-PPO-PEO triblocks: a new family of reverse thermo-responsive polymers.

Biomaterials **25,** 2851–8 (2004).

126. Vincent, T., Jourdan, M., Sy, M.-S., Klein, B. & Mechti, N. Hyaluronic Acid Induces Survival and Proliferation of Human Myeloma Cells through an Interleukin-6-mediated Pathway Involving the Phosphorylation of Retinoblastoma Protein. *J. Biol. Chem.* **276,** 14728–14736 (2001).

127. Matsui, Y. *et al.* Hyaluronic acid stimulates tumor-cell proliferation at wound sites. *Gastrointest. Endosc.* **60,** 539–543 (2004).

128. Murakami, T. *et al.* Hyaluronic acid promotes proliferation and migration of human meniscus cells via a CD44-dependent mechanism. *Connect. Tissue Res.* 1–11 (2018). doi:10.1080/03008207.2018.1465053

129. Moraima Morales-Cruz, C. M. F. & Jean C Fernández, B. N. S. Induction of Cancer Cell Death by Hyaluronic Acid-Mediated Uptake of Cytochrome C. *J. Nanomed. Nanotechnol.* **06,** (2015).

130. *Guidance for Industry Nonclinical Studies for the Safety Evaluation of Pharmaceutical Excipients.* (2005).

131. Weber, M. *et al.* Blood-Contacting Biomaterials: In Vitro Evaluation of the Hemocompatibility. *Front. Bioeng. Biotechnol.* **6,** 99 (2018).

132. Molinaro, G., Leroux, J.-C., Damas, J. & Adam, A. Biocompatibility of thermosensitive chitosan-based hydrogels: an in vivo experimental approach to injectable biomaterials. *Biomaterials* **23,** 2717–22 (2002).

133. Sun, J., Jiang, G., Wang, Y. & Ding, F. Thermosensitive chitosan hydrogel for implantable drug delivery: Blending PVA to mitigate body response and promote bioavailability. *J. Appl. Polym. Sci.* **125,** 2092–2101 (2012).

134. Søndenaa, K. & Kjellevold, K. H. A prospective study of the length of the distal margin after low anterior resection for rectal cancer. *Int. J. Colorectal Dis.* **5,** 103–5 (1990).

135. Zhang, Q.-S., Han, B., Xu, J.-H., Gao, P. & Shen, Y.-C. Clip closure of defect after endoscopic resection in patients with larger colorectal tumors decreased the adverse events. *Gastrointest. Endosc.* **82,** 904–909 (2015).

136. Maeng, J. H. *et al.* Endoscopic application of EGF-chitosan hydrogel for precipitated healing of GI peptic ulcers and mucosectomy-induced ulcers. *J. Mater. Sci. Mater. Med.* **25,** 573–82 (2014).

137. Lorenzo-Zuniga, V. *et al.* Efficacy of platelet-rich plasma as a shielding technique after endoscopic mucosal resection in rat and porcine models. *Endosc Int Open* **4,** E859-64 (2016).

138. Moseley, R. *et al.* Comparison of the antioxidant properties of HYAFF-

11p75, AQUACEL and hyaluronan towards reactive oxygen species in vitro. *Biomaterials* **23,** 2255–64 (2002).

139. Sheehan, K. M., DeLott, L. B., Day, S. M. & DeHeer, D. H. Hyalgan has a dose-dependent differential effect on macrophage proliferation and cell death. *J. Orthop. Res.* **21,** 744–51 (2003).

140. Dougados, M. Sodium hyaluronate therapy in osteoarthritis: arguments for a potential beneficial structural effect. *Semin. Arthritis Rheum.* **30,** 19–25 (2000).

141. Roth, A. *et al.* Intra-articular injections of high-molecular-weight hyaluronic acid have biphasic effects on joint inflammation and destruction in rat antigen-induced arthritis. *Arthritis Res. Ther.* **7,** R677-86 (2005).

142. Cabrera, P. V *et al.* CD44 and hyaluronic acid regulate in vivo iNOS expression and metalloproteinase activity in murine air-pouch inflammation. *Inflamm. Res.* **53,** 556–66 (2004).

143. Chen, W. Y. & Abatangelo, G. Functions of hyaluronan in wound repair. *Wound Repair Regen.* **7,** 79–89

144. Bartolí, R. *et al.* Effect of the administration of fermentable and non-fermentable dietary fibre on intestinal bacterial translocation in ascitic cirrhotic rats. *Clin. Nutr.* **26,** 383–387 (2007).

145. Metz, A. J. *et al.* A blinded comparison of the safety and efficacy of hot biopsy forceps electrocauterization and conventional snare polypectomy for diminutive colonic polypectomy in a porcine model. *Gastrointest. Endosc.* **77,** 484–490 (2013).

146. Lee, H. *et al.* Clinical features and predictive factors of coagulation syndrome after endoscopic submucosal dissection for early gastric neoplasm. *Gastric Cancer* **15,** 83–90 (2012).

147. Patel, M. M. Cutting-edge technologies in colon-targeted drug delivery systems. *Expert Opin. Drug Deliv.* **8,** 1247–1258 (2011).

148. Bak, A., Ashford, M. & Brayden, D. J. Local delivery of macromolecules to treat diseases associated with the colon. *Adv. Drug Deliv. Rev.* **136–137,** 2–27 (2018).

149. Leung Ki, E.-L. & Lau, J. Y. W. New endoscopic hemostasis methods. *Clin. Endosc.* **45,** 224–9 (2012).

150. Bang, Byoung Wook, Jin Hee Maeng, Min-Kyoung Kim, Don Haeng Lee, S.-G. Y. Hemostatic action of EGF-endospray on mucosectomy-induced ulcer bleeding animal models. *Biomed. Mater. Eng.* **25,** (2015).

151. Antoniou, E. *et al.* The TNBS-induced colitis animal model: An overview. (2016). doi:10.1016/j.amsu.2016.07.019

152. Sufeng Zhang, Joerg Ermann, Marc D. Succi, Allen Zhou, M. J., Hamilton, Bonnie Cao, Joshua R. Korzenik, Jonathan N. Glickman, P. K., Vemula, Laurie H. Glimcher, Giovanni Traverso, Robert Langer, and J. & Karp, M. An inflammation-targeting hydrogel for local drug delivery in inflammatory bowel disease. *Sci Transl Med* **7,** (2015).

153. Ben–Horin, S. *et al.* Addition of an Immunomodulator to Infliximab Therapy Eliminates Antidrug Antibodies in Serum and Restores Clinical Response of Patients With Inflammatory Bowel Disease. *Clin. Gastroenterol. Hepatol.* **11,** 444–447 (2013).

154. Meriggi, F., Di Biasi, B., Abeni, C. & Zaniboni, A. Anti-EGFR therapy in colorectal cancer: how to choose the right patient. *Curr. Drug Targets* **10,** 1033–40 (2009).

155. Takahashi, M. & Wakabayashi, K. Gene mutations and altered gene expression in azoxymethane-induced colon carcinogenesis in rodents. *Cancer Sci.* **95,** 475–80 (2004).

156. Chiron, M. *et al.* Differential antitumor activity of aflibercept and bevacizumab in patient-derived xenograft models of colorectal cancer. *Mol. Cancer Ther.* **13,** 1636–44 (2014).

ANNEXES

I.   Lorenzo-Zúñiga V, Boix J, Moreno de Vega V, **Bon I**, Marín I, Bartolí R. Endoscopic shielding technique with a newly developed hydrogel to prevent thermal injury in two experimental models. Dig Endosc. 2017 Sep;29(6):702-711. doi: 10.1111/den.12864. Impact factor: 3.375.

II.   **Bon I,** Bartoli R, Lorenzo-Zúñiga V. Endoscopic Shielding technique, a new method in therapeutic endoscopy. World J Gastroenterol 2017 Jun7: 23(21): 3761-3764. doi: 10.3748/wjg.v23.i21.3761. Impact factor: 3.3.

III.   **Bon I**, Bartolí R, Cano-Sarabia M, de la Ossa N, Moreno de Vega V, Marín I, Boix J, Lorenzo-Zúñiga V. Comparative study of electrical and rheological properties of different solutions used in EMR. Dig Endosc. 2018 Nov 14. doi: 10.1111/den.13297. Impact factor: 3.375.

Original Article

Endoscopic shielding technique with a newly developed hydrogel to prevent thermal injury in two experimental models

Vicente Lorenzo-Zúñiga,[1,3] Jaume Boix,[1,3] Vicente Moreno de Vega,[1,3] Ignacio Bon,[1,2] Ingrid Marín[1] and Ramón Bartolí[2,3]

[1]*Endoscopy Unit, Germans Trias i Pujol University Hospital,* [2]*Germans Trias i Pujol Research Institute (IGTP), and* [3]*Centro de Investigación Biomédica en Red de Enfermedades Hepáticas y Digestivas (CIBEREHD), Barcelona, Spain*

Background and Aim: A newly developed hydrogel, applied through the endoscope as an endoscopic shielding technique (EndoSTech), is aimed to prevent deep thermal injury and to accelerate the healing process of colonic induced ulcers after therapeutic endoscopy.

Methods: Lesions were performed in rats (*n* = 24) and pigs (*n* = 8). Rats were randomized to receive EndoSTech (eight rats each) with: saline (control), hyaluronic acid and product. In pigs, three ulcer sites were produced in each pig: endoscopic mucosal resection (EMR)-ulcer with prior saline injection (A; EMR-saline), EMR-saline plus EndoSTech with product (B; EMR-saline-P), and EMR with prior injection of product plus EndoSTech-P (C; EMR-P-P). At the end of the 14-day study, the same lesions were performed again in healthy mucosa to assess acute injury. Animals were sacrificed after 7 (rats) and 14 (pigs) days. Ulcers were macroscopically and histopathologically evaluated. Thermal injury (necrosis) was assessed with a 1-4 scale.

Results: In rats, treatment with product improved mucosal healing comparing with saline and hyaluronic acid (70% vs 30.3% and 47.2%; *P* = 0.003), avoiding mortality (0% vs 50% and 25%; *P* = 0.038), and perforation (0% vs 100% and 33.3%; *P* = 0.02); respectively. In pigs, submucosal injection of product induced a marked trend towards a less deep thermal injury (C = 2.25-0.46 vs A and B = 2.75-0.46; *P* = 0.127). Mucosal healing rate was higher with product (B = 90.2-3.9%, C = 91.3-5.5% vs A = 73.1-12.6%; *P* = 0.002).

Conclusions: This new hydrogel demonstrates strong healing properties in preclinical models. In addition, submucosal injection of this product is able to avoid high thermal load of the gastrointestinal wall.

Key words: deep thermal injury, delayed complications, endoscopic shielding technique, hydrogel, mucosal healing

INTRODUCTION

ADVANCED ENDOSCOPIC TECHNIQUES, endoscopic mucosal resection (EMR) or endoscopic submucosal dissection (ESD), have true advantages over surgery, but can induce adverse events, including bleeding and perforation. These adverse events are likely to increase because of the widespread implementation of endoscopic screening programs.[1] Besides this, electrocautery may

induce deep thermal damage with transmural necrosis, named coagulation syndrome (CS) or post-polypectomy electrocoagulation syndrome, with a high risk of delayed perforation.[2] Until now, we do not have any valid endoscopic treatment to prevent this delayed complication; therefore, new methods are needed. In this sense, our group has proposed that endoscopic shielding technique (EndoSTech) is a new and easy way to manage lesions resulting from therapeutic endoscopy.[3] As an important unmet topic in this field, we have developed a new topical composition, applied as a shield, to prevent CS. The purpose of the present study was to assess the protective effect of a shield with this newly developed hydrogel in two experimental models with rats and pigs. Moreover, we wanted to test its effectiveness in the prevention of deep thermal injury when used as a submucosal injection solution.

METHODS

Animals

TWENTY -FOUR MALE rats (Harlan Laboratories Models SL, Barcelona, Spain), and eight female pigs (Specipig, Barcelona, Spain) were used in this study. All procedures were approved by the Institutional Animal Care and Use Committee of Hospital Universitari Germans Trias i Pujol (protocol number DAAM 6710).

Endoscopy

Colonoscopies were carried out with the same endoscope: Olympus FQ260Z (Olympus, Tokyo, Japan), with an outer diameter of 9.5 mm, working channel diameter of 2.8 mm. Room air was used for insufflation during the endoscopy.

Development of new hydrogel

The inventors have developed a topical composition comprising specific amounts of hyaluronic acid (HA), methylcellulose, poloxamer 407 and a non-absorbable antibiotic. This hydrogel has been patented (PCT/EP2016/053928). The composition of this product is based on the combination of different substances to create this solution, which can be prepared before the procedure.

Our group carried out a pilot study based on previous reports of these components, alone or mixed in different concentrations, for the ability to improve the outcome of different surgical procedures. Our goal was to improve the beneficial effects of HA onto the colonic mucosa by adding different substances that could enhance its properties and make it suitable to be given though the endoscope working channel. For this, we worked with different substances and evaluated different aspects of the obtained hydrogels (viscosity, adherence, and biological activity), and came to the conclusion that the best composition for the hydrogel was the one described in the present study (different percentages of methylcellulose, HA and poloxamer 407). Unfortunately, these data have not been published because of patent restrictions. All compounds of the product are well known and have proved safety. The composition of the invention is biodegradable and has the advantage that it can easily and rapidly be applied without requiring any special or complex devices and, as a result of its viscosity and adhesion properties at body temperature, has the ability to remain adhered to the affected area for a long period of time, thus facilitating the physiological healing process of the wound. A rheological study was carried out in a rheometer Haake RheoStress (Thermo Fisher Scientific, Waltham, MA

USA) with a C60/1°Ti probe and a gap set of 0.053 mm. Viscosity (η) was measured as a function of shear rate (γ) of 0–300 s^{-1} at 22°C and 37°C. Figure 1 shows the evolution of the viscosity of the hydrogel according to the speed of shear. The product showed an increase in viscosity with temperature, as the initial viscosity (22°C) increased from <1 Pa s to 1550 Pa s at 37°C. In particular, when the composition contacts the mucosa at body temperature, it has the consistency of a gel, and has the ability to remain adhered to the affected area. The term 'adhesion' refers to the ability of the hydrogel to bind to the site of administration, and was measured by a texture analyzer TA.XT Plus (Stable Micro Systems, Surrey, UK). The more negative the value in mN/s, the more adhesive the topical composition will be. A 40-mm (diameter) disk was compressed into the gel and redrawn. The method settings, including speed rate at 1 mm/s and distance (depth of the insertion) of 9 mm were assessed at 22°C and 37°C. Texture properties of the hydrogel are shown in Table 1, where a temperature rise resulted in a significant higher adhesion of the product. This composition can be given smoothly through a catheter (diameter 2.0–2.2 mm) by applying a force of 370 mmHg (0.48 atmospheres).

To assess the adhesion lasting power, *in vivo* X-ray Microtomograph (SkyScan 2002; SkyScan, Aartselaar,

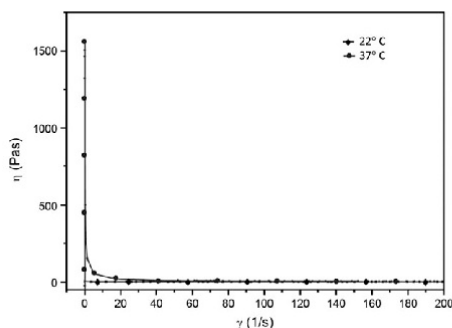**Figure 1** Evolution of the viscosity of the hydrogel according to the speed of shear. ━━, 22°C; ━━, 37°C.

Table 1 Texture properties of the hydrogel

	At 22°C		At 37°C	
	Adhesion (mN/s)	SD	Adhesion (mN/s)	SD
Hydrogel	−24.48	5.34	−3992.93	536.21

Belgium) was used in order to obtain 3D images of the distal colon (scar area) in three rats treated with product, not included in the protocol. Briefly, after therapeutic endoscopy, animals were placed in the scanning area under anesthesia with isofluorane. To visualize the hydrogel, barium contrast was mixed with the product. Acquisition images for 3D reconstruction of the distal colon lasted over 20 min with a resolution of 32 μm. Computed tomography (CT) study showed that hydrogel remained adhered to the scar area for at least 36 h after endoscopic administration.

Flowchart of the study

Flowchart of the present study is shown in Figure 2.

Shielding technique

To carry out EndoSTech, agents were applied over mucosal lesions as a coverage shield, with a catheter through the endoscope channel, positioning the tip of the catheter over the ulcer. An amount of 1 mL in rats and 5 mL in pigs was applied in each animal (Fig. 3), approximately 0.5–2 mL per cm^2 of mucosal lesion.

Colonic induced lesions in rats

After a 24-h fasting period with free access to drinking water, rats were anesthetized by isoflurane inhalation (1.5% with 98% O_2) and placed in a supine position. Remaining feces were flushed away by injecting water through the anus. A drop of lubricating jelly (Aquagel; Ecolab, Leeds, UK) was applied on the anal sphincter to facilitate insertion of the endoscope. The endoscope was then gently passed through the anus and further introduced under endoscopic vision. Water was injected through the endoscope's working channel to visualize the lumen of the colon. Occasionally, the colon was inflated with air for better visualization of the lumen.

Conventional EMR technique with prior submucosal injection was not able to be done as a result of wall thickness.[4] Lesions were created in the left colon, 6 cm to the anal margin, by Coagrasper Hemostatic Forceps (Olympus), with a power setting of forced coagulation 40 W during 4 s.[5] This technique induces deep thermal damage in the acute phase (48 h), with development of CS and large mucosal defects in the late phase, 1 week after the injury. Animals were randomly divided into three groups
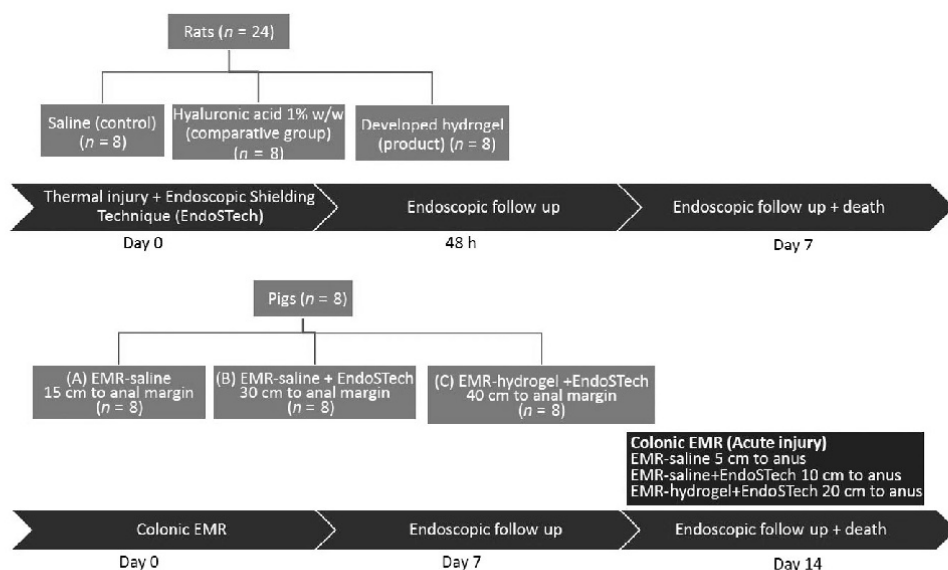

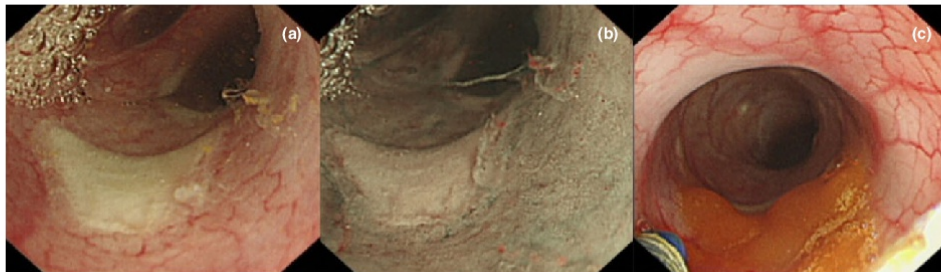**Figure 2** Flowchart of the present study.

Figure 3 Endoscopic shielding technique with the hydrogel applied on colonic induced lesions by Coagrasper Hemostatic Forceps (Olympus, Tokyo, Japan) in the rat model (40 W × 4 S). (a) Endoscopic view with high-resolution white-light imaging and (b) the corresponding narrow-band image. (c) Hydrogel was applied onto the lesion.

(n = 8, each) for EndoSTech with saline (control), sodium hyaluronic acid sodium salt 1% w/w (comparative example) and product. Rats underwent endoscopic follow up at 48 h and 7 days, and were killed by anesthetic overdose.

After death, the colon was opened longitudinally to examine colonic mucosa. Full-thickness samples of approximately 4 cm were taken from the proximal left colon surrounding endoscopic lesions.

Colonic induced lesions in pigs

In the porcine model, food was not allowed 12 h prior to the procedure. Preparation for colonoscopy was done with saline irrigation. Colonoscopy was carried out under sedation with propofol. Three ulcers sites were prepared in each pig: Mucosal elevation by submucosal injection of saline was created at 15 cm to the anal margin, then EMR with snare polypectomy and forced coagulation was carried out (A; EMR-saline; Fig. 4), EMR-saline plus EndoSTech with product at 30 cm to anus (B; EMR-saline-P; Fig. 5), and EMR with prior injection of product plus EndoSTech-P at 40 cm to anal verge (C; EMR-P-P; Fig. 6). At the end of the 14-day study, new lesions (EMR-saline; EMR-saline-P and EMR-P-P) were created in healthy colonic mucosa to assess the basal injury of the different approaches, at 5, 10 and 20 cm to anal margin; respectively. These new lesions were not used to assess mucosal healing. Animals underwent endoscopic follow up at 7 and 14 days after EMR. After this time, pigs were killed and necropsied to obtain colonic samples as described above.

Assessments

Mucosal healing was evaluated as mean ulcerated area after 48 h and 7 days in rats, and after 7 and 14 days in pigs.

Mucosal healing rate was defined as percentage of mucosal restoration. Measurement of mucosal lesion was carried out as comparison with opened forceps (5 mm) or by direct measurement with the specimen. We calculated the mean ulcerated and mucosal healing rate by the use of ImageJ public software (Image Processing and Analysis in Java; https://imagej.nih.gov/ij/). Physiological or fibrotic healing, as absence or presence of fibrosis, was evaluated with histological study of the specimen.

Thermal injury was evaluated with a 1–4 scale[5]: (i) mucosal necrosis; (ii) submucosal necrosis; (iii) transmural necrosis; and (iv) peritonitis and/or microperforation, in hematoxylin and eosin (HE) histological sections using a conventional microscope (Olympus).

Statistical analysis

Unless otherwise indicated, results are expressed as mean ± SEM or proportions as required. Comparison of means among groups was done using the one-way ANOVA or its corresponding non-parametric (Kruskal-Wallis) test. Post-hoc comparisons, to identify pairs of groups significantly different at the 0.05 level, were made with the Duncan test or the Mann–Whitney U-test, respectively. Comparisons of proportions among groups were made with the χ^2-test. Statistical analyses were carried out with SPSS for Windows version 14.0 (SPSS Inc., Chicago, IL, USA).

RESULTS

Thermal injury

ENDOSTECH WITH PRODUCT induced a marked trend towards a less deep thermal injury on the pathological specimen in both animal models (Fig. 7). In rats, treatment with product showed the best results in
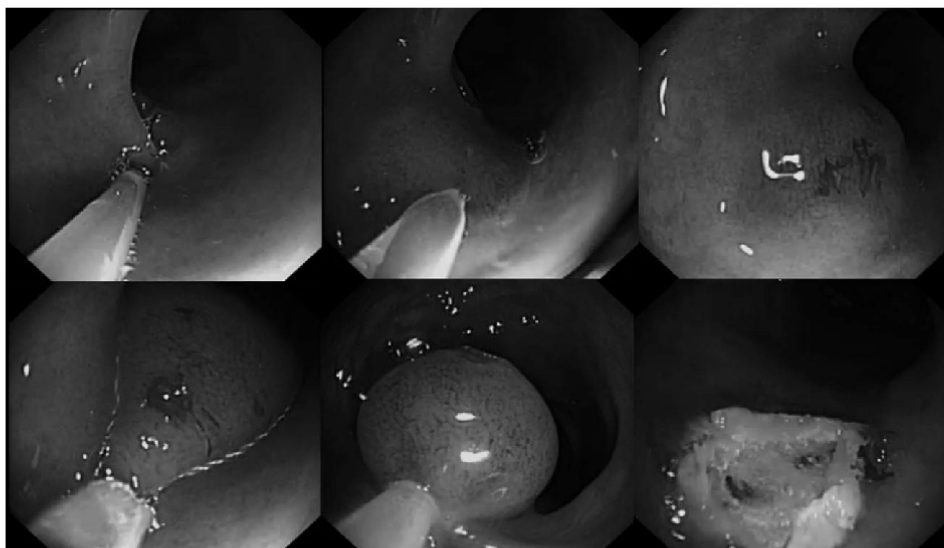
Figure 4 Mucosal elevation by submucosal injection of saline was created at 15 cm to the anal margin in the porcine model. Endoscopic mucosal resection was carried out with snare polypectomy with blended current.
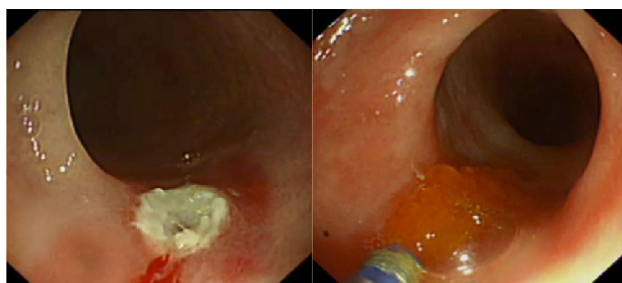

Figure 5 Endoscopic mucosal resection-induced lesion in the porcine model with prior saline injection was created at 30 cm to the anus. Endoscopic shielding technique with hydrogel was applied onto the lesion.

comparison with control and comparative groups, avoiding mortality (0% *vs* 50% and 25%; $P = 0.038$), and avoiding or reducing the risk of perforation at 7 days (0% *vs* 100% and 33.3%; $P = 0.02$); respectively (Table 2). Mortality in rats happened during the first 48 h after the procedure. We detected perforation in dead rats with necropsy, which confirmed open perforations. In those rats, only macroscopic assessment was obtained. In the surviving animals, delayed

perforation was observed in histological studies. Although we have not observed statistical significance between groups, because of the number of animals, non-treated animals showed higher deep thermal injury (1.45 ± 0.88 *vs* 2.25 ± 1.38 and 1.50 ± 1.19; $P = $ n.s.). In the porcine protocol, all animals survived at the end of the study. Submucosal injection of product induced a marked trend towards a less deep thermal injury in acute lesions induced
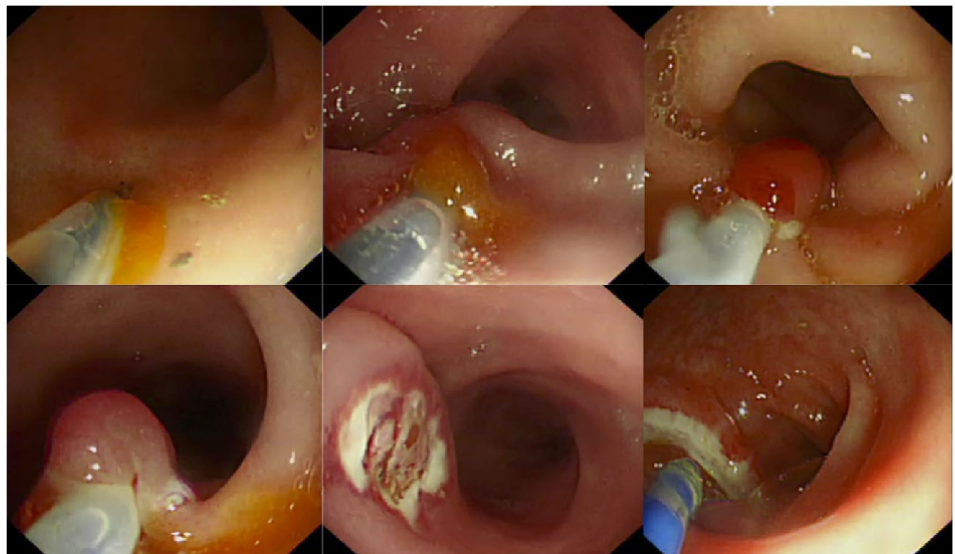
Figure 6 Endoscopic mucosal resection-induced lesion with prior hydrogel submucosal injection was performed at 40 cm to the anus. Endoscopic shielding technique with hydrogel was applied onto the lesion.

Table 2 Thermal injury and mucosal healing in rat model treated with saline, hyaluronic acid (comparative example) or developed hydrogel (product)

	Saline (*n* = 8)	Comparative (*n* = 8)	Product (*n* = 8)	*P*-value
Mortality *n* (%)	4/8 (50)	2/8 (25)	0/8 (0)	0.038
Delayed perforation *n* (%)	4/4 (100)	2/6 (33.3)	0/8 (0)	0.02
Mean ulcerated area at 48 h (cm^2)	0.56 ± 0.10	0.55 ± 0.01	0.57 ± 0.34	n.s.
Mean ulcerated area at 1 week (cm^2)	0.39 ± 0.04	0.29 ± 0.01	0.17 ± 0.07	0.01
Mucosal healing rate (%)	30.3	47.2	70.3	0.03
Physiological healing *n* (%)	0/4 (0)	4/6 (66.6)	6/8 (75)	0.02
Fibrotic healing *n* (%)	4/4 (100)	2/6 (33.3)	2/8 (25)	0.01
Thermal injury	2.25 ± 1.38	1.50 ± 1.19	1.45 ± 0.88	n.s.

Values are given as mean ± SD.
n.s., not significant.

at the end of the 14-day study (C = 2.25 ± 0.46 *vs* A and B = 2.75 ± 0.46; *P* = 0.127) (Table 3).

Mucosal healing

In rats (see results in Table 2), ulcers at 48 h were similar in all treatment groups (0.56 ± 0.10 cm^2 with saline *vs* 0.55 ± 0.01 cm^2 with comparative *vs* 0.57 ± 0.34 cm^2 with product; *P* = n.s.). Mean ulcerated area after 7 days was significantly smaller with product than with saline and comparative (0.17 ± 0.07 cm^2 *vs* 0.39 ± 0.04 cm^2 and 0.29 ± 0.01 cm^2; *P* < 0.01). Mucosal healing rate (percentage of mucosal restoration) at 7 days was significantly higher with product (70.3% *vs* 30.3% and 47.2%; *P* = 0.003). Physiological healing (absence of submucosal fibrosis) was significantly higher with product (6 of 8 animals, 75%) than in saline (0 of 4 animals, 0%) and hyaluronic acid (4 of 6 animals, 66.6%) (*P* = 0.02). In the
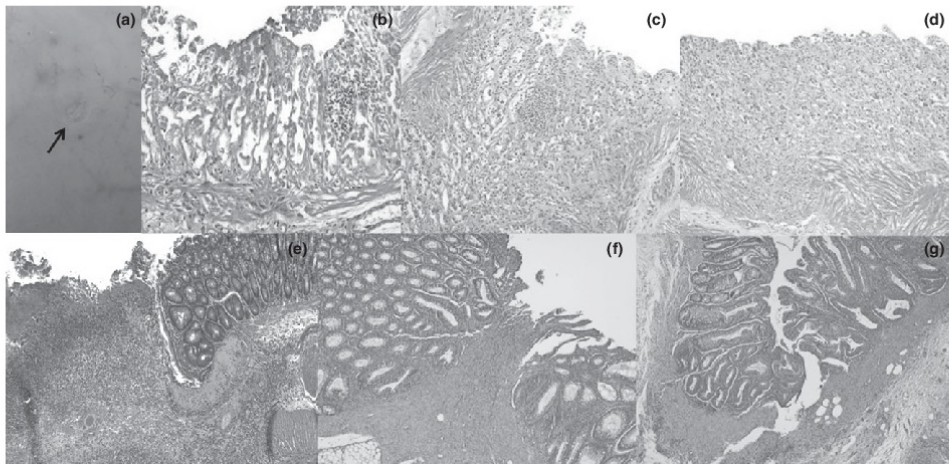
Figure 7 Pathological findings in (a–d) rats at day 7 and (e–g) porcine models at basal time. (a) Open perforation (arrow) on dead rat with macroscopic assessment. (b) Transmural necrosis in control rats. Absence of deep thermal injury in rat treated with (c) hyaluronic acid or (d) hydrogel. Necrosis of the muscularis propria in animals with endoscopic mucosal resection (EMR) carried out with prior submucosal injection of saline, without (e) or with (f) shielding with hydrogel. (g) Superficial necrosis in animals with EMR carried out with prior submucosal shielding with hydrogel.

porcine protocol (see results in Table 3), basal mean ulcerated area induced by EMR was comparable in the three groups (A = 2.12 ± 1.45 cm^2, B = 2.57 ± 1.53 cm^2, C = 2.66 ± 1.64 cm^2; P = n.s.). Mucosal healing rate at week 2 (percentage of mucosal restoration) was significantly higher in animals treated with product (B = $90.2 \pm 3.9\%$, C = $91.3 \pm 5.5\%$ *vs* A = $73.1 \pm 12.6\%$; P = 0.002), as can be observed during endoscopic follow up (Fig. 8).

DISCUSSION

THIS STUDY SHOWS that the use of EndoSTech with this newly developed hydrogel, applied directly onto endoscopic induced mucosal lesions in the colon, is able to reduce the depth of thermal injury in both experimental models. In addition, EndoSTech with this product has a protective effect for the appearance of delayed perforation and CS in rats.

Previous reports in clinical practice have demonstrated that clipping closure[6] or sealing bowel defects with tissue adhesives[7] have achieved promising results in the prevention of delayed perforation by maintaining high mechanical strength; despite this, the use of clips sometimes is complex or is limited to lesions smaller than 40 mm.[5] Tissue-shielding method also has the disadvantage of being time-consuming.[7,8] In this sense, sealing mucosal lesions with endoscopic applied chitosan hydrogel containing epidermal growth factor induced both, a significant reduction in mucosal resection-induced gastric ulcers in rabbits and pigs, and the appearance of deep scar formation and fibrotic

Table 3 Mucosal healing and thermal injury in porcine model treated with EMR-saline (Group A), EMR-saline plus EndoSTech with hydrogel (Group B) and EMR-hydrogel with EndoSTech with hydrogel (Group C)

	Group A (n = 8)	Group B (n = 8)	Group C (n = 8)	P-value
Basal ulcer (cm^2)	2.12 ± 1.45	2.57 ± 1.53	2.66 ± 1.64	n.s.
Mucosal healing rate (%)	73.1 ± 12.6	90.2 ± 3.9	91.3 ± 5.5	0.002
Thermal injury	2.75 ± 0.46	2.75 ± 0.46	2.25 ± 0.46	n.s.

Values are given as mean ± SD.
EMR, endoscopic mucosal resection; EndoSTech, Endoscopic Shielding Technique; n.s., not significant.
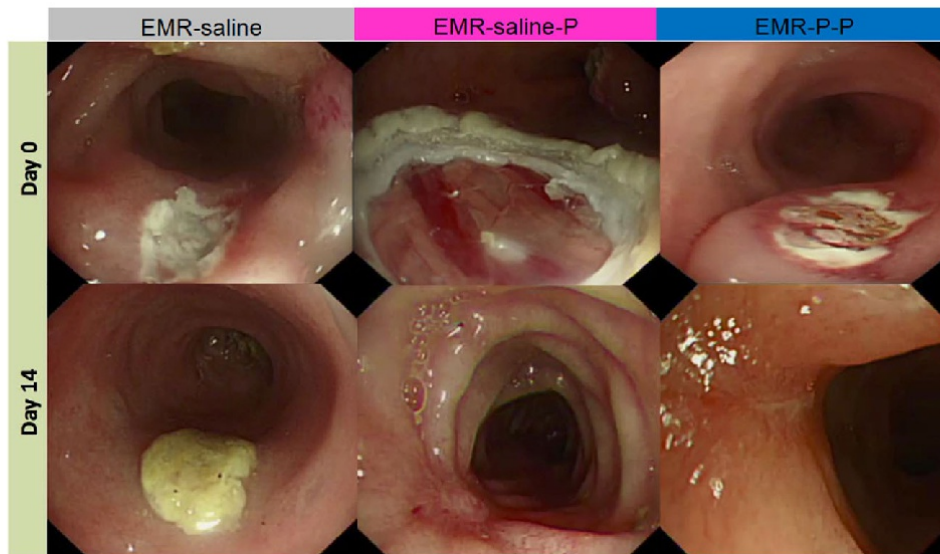
Figure 8 Endoscopic follow up in the porcine model in three treated animals: endoscopic mucosal resection (EMR)-saline (left), EMR-saline with endoscopic shielding technique (EndoSTech) with hydrogel (center), and EMR-hydrogel plus EndoSTech with hydrogel (right), at basal time and at week 2 of follow up.

submucosa in untreated lesions.[9] More recently, our group has assessed the utility of platelet-rich plasma applied onto colonic-induced lesions, showing strong healing properties in preclinical studies.[3]

Our study suggests that carrying out EndoSTech with this newly developed hydrogel, which is able to gel over induced lesions after therapeutic endoscopy, is a quick (<5 min) and safe method to prevent complications secondary to deep thermal injuries. This product has some beneficial effects: biodegradation, easy to apply without requiring any special or complex devices and it also facilitates the physiological healing process of the wound. Our data confirmed that the hydrogel had adhered to the colon for at least 36 h. The duration of the adhesion to the affected area has not been calculated in this study, but is sufficient to improve mucosal healing, promoting physiological tissue repair, and avoiding perforation.

HA is a polysaccharide of the glycosaminoglycan type. HA has an important role in tissue reparation as a result of its inmunomodulator, proliferative and tissue-repairing effects, which promote the re-epithelialization rather than cicatrization. Because of its high biocompatibility, this

substance is being used in oropharyngeal and maxillofacial surgery[10] as a base of a hydrogel capable of presenting therapeutic molecules. The addition of a bioadhesive substance such as methylcellulose has demonstrated its trophic and protective effect toward the mucosal layer of the intestine, preventing bacterial translocation in different experimental models, as we have demonstrated in previous work.[11] Moreover, methylcellulose is characterized for its bioadhesive capacity, as well as its ability to liberate, for a period of time, therapeutic substances. Finally, rifaximin is a low-absorbance, wide-spectrum antibiotic that has been used in several pathologies to clean the intestine. Giving rifaximin would ensure a lower rate of infection of the wounded area, reducing local inflammation and bacterial translocation, thereby facilitating the healing process in a faster way. Poloxamer 407 (Sigma-Aldrich, Madrid, Spain) shows suitable viscosity and adhesion properties. In particular, when the composition contacts the mucosa at body temperature, it has the consistency of a gel, and has the ability to remain adhered to the affected area.

Submucosal fluid cushion is the simplest way to prevent complications, especially perforation. Finding the most

adequate solution is essential to prevent not only perforation but also the cautery effect on the intestinal wall, as electrical conductivity may vary according to the type of solution injected.[12] CS is a condition characterized by the development of fever, abnormal levels of inflammatory markers, and abdominal pain, with or without symptoms of peritoneal irritation, as has been described with the use of hot forceps biopsy in the right colon.[13] The incidence of CS ranges from 0.07% to 1.0% in patients submitted for polypectomy, being higher in ESD, where more frequent and repetitive electrocoagulation is needed, reaching an incidence of 7.1% in gastric lesions.[14] Arterial hypertension, lesions larger than 20 mm, and laterally spreading flat mucosal neoplasms were independently associated with CS in patients undergoing colonoscopic polypectomies,[15] whereas for early gastric neoplasms, large lesions, long-term procedures, and tumor location in the middle third of the stomach were the predictive factors. In our study, the application of this hydrogel had a positive influence by reducing the depth of the thermal injury and preventing mortality and peritonitis. As a consequence of its biological and adhesion properties, it also improves mucosal restoration and the physiological healing process, avoiding mechanical damage and providing a safe and wet environment surrounding the affected area. Delayed perforation was observed in non-treated rats. Delayed bleeding was not observed in any case, and thus was not reported in the present study.

In the prevention of CS it is important to avoid high thermal load of the intestinal wall, optimizing the impedances of the tissue. In this sense, clinically injected solutions have high significant differences of specific impedances.[16] Furthermore, submucosal injection of our product reduced thermal damage in the porcine model by maintaining a good elevation of the area to be resected. Despite these promising results, our study has limitations because it is preclinical and preliminary. More data are needed in future studies in order to check the electrical properties of this hydrogel, as well as the possibility of preventing stenosis after circumferential endoscopic resections.

In conclusion, this newly developed hydrogel, which can be easily applied through the endoscope channel directly onto the lesions as a shield, is able to prevent deep thermal injury in both preclinical models. In addition, submucosal injection of this product avoids high thermal load of the gastrointestinal wall.

ACKNOWLEDGEMENTS

CONFLICTS OF INTEREST

VICENTE LORENZO-ZÚÑIGA, Ramon Bartolí and Jaume Boix are the authors of the patent (PCT/EP2016/053928). Vicente Moreno de Vega, Ingrid Marín and Ignacio Bon have no conflicts of interest or financial ties to disclose.

REFERENCES

1 Paspatis GA, Dumonceau JM, Barthet M *et al.* Diagnosis and management of iatrogenic endoscopic perforations: European Society of Gastrointestinal Endoscopy (ESGE) position statement. *Endoscopy* 2014; **46**: 693–711.

2 Lee SH, Kim KJ, Yang DH *et al.* Postpolypectomy Fever, a rare adverse event of polypectomy: nested case-control study. *Clin. Endosc.* 2014; **47**: 236–41.

3 Lorenzo-Zúñiga V, Boix J, Moreno de Vega V, Bon I, Marín I, Bartolí R. Efficacy of platelet-rich plasma as a shielding technique after endoscopic mucosal resection in rat and porcine models. *Endosc. Int. Open* 2016; **04**: E1–6.

4 Bartoli R, Boix J, Odena G, de la Ossa ND, Moreno de Vega V, Lorenzo-Zúñiga V. Colonoscopy in rats: an endoscopic, histological and tomographic study. *World J. Gastrointest. Endosc.* 2013; **5**: 226–30.

5 Lorenzo-Zúñiga V, Boix J, Moreno-de-Vega V, de la Ossa ND, Òdena G, Bartolí R. Microperforation of the colon: animal model in rats to reproduce mucosal thermal damage. *J. Surg. Res.* 2014; **188**: 415–8.

6 Zhang QS, Han B, Xu JH, Gao P, Shen YC. Clip closure of defect after endoscopic resection in patients with larger colorectal tumors decreased the adverse events. *Gastrointest. Endosc.* 2015; **82**: 904–5.

7 Tsuji Y, Ohata K, Gunji T *et al.* Endoscopic tissue shielding method with polyglycolic acid sheets and fibrin glue to cover wounds after colorectal endoscopic submucosal dissection (with video). *Gastrointest. Endosc.* 2014; **79**: 151–4.

8 Takimoto K, Toyonaga T, Matsuyama K. Endoscopic tissue shielding to prevent delayed perforation associated with endoscopic submucosal dissection for duodenal neoplasms. *Endoscopy* 2012; **44**: E414–5.

9 Maeng JH, Bang WB, Lee E, Kim HG, Lee DH, Yang SG. Endoscopic application of EGF-chitosan hydrogel for precipitated healing of GI peptic ulcers and mucosectomy-induced ulcers. *J. Mater. Sci. Mater. Med.* 2014; **25**: 573–82.

10 Fong E, Garcia M, Woods CM, Ooi E. Hyaluronic acid for post sinus surgery care: systematic review and meta-analysis. *J. Laryngol. Otol.* 2017; **131**: S2–11.

11 Bartolí R, Mañé J, Cabré E *et al.* Effect of the administration of fermentable and non-fermentable dietary fibre on intestinal

bacterial translocation in ascitic cirrhotic rats. *Clin. Nutr.* 2007; **26**: 383–7.

12 Park S, Chun HJ, Kim CY *et al.* Electrical characteristics of various submucosal injection fluids for endoscopic mucosal resection. *Dig. Dis. Sci.* 2008; **53**: 1678–82.

13 Metz AJ, Moss A, McLeod D *et al.* A blinded comparison of the safety and efficacy of hot biopsy forceps electrocauterization and conventional snare polypectomy for diminutive colonic polypectomy in a porcine model. *Gastrointest. Endosc.* 2013; **77**: 484–90.

14 Lee H, Cheoi KS, Chung H *et al.* Clinical features and predictive factors of coagulation syndrome after endoscopic submucosal dissection for early gastric neoplasm. *Gastric Cancer* 2012; **15**: 83–90.

15 Cha JM, Lim KS, Lee SH *et al.* Clinical outcomes and risk factors of post-polypectomy coagulation syndrome: a multicenter, retrospective, case-control study. *Endoscopy* 2013; **45**: 202–7.

16 Uraoka T, Kawahara Y, Ohara N *et al.* Carbon dioxide submucosal injection cushion: an innovative technique in endoscopic submucosal dissection. *Dig. Endosc.* 2011; **23**: 5–9.

Endoscopic shielding technique, a new method in therapeutic endoscopy

Ignacio Bon, Ramon Bartolí, Vicente Lorenzo-Zúñiga

Ignacio Bon, Ramon Bartolí, Vicente Lorenzo-Zúñiga, Institut Investigació en Ciències de la Salut Germans Trias i Pujol, Badalona, 08916 Badalona, Spain

Ramon Bartolí, Vicente Lorenzo-Zúñiga, Centro de Investigación Biomédica en Red de Enfermedades Hepáticas y Digestivas, 08916 Badalona, Spain

Vicente Lorenzo-Zúñiga, Endoscopy Unit, Department of Gastroenterology, Hospital Universitari Germans Trias i Pujol, 08916 Badalona, Spain

Abstract

Prevention of late complications after large endoscopic resection is inefficient with current methods. Endoscopic shielding, as a simple and safe technique, has been proposed to improve the incidence of these events. Different methods, sheets or hydrogels, have showed proven efficacy in the prevention of late bleeding and perforation, as well as the improvement of tissue repair, in experimental models and in clinical practice.

Key words: Endoscopic shielding technique; Late complication; Therapeutic endoscopy

Core tip: Prevention of late complications after large endoscopic resection is inefficient with current methods. Endoscopic shielding technique is a simple and safe method to reduce the incidence of late bleeding and perforation.

INTRODUCTION

Endoscopic resection of large lesions leads to extensive mucosal defects and submucosal exposure, with a substantial risk of complications. Late complications (bleeding, stricture, and perforation) are well known by endoscopists that perform advanced techniques[1]. There are several techniques can be used to prevent

Table 1 Outcomes of endoscopic shielding techniques with different experimental models

Ref.	Year	*n*	Species	Location of lesions	Substance	Primary endpoint	Efficacy
Maeng *et al*[4]	2014	12/2	Rabbit/pigs	Stomach	EGF-CS	Mucosal healing	90%-95%
Takao *et al*[5]	2015	9	Pigs	Stomach	PGA-FG	Prevent late complications	100%
Hiroyuki *et al*[6]	2016	20	Canine	Stomach	PGA-FG with suture	Prevent late complications	100%
Lorenzo-Zúñiga *et al*[7]	2016	4/16	Pigs/rats	Colon	PRP	Prevent late perforation and mucosal healing	100% and 2.4% (control) *vs* 80% (treated)
Lorenzo-Zúñiga *et al*[8]	2017	8/24	Pigs/rats	Colon	HAMPA	Prevent late perforation	100%

PGA: Polyglycolic acid sheets; FG: Fibrin glue; EGF-CS: Hydrogel epidermal growth factor with chitosan; PRP: Platelet rich plasma; HAMPA: Hydrogel based on the combination of hyaluronic acid, methylcellulose, poloxamer 407 and a non-absorbable antibiotic.

these adverse effects, such as adding adrenaline to the submucosal cushion, applying argon plasma coagulation, or clipping closure of the mucosal defect. However, these approaches are inefficient in the management of extensive submucosal exposure[2].

A shielding technique refers to the application of different biocompatible substances with proven biological activity to cover the lesion after therapeutic endoscopy. There are different techniques to perform this procedure. All of them are simple and safe methods to provide shielding protection of the resected area as a way to prevent late complications[3]. Due to the experience we have gained using this technique, we aim to review our evidence, as well as the experimental models used in clinical practice.

SEARCH STRATEGIES

Studies in English studies were identified by using a comprehensive search of PUBMED. The key words and search strategies were as follows: 1, ("endoscopy" [All Fields] AND ("shielding" [All Fields]). 2, ("hydrogel" [All Fields] AND "mucosectomy" [All Fields]). The Reference lists of primary study publications were searched manually. We did not consider abstracts or unpublished reports for inclusion.

EXPERIMENTAL MODELS

Endoscopic shielding techniques have been evaluated in some preclinical models (Table 1). Aimed to increase mucosal healing, to prevent late bleeding secondary to acetic acid or EMR-induced gastric ulcers, a hydrogel based on epidermal growth factor-containing chitosan hydrogel was tested in rabbits and pigs[4]. Feasibility of endoscopic application of this hydrogel was observed in both models, with a significant reduction in the ulcer size in animals treated with this hydrogel. Moreover, the depth of the untreated ulcers was greater, and the underlying muscle layer remained exposed one week after treatment, with deep scar formation and fibrotic submucosa six weeks after endoscopic resection. Other studies refer to the use of polyglycolic acid sheets (PGA) and fibrin glue (FG) to prevent late complications of ESD-induced ulcers in the stomach of two animal

models, porcine[5] and canine[6]. PGA-FG exhibited a protective effect against gastric juice, and no peeling of the sheet was observed despite the influence of peristalsis and gastric acid. Histopathological examination revealed excellent long-term tissue repair, with no adverse events.

Shielding with platelet rich plasma (PRP) has been successfully tested in colonic EMR-induced ulcers to prevent late perforations in rats and pigs[7]. On the other hand, PRP showed strong healing properties in both models, with a significant reduction of the ulcer size (2.4% in control groups *vs* 80% in treated animals). More recently, the application of other new hydrogel based on the combination of hyaluronic acid, methylcellulose, poloxamer 407 and a non-absorbable antibiotic, is able to increase mucosal healing rate and to prevent late perforation secondary to deep thermal injury in two experimental models, murine and porcine[8].

CLINICAL EXPERIENCE

According to our study, 9 articles were identified with around one hundred patients included, and are summarized in Table 2. The first report was published in 2012[3] as a case report using PGA-FG to prevent late perforation associated with ESD for a duodenal tumor 20mm in diameter. The ulcer was covered with pieces of PGA sheets using biopsy forceps and fixed in place with sprayed FG, that were spontaneously absorbed within 4-15 wk. FG is the result of spraying fibrinogen and thrombin with different tubes. This method, considered to be useful, simple and safe, can sometimes present problems because of gravitational influence, with early slipping of the sheets. To resolve this and to improve the coverage, adding clips to PGA-FG has been successfully assessed in endoscopic resection of duodenal lesions, with a median covering procedure time of 22 min[9,10].

The usefulness of the shielding technique in the prevention of late complications has been evaluated in colorectal ESD with large sheets of PGA-FG[11] or Surgicel®[12]. Both substances showed a success rate of 100%. Regarding total procedure time, Surgicel®, an oxidized cellulose polymer that swells into a gelatinous

Table 2 Outcomes of endoscopic shielding with different substances to prevent late complications after endoscopic resection

Ref.	Year	*n*	Location of lesions	Size (mm)	Substance	Procedure time (min)	Primary endpoint	Efficacy
Takimoto *et al*[3]	2012	1	Duodenum	20.0	PGA-FG	NR	Prevent late perforation	100%
Doyama *et al*[9]	2014	3	Duodenum	17.5	PGA-FG with clips	22	Prevent late perforation	100%
Takimoto *et al*[10]	2014	2	Duodenum	17.5	PGA-FG with clips	NR	Prevent late perforation	100%
Tsuji *et al*[11]	2014	10	Colorectal	39.7	PGA-FG	18.7	Prevent late complications	100%
Tsuji *et al*[13]	2015	41	Stomach	40.1	PGA-FG	20.4	Prevent late bleeding	93.3%
Kataoka *et al*[16]	2015	1	Esophagus	55.0	PGA-FG-T	NR	Prevent late stricture	100%
Myung *et al*[12]	2016	35	Colorectal	38.8	Surgicel®	5	Prevent late complications	100%
Sakaguchi *et al*[15]	2016	11	Esophagus	38.3	PGA-T	12	Prevent late stricture	81.8%
Takimoto *et al*[14]	2016	3	Stomach	25.0	PGA-FG	NR	Treatment of postoperative perforations	100%

PGA: Polyglycolic acid sheets; FG: Fibrin glue; T: Triamcinolone; NR: Not reported.

mass with hemostatic and bactericidal effects, showed the best results as a rapid technique (mean time 5 min), in comparison with PGA-FG (19 min). Despite the use of large PGA sheets being less time consuming than many small PGA sheets, is not comparable with the use of a gel agent.

PGA-FG decreased the risk of bleeding after ESD of a large gastric neoplasm, with a mean resection size of 40 mm[13]. The post-ESD bleeding occurred at a rate of 6.7% in the study group, compared to 22% in the historical control group. Furthermore, another study[14] reported the efficacy of PGA-FG in the closure of postoperative gastric perforations without large and deep cavities.

The prevention of late esophageal strictures after circumferential ESD has been evaluated with the combination of intra-lesional steroid injections (triamcinolone 40 mg, 5 mg/mL) and shielding with PGA sheets and FG[15,16] with and incidence of stricture around 18%.

CONCLUSION

Significant technological advancements have led to a rapid expansion of the indications of therapeutic endoscopy, which carries a small, but significant, risk of complications. Adverse events associated with large endoscopic resections cannot be overlooked. To prevent these events we should close the submucosal exposure, although it is difficult to completely close ones > 30 mm in diameter with clipping closure[17]. In our opinion, endoscopic shielding technique is a very promising method that does not require special or complex devices. Shielding large mucosal defects has been demonstrated in experimental models and in clinical practice with around one hundred patients included, showing effectiveness in the prevention of late complications (perforation, bleeding or stricture). There are now different substances, sheets or hydrogels, with different mechanisms of action, which can be used as covering agents. We believe that the use of a single gelling agent seems to have more advantages, as it is the simplest and quickest method to cover large lesions. Moreover, these agents typically have bioactive properties that can accelerate mucosal healing. However, larger prospective studies with control groups are needed to perform a comparison of the different substances.

REFERENCES

1   **Paspatis GA**, Dumonceau JM, Barthet M, Meisner S, Repici A, Saunders BP, Vezakis A, Gonzalez JM, Turino SY, Tsiamoulos ZP, Fockens P, Hassan C. Diagnosis and management of iatrogenic endoscopic perforations: European Society of Gastrointestinal Endoscopy (ESGE) Position Statement. *Endoscopy* 2014; **46**: 693-711 [PMID: 25046348 DOI: 10.1055/s-0034-1377531]

2   **Toyonaga T**, Man-i M, East JE, Nishino E, Ono W, Hirooka T, Ueda C, Iwata Y, Sugiyama T, Dozaiku T, Hirooka T, Fujita T, Inokuchi H, Azuma T. 1,635 Endoscopic submucosal dissection cases in the esophagus, stomach, and colorectum: complication rates and long-term outcomes. *Surg Endosc* 2013; **27**: 1000-1008 [PMID: 23052530 DOI: 10.1007/s00464-012-2555-2]

3   **Takimoto K**, Toyonaga T, Matsuyama K. Endoscopic tissue shielding to prevent delayed perforation associated with endoscopic submucosal dissection for duodenal neoplasms. *Endoscopy* 2012; **44** Suppl 2 UCTN: E414-E415 [PMID: 23169042 DOI: 10.1055/s-0032-1325739]

4   **Maeng JH**, Bang BW, Lee E, Kim J, Kim HG, Lee DH, Yang SG. Endoscopic application of EGF-chitosan hydrogel for precipitated healing of GI peptic ulcers and mucosectomy-induced ulcers. *J Mater Sci Mater Med* 2014; **25**: 573-582 [PMID: 24338378 DOI: 10.1007/s10856-013-5088-x]

5   **Takao T**, Takegawa Y, Shinya N, Tsudomi K, Oka S, Ono H. Tissue shielding with polyglycolic acid sheets and fibrin glue on ulcers induced by endoscopic submucosal dissection in a porcine model. *Endosc Int Open* 2015; **3**: E146-E151 [PMID: 26135658 DOI: 10.1055/s-0034-1391391]

6   **Hiroyuki T**, Kohki Y, Hiroe M, Tsunehito H, Rie A, Shota T, Hiroko T, Yuki O, Takagi T, Kengo T, Takashi T, Hideyuki K, Hideki T, Akeo H. A basic study of the effect of the shielding method with polyglycolic acid fabric and fibrin glue after endoscopic submucosal dissection. *Endosc Int Open* 2016; **4**: E1298-E1304 [PMID: 27995192 DOI: 10.1055/s-0042-118208]

7   **Lorenzo-Zúñiga V**, Boix J, Moreno de Vega V, Bon I, Marín I, Bartoli R. Efficacy of platelet-rich plasma as a shielding technique after endoscopic mucosal resection in rat and porcine models. *Endosc Int Open* 2016; **4**: E859-E864 [PMID: 27540573 DOI: 10.1055/s-0042-109170]

8   **Lorenzo-Zúñiga V**, Boix J, Moreno de Vega V, Bon I, Marín I,

Bartoli R. Endoscopic shielding technique with a newly developed hydrogel to prevent thermal injury in two experimental models. *Dig Endosc* 2017; Epub ahead of print [PMID: 28294423 DOI: 10.111/den.12864]

9   **Doyama H**, Tominaga K, Yoshida N, Takemura K, Yamada S. Endoscopic tissue shielding with polyglycolic acid sheets, fibrin glue and clips to prevent delayed perforation after duodenal endoscopic resection. *Dig Endosc* 2014; **26** Suppl 2: 41-45 [PMID: 24750147 DOI: 10.1111/den.12253]

10   **Takimoto K**, Imai Y, Matsuyama K. Endoscopic tissue shielding method with polyglycolic acid sheets and fibrin glue to prevent delayed perforation after duodenal endoscopic submucosal dissection. *Dig Endosc* 2014; **26** Suppl 2: 46-49 [PMID: 24750148 DOI: 10.1111/den.12280]

11   **Tsuji Y**, Ohata K, Gunji T, Shozushima M, Hamanaka J, Ohno A, Ito T, Yamamichi N, Fujishiro M, Matsuhashi N, Koike K. Endoscopic tissue shielding method with polyglycolic acid sheets and fibrin glue to cover wounds after colorectal endoscopic submucosal dissection (with video). *Gastrointest Endosc* 2014; **79**: 151-155 [PMID: 24140128 DOI: 10.1016/j.gie.2013.08.041]

12   **Myung YS**, Ko BM, Han JP, Hong SJ, Jeon SR, Kim JO, Moon JH, Lee MS. Effectiveness of Surgicel® (Fibrillar) in patients with colorectal endoscopic submucosal dissection. *Surg Endosc* 2016; **30**: 1534-1541 [PMID: 26201411 DOI: 10.1007/s00464-015-4369-5]

13   **Tsuji Y**, Fujishiro M, Kodashima S, Ono S, Niimi K, Mochizuki S, Asada-Hirayama I, Matsuda R, Minatsuki C, Nakayama C, Takahashi Y, Sakaguchi Y, Yamamichi N, Koike K. Polyglycolic acid sheets and fibrin glue decrease the risk of bleeding after endoscopic submucosal dissection of gastric neoplasms (with video). *Gastrointest Endosc* 2015; **81**: 906-912 [PMID: 25440679 DOI: 10.1016/j.gie.2014.08.028]

14   **Takimoto K**, Hagiwara A. Filling and shielding for postoperative gastric perforations of endoscopic submucosal dissection using polyglycolic acid sheets and fibrin glue. *Endosc Int Open* 2016; **4**: E661-E664 [PMID: 27556075 DOI: 10.1055/s-0042-105867]

15   **Sakaguchi Y**, Tsuji Y, Fujishiro M, Kataoka Y, Takeuchi C, Yakabi S, Saito I, Shichijo S, Minatsuki C, Asada-Hirayama I, Yamaguchi D, Niimi K, Ono S, Kodashima S, Yamamichi N, Koike K. Triamcinolone Injection and Shielding with Polyglycolic Acid Sheets and Fibrin Glue for Postoperative Stricture Prevention after Esophageal Endoscopic Resection: A Pilot Study. *Am J Gastroenterol* 2016; **111**: 581-583 [PMID: 27125718 DOI: 10.1038/ajg.2016.60]

16   **Kataoka Y**, Tsuji Y, Sakaguchi Y, Kodashima S, Yamamichi N, Fujishiro M, Koike K. Preventing esophageal stricture after endoscopic submucosal dissection: steroid injection and shielding with polyglycolic acid sheets and fibrin glue. *Endoscopy* 2015; **47** Suppl 1 UCTN: E473-E474 [PMID: 26465191 DOI: 10.1055/s-0034-1392975]

17   **Liaquat H**, Rohn E, Rex DK. Prophylactic clip closure reduced the risk of delayed postpolypectomy hemorrhage: experience in 277 clipped large sessile or flat colorectal lesions and 247 control lesions. *Gastrointest Endosc* 2013; 77: 401-407 [PMID: 23317580 DOI: 10.1016/j.gie.2012.10.024]

Original Article

Comparative study of electrical and rheological properties of different solutions used in endoscopic mucosal resection

Ignacio Bon,[1] Ramón Bartolí,[2] Mary Cano-Sarabia,[3] Napoleón de la Ossa,[4] Vicente Moreno de Vega,[1] Ingrid Marín,[1] Jaume Boix[1,2] and Vicente Lorenzo-Zúñiga[1,2] (iD)

[1]*Endoscopy Unit, Germans Trias i Pujol University Hospital, Barcelona,* [2]*Network Biomedical Research Center of Hepatic and Digestive Diseases (CIBERehd), Madrid,* [3]*Catalan Institute of Nanoscience and Nanotechnology, CSIC and The Barcelona Institute of Science and Technology, Barcelona,   and* [4]*Departament of Pathology, Germans Trias i Pujol University Hospital, Barcelona, Spain*

Background and Aim: The study of electrical and rheological properties of solutions to carry out endoscopic resection procedures could determinate the best candidate. An *ex vivo* study with porcine stomachs was conducted to analyze electrical resistivity (*R*) and rheological properties (temperature, viscosity, height and lasting of the cushion) of different substances used in these techniques.

Methods: Tested solutions were: 0.9% saline (S), platelet-rich plasma (PRP), Gliceol (GC), hyaluronic acid 2% (HA), Pluronic-F127 20% (PL), saline with 10% glucose (GS), Gelaspan (GP), Covergel-BiBio (TB) and PRP with TB (PRP+TB). Measurements of electrical and rheological properties were done at 0, 15, 30, 45 and 60 min after submucosal injection.

Results: Solutions showed a wide variability of transepithelial *R* after submucosal injection. Substances able to maintain the highest *R* 60 min postinjection were TB (7×10^4 Ω), HA (7×10^4 Ω) and PL (7×10^4 Ω). Protective solutions against deep thermal injury (*T*ª lower than 60°C) were PL (47.6°C), TB (55°C) and HA (56.63°C). Shortest time to carry out resections were observed with GC (17.66″), PRP (20.3″) and GS (23.45″). Solutions with less cushion decrease (<25%) after 60 min were TB (11.74%), PL (18.63%) and PRP (22.12%).

Conclusions: Covergel-BiBio, PL and HA were the best solutions with long-term protective effects (transepithelial *R*, lower thermal injury and less cushion decrease). Solutions with quicker resection time were GC, PRP and GS.

Key words: electrical property, endoscopic mucosal resection, endoscopic submucosal dissection, rheological property, submucosal injection

INTRODUCTION

DIFFERENT SOLUTIONS ARE widely used in endoscopic mucosal resection (EMR) or endoscopic submucosal dissection (ESD) as submucosal injection to facilitate en bloc resection or to reduce the incidence of adverse events.[1,2] The ideal solution with which to carry out submucosal injection must contribute to a better clinical outcome. This solution should achieve and maintain a long-lasting cushion to safely allow the physician to carry out the required techniques, be non-toxic so as not to influence histological evaluation and should be an inexpensive, readily available and easily administered solution.[2–7] Endoscopic resection techniques are carried out using an electrosurgical unit (ESU) which works by applying an electrical current through an electrode in contact with the tissue and, depending on the setting of the machine, carrying out coagulation or cutting. The electric circuit that forms between the ESU, the electrode and the tissue can be affected by many variables, influencing the outcome of the procedure. Thus, electrical characteristics of the submucosal injection solution used also have an effect on this outcome.[8] Hence, measurement of electrical resistivity (i.e. the fundamental property of a material that quantifies how strongly that material opposes the flow of electric current), viscosity or osmolarity are of great importance for the outcome of the procedure.

Therefore, we aim to analyze electrical (resistivity) and rheological properties (temperature, viscosity, height and lasting of the cushion) of different solutions to carry out EMR in an ex vivo model of porcine stomachs.

METHODS

FRESH PORCINE STOMACHS were used to analyze submucosal injection solution properties. Measurements

Corresponding: Vicente Lorenzo-Zúñiga, Endoscopy Unit, Department of Gastroenterology/CIBERehd, Hospital Universitari Germans Trias i Pujol, Carretera del Canyet s/n, 08916 Badalona, Spain. Email: vlorenzo.germanstrias@gencat.cat

were carried out in the fundus. Each solution (2 mL) was injected using a 22 G needle. For measurement of cushion decrease and transepithelial resistance, stomach portions of 8 × 5 cm were used. Stomach portions were maintained at 37°C during the test. EMR resection was carried out after prior submucosal injection with a standard polypectomy snare (Olympus Medical Systems, Tokyo, Japan) with blended current on full stomachs for the measurement of EMR time and muscle temperature. To standardize the same force applied to the polypectomy snare in all procedures, the snare was placed in a laboratory syringe pump (Advance Infusion Pump Series 1200; Parkland Scientific, Coral Springs, FL, USA) with a linear force of 10000 g.

Solutions

The following solutions were tested: 0.9% saline (S), platelet-rich plasma (PRP), Gliceol (GC), hyaluronic acid 2% (HA), Pluronic-F127 20% (PL), saline with 10% glucose (GS), Gelaspan (GP), Covergel-BiBio (TB) and PRP with TB (PRP+TB).

Saline, GS and GP were acquired from the hospital pharmacy service (Germans Trias i Pujol University Hospital, Barcelona, Spain). GC was manufactured in our laboratory (Helath Research Institute Germans Trias i Pujol, Barcelona, Spain). PRP was obtained by extraction of blood with a syringe containing 1/10 total blood volume of 10% sodium citrate. Then, blood was centrifuged at 160 g for 20 min at room temperature; this resulted in a two-phases tube, the top one containing plasma. Plasma was recollected and transferred to a new centrifuge tube, and further centrifuged at 400 g for 15 min. The result of this was platelet-poor plasma (2/3 of total volume) and PRP (the bottom 1/3 of the total volume). PRP was activated by addition of 0.05 mL/1 mL PRP of 10% calcium chloride.

Covergel-BiBio is a mixture of four components[9]: Pluronic-F127 modified to add acrylate motifs for its irreversible gelation, hyaluronic acid (TCI Europe, Zwijndrecht, Belgium), methylcellulose (Sigma, St Louis, MO, USA), Rifaximine (Sigma) and Irgarcure 2959 as a photoinitiator (Sigma).

Evaluation of electrical and rheological properties

Electrical resistivity or resistance (R) of materials to the flow of an electric current was evaluated using a multimeter SK-7707 (KAISE Corporation, Ueda City, Japan) with conventional electrodes; one electrode was positioned at the apical surface of the cushion (gastric mucosa) and the other on the basal surface of the cushion (serosa layer), to evaluate the

Figure 1 Evaluation of electrical resistivity with a multimeter.

transepithelial R that the stomach wall had with the submucosal solution injected. Measurements were done at 0, 15, 30, 45 and 60 min after submucosal injection (Fig. 1).

Temperature (T^n) analysis was carried out using a thermometer K/J type thermocouple (Uxcell, Kwai Fong, Hong Kong) with the sensor located at the muscle layer to check the risk of deep thermal injury (Fig. 2). Measurement started after submucosal injection and finished after EMR was done. Moreover, time needed to carry out EMR was registered with each solution.

Submucosal cushion height was studied taking into account three different aspects: differences of height at time 0 after injection, differences of height at time 60 min after injection and the percentage of decrease for each substance. We evaluated this by taking standardized pictures at times: 0, 15, 30, 45 and 60 min. Images were evaluated using ImageJ software (NIH, Bethesda, MD, USA). Decrease of the cushion is shown as % of the original height of each solution.

All determinations were carried out in triplicate to calculate mean data.

Osmolarity and viscosity of each solution were obtained from each manufacturer.

Statistical analysis

A descriptive analysis was carried out for each experiment. ANOVA tests were carried out to compare groups. Tuckey tests were done as post-hoc analysis. SPSS software, 15.0 version was used). A nonparametric Spearman correlation study was carried out between all the characteristics evaluated using SPSS software, 15.0 version software.

Figure 2 Analysis of temperature during endoscopic mucosal resection with a thermometer on the apical face of the stomach and the other (black arrow) on the serosa layer.

RESULTS

Electrical and rheological properties

TRANSEPITHELIAL R WAS measured at times 0, 15, 30, 45 and 60 min after substance injection on the submucosal layer. Resistivity of porcine stomach without submucosal injection was 5×10^4 Ω. Solutions showed a wide variability of transepithelial R after submucosal injection (time 0: GP 20×10^4 Ω, TB 20×10^4 Ω, GC 16×10^4 Ω, GS 13×10^4 Ω, HA 9×10^4 Ω, PL 8×10^4 Ω, PRP 6.5×10^4 Ω, S 6×10^4 Ω, and PRP+TB 6×10^4 Ω; Table 1). Next, measurements at 15, 30 and 45 min showed a trend to decrease R in all solutions except HA, PL, PRP and PRP+TB, which maintained stable values. Substances that were able to maintain a higher R after 60 min postinjection were TB $(7 \times 10^4$ Ω), HA $(7 \times 10^4$ Ω) and PL $(7 \times 10^4$ Ω). Values represent the mean of three separate experiments for each substance (Fig. 3).

Endoscopic mucosal resection without any solution used to create a cushion resulted in a muscle layer T^a of 79.48°C and total time for resection of 31 s (basal determinations). Solutions showed very different patterns in T^a increase during EMR at the muscle layer (Fig. 4). High risk of deep thermal injury (T^a higher than 60°C) was observed with S (198.4°C), GP (133.55°C), PRP (110.4°C), GS (82.85°C), GC (82.4°C) and PRP+TB (80.1°C). In contrast, protective solutions were PL (47.6°C), TB (55°C) and HA (56.63°C).

Time to carry out EMR was comparable or higher than basal with HA (28″), GP (30.73″), PRP+TB (33″), S (33.41″), PL (34.64″) and TB (51.67″). Solutions able to shorten this time were GC (17.66″), PRP (20.3″) and GS (23.45″) (Fig. 5).

Submucosal cushion height with the different solutions at time 0 and 60 min after injection is shown in Table 1. Substances capable of maintaining at least 75% of the original height after 1 hour were (cushion decrease <25%): TB (11.74%), PL (18.63%) and PRP (22.12%) (Fig. 6).

Osmolarity and viscosity of each solution are shown in Table 1.

A nonparametric Spearman's correlation study was done for all the characteristics evaluated and results are shown in Table 2. Correlation quantifies the degree to which two variables are related. Correlation tests compute a correlation coefficient (r) that shows how much one variable tends to change when the other variable changes. When r is 0.0, there is no relationship. When r is positive, there is a trend that one variable goes up as the other one goes up. When r is negative, there is a trend that one variable goes up as the other one goes down. Statistical correlation study showed a significant correlation only between: resistivity of the solutions and the muscular temperature reached after EMR (-0.7851 P-value 0.002, negative correlation, the higher the resistivity, the lower the temperature reached); resistivity of the solutions and the time to carry out EMR (0.6938 P-value

Table 1 Electrical and rheological properties of different solutions used to carry out submucosal injection

Solutions	Resistivity $(10^4$ Ω)	T^a muscle (°C)	Heigh t = 0 (cm)	Heigh t = 60 (cm)	Cushion decrease (%)	Time (s)	Osmolarity (mOsm/L)	Viscosity (Pa)
Saline	6	198.4	1.68	1.22	27.46	33.4	286	0.0043
PRP	6.5	110.4	2.14	1.67	22.12	20.3	278	0.01
Gliceol	16	82.4	2.12	1.53	28.74	17.6	288	0.009
HA	9	56.6	2.41	1.76	27.06	28	282	0.04
PL	8	47.6	2.37	1.93	18.63	34.6	300	0.9
GS	13	82.9	2.33	1.15	50.84	23.5	556	0.008
Gelaspan	20	133.6	2.45	1.73	30.51	30.7	284	0.009
TB	20	55	2.63	2.32	11.74	51.7	300	0.9
PRP+TB	6	80.1	2.60	1.65	36.55	33	280	0.045

PRP, platelet-rich plasma; HA, hyaluronic acid 2%; PL, pluronic-F127 20%; GS, saline with 10% glucose; TB, Covergel-BiBio.
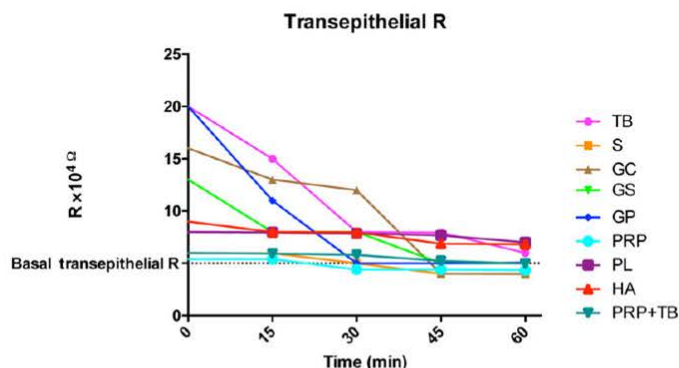
Time	Mean	Median	SD	SEM	Substance
0 min	19.89	20.20	2.61	1.50	TB
	5.93	5.90	0.80	0.46	S
	15.98	15.80	0.92	0.53	GC
	12.95	13.10	1.45	0.84	GS
	19.93	19.20	2.02	1.17	GP
	5.34	5.40	1.00	0.58	PRP
	7.82	8.50	2.00	1.15	PL
	8.91	8.90	1.55	0.90	HA
	5.98	5.90	0.66	0.38	PRP+TB
15 min	14.86	15.40	2.42	1.40	TB
	5.93	5.90	0.80	0.46	S
	12.99	13.00	0.50	0.29	GC
	7.93	8.30	1.28	0.74	GS
	10.83	9.90	2.44	1.41	GP
	5.36	5.30	0.85	0.49	PRP
	7.79	8.50	1.96	1.13	PL
	7.93	7.70	1.28	0.74	HA
	5.92	5.70	0.49	0.28	PRP+TB
30 min	7.82	8.40	2.03	1.17	TB
	4.97	5.30	0.61	0.35	S
	11.98	12.40	0.78	0.45	GC
	7.91	8.40	1.44	0.83	GS
	4.86	4.90	1.45	0.84	GP
	4.36	4.30	0.75	0.44	PRP
	7.69	8.30	1.99	1.15	PL
	7.89	7.60	1.39	0.80	HA
	5.79	5.80	0.50	0.29	PRP+TB
45 min	7.82	7.90	1.65	0.95	TB
	3.94	4.40	0.78	0.45	S
	3.94	4.20	0.82	0.47	GC
	4.76	5.20	1.81	1.04	GS
	4.92	5.00	1.10	0.64	GP
	4.34	4.40	0.90	0.52	PRP
	7.51	7.90	1.86	1.07	PL
	6.80	6.30	1.16	0.67	HA
	5.21	4.90	0.58	0.33	PRP+TB
60 min	5.96	6.20	0.82	0.47	TB
	3.94	4.40	0.78	0.45	S
	3.94	4.00	0.55	0.32	GC
	4.79	5.30	1.67	0.96	GS
	5.02	5.10	0.85	0.49	GP
	4.28	4.20	0.81	0.47	PRP
	6.80	7.30	1.97	1.14	PL
	6.74	6.20	1.13	0.65	HA
	4.93	4.70	0.74	0.43	PRP+TB

Figure 3 Transepithelial resistivity (R) of different solutions in fresh porcine stomach at baseline, 15, 30, 45 and 60 min after submucosal injection. Solutions used were platelet-rich plasma (PRP), 0.9% saline (S), Gliceol (GC), Pluronic-F127 20% (PL), hyaluronic acid 2% (HA), saline with 10% glucose (GS), Gelaspan (GP), Covergel-BiBio (TB) and PRP+TB.

0.042, positive correlation, the higher the resistivity, the longer the time to carry out EMR); and between viscosity and the muscle temperature reached after EMR (−0.8740 *P*-value 0.003, negative correlation, the higher the viscosity the lower the temperature reached). The rest of the correlations, although not statistically significant, show a clear trend. For example, the risk of thermal injury seems to be higher with higher osmolarity, and EMR time is higher with higher resistivity, viscosity and osmolarity of the substance.

DISCUSSION

ENDOSCOPIC MUCOSAL RESECTION and ESD have been established as safe and feasible techniques for the removal of large lesions throughout the gastrointestinal tract. Avoiding the main complications associated with bleeding and perforation is of interest in the field of endoscopy and, to achieve this, many improvements in resection techniques have been developed. Submucosal injection, as the introduction of a substance into the submucosal layer of the gastrointestinal wall to elevate the mucosal layer, thus protecting the muscle layer, has been proven effective to prevent these complications and to improve the clinical outcomes of the procedure.

The search for the most appropriate solution to carry out this submucosal injection is still a matter of debate. Studies have been focused on the capacity of the solution to elevate the mucosa and to maintain this elevation, ignoring some other important aspects of these solutions that may have an
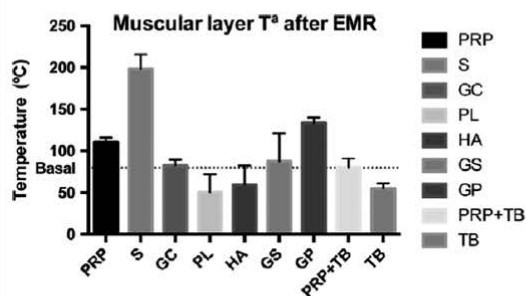
Figure 4 Temperature after endoscopic mucosal resection (EMR) reached muscular layer. Values are the mean of three separate experiments for each substance. Solutions used were platelet-rich plasma (PRP), 0.9% saline (S), Gliceol (GC), Pluronic-F127 20% (PL), hyaluronic acid 2% (HA), saline with 10% glucose (GS), Gelaspan (GP), Covergel-BiBio (TB) and PRP+TB.

Figure 5 Time required to carry out endoscopic mucosal resection (EMR) with different substances using a standard polypectomy snare. Values are the mean of three separate experiments for each substance. Solutions used were platelet-rich plasma (PRP), 0.9% saline (S), Gliceol (GC), Pluronic-F127 20% (PL), hyaluronic acid 2% (HA), saline with 10% glucose (GS), Gelaspan (GP), Covergel-BiBio (TB) and PRP+TB.
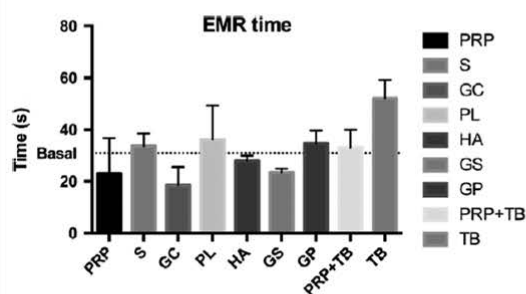
important role on the outcome of the procedure. Endoscopic resections are carried out using an ESU which applies an electrical current to carry out the desired coagulation or cutting for the procedure; thus, studying the electrically related properties of the solutions is of great interest.[4,6–8]

In the present study, we have tested both commercial and non-commercial solutions to carry out submucosal injection and we have tried to connect electrical resistivity, viscosity and osmolarity of the solutions with clinical aspects that will have an impact on the clinical outcome, such as height and duration of the elevation, time to carry out EMR or temperature reached after EMR.

Resistivity is a property of a material that quantifies the opposition of said material to the flow of an electric current. Osmolarity is the measure of a solute concentration, the number of osmoles of solute particles per unit of volume in a solution. This value is indicative of the osmotic pressure of a solution which will determine how this solution will diffuse across a semipermeable membrane (osmosis). Viscosity is often referred to as the thickness of a fluid and, at a molecular level, it is a result of the interaction between the different molecules in a fluid and it will determine the energy needed to make a fluid flow. Previous studies related the electrical resistivity of blood to its viscosity, affected by the quantity of fibrinogen.[10,11]

Our results showed wide variability of transepithelial R after submucosal injection. Substances with high viscosity were associated with higher and maintained stable values of R (TB, PL and HA). These solutions also have a higher protective effect against deep thermal injury and less cushion decrease. In contrast, solutions able to carry out EMR in a shorter time were GC, PRP and GS. Statistical correlation study showed a significant correlation only between: resistivity of the solutions and the muscle temperature reached after EMR, resistivity of the solutions and the time to carry out EMR and between viscosity and the muscle temperature reached after EMR.

Our study was an attempt to explore electrical and rheological properties of different solutions used in EMR. An *ex vivo* model to study any organ physiology has some drawbacks such as absence of perfusion and active absorption that, in this case, can mean a longer time for the submucosal fluid to resolve; nonetheless, we tried to minimize this problem by using porcine stomachs within the first hour after the animal's death, which avoids significant tissue changes.[12]

In the present study, we tried to standardize all procedures as much as possible by using the same part of the stomach for each substance, creating a 2-mL submucosal cushion, applying the same force to the polypectomy snare by using a laboratory syringe pump at a set value and cutting the same amount of stomach mucosal layer. The small-sized mucosal resections we carried out do not usually require a submucosal injection clinically as lesions smaller than 2 cm do not require submucosal injection for EMR or, if it is done, the solution used does not have much impact on the final outcome.[7] Nonetheless, we prioritized standardization of the lesions and the EMR technique for better comparison of the results.

We also note our small size sample and the lack of *in vivo* data, as this was a proof of concept research work in which we wanted to see a possible correlation or trend between the characteristics studied and, thus, open the door for a future *in vivo* study that is more clinically representative.
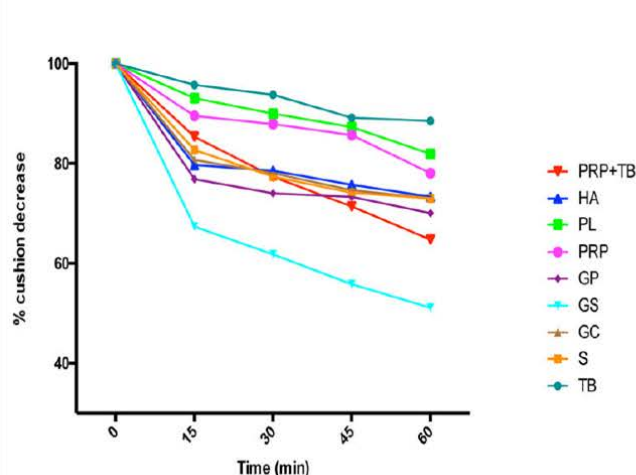
Time	Mean	Median	SD	SEM	Substance
	76.67	74.20	7.05	4.07	GP
	95.63	97.08	5.05	2.91	TB
	82.67	82.27	2.80	1.62	S
	80.11	83.55	11.49	6.63	GC
15 min	66.46	68.68	13.20	7.62	GS
	85.26	85.66	4.57	2.64	PRP+TB
	89.06	90.28	10.88	6.28	PRP
	92.98	95.08	5.37	3.10	PL
	79.41	83.02	8.07	4.66	HA
	73.28	66.39	13.30	7.68	GP
	93.59	97.08	6.51	3.76	TB
	77.00	79.46	9.29	5.36	S
	77.06	81.34	14.80	8.55	GC
30 min	60.33	61.92	16.12	9.30	GS
	77.27	75.88	4.15	2.39	PRP+TB
	87.41	87.97	11.04	6.38	PRP
	89.88	90.20	4.27	2.46	PL
	78.25	82.02	7.88	4.55	HA
	72.48	65.24	14.11	8.15	GP
	88.96	89.45	7.10	4.10	TB
	73.66	74.57	10.13	5.85	S
	72.89	80.67	19.06	11.01	GC
45 min	53.96	54.93	17.57	10.14	GS
	70.87	72.38	10.44	6.03	PRP+TB
	85.21	86.11	10.84	6.26	PRP
	87.18	85.46	5.51	3.18	PL
	75.45	79.20	7.78	4.49	HA
	69.49	64.36	11.30	6.52	GP
	88.26	87.99	8.54	4.93	TB
	72.54	73.15	10.16	5.87	S
	71.26	78.93	18.90	10.91	GC
60 min	49.16	49.28	17.19	9.92	GS
	63.45	67.19	15.42	8.91	PRP+TB
	77.88	75.98	6.14	3.55	PRP
	81.37	82.40	11.64	6.72	PL
	72.94	78.67	9.54	5.51	HA

Figure 6 Percentage of submucosal cushion decrease of the height acquired by each substance at time 0. Values are the mean of three separate experiments for each substance. Solutions used were platelet-rich plasma (PRP), 0.9% saline (S), Gliceol (GC), Pluronic-F127 20% (PL), hyaluronic acid 2% (HA), saline with 10% glucose (GS), Gelaspan (GP), Covergel-BiBio (TB) and PRP+TB.

Table 2 Nonparametric Spearman's correlation for all characteristics evaluated

	Resistivity	Viscosity	Osmolarity	Muscle T^a	EMR time	Cushion decrease
Resistivity	—	0.6352	0.3575	−0.7851**	0.6938*	−0.5295
Viscosity	0.6352	—	−0.3376	−0.8740**	0.4958	−0.6051
Osmolarity	0.3575	−0.3376	—	0.02510	0.3904	0.07531
Muscle T^a	−0.7851**	−0.8740**	0.02510	—	−0.3833	0.4833
EMR time	0.6938*	0.4958	0.3904	−0.3833	—	−0.4500
Cushion decrease	−0.5295	−0.6051	0.07531	0.4833	−0.4500	—

*P-value <0.05.
**P-value <0.01.
EMR, endoscopic mucosal resection.

In conclusion, HA, PL and TB were the best solutions with long-term protective effects (transepithelial R, lower thermal injury and less cushion decrease). Solutions with quicker resection time were GC, PRP and GS.

CONFLICTS OF INTEREST

V. LORENZO -ZÚÑIGA, R. Bartolí and J. Boix declare patent authorship of one of the tested solutions

(Covergel-BiBio). Other authors have no conflicts of interest to disclose. The authors who have taken part in this study do not have a relationship with the manufacturers of the drugs involved either in the past or present and did not receive funding from the manufacturers to carry out their research.

REFERENCES

1 Conio M. Endoscopic mucosal resection. *Gastroenterol. Hepatol.* 2011; **7**: 248–50.
2 Ferreira A, Moleiro J, Torres J, Dinis-Ribeiro M. Solutions for submucosal injection in endoscopic resection: a systematic review and meta-analysis. *Endosc. Int. Open.* 2015; **04**: E1–16.
3 Polymeros D, Kotsalidis G, Triantafyllou K, Karamanolis G, Panagiotides JG, Ladas SD. Comparative performance of novel solutions for submucosal injection in porcine stomachs: an *ex vivo* study. *Dig. Liver Dis.* 2010; **42**: 226–9.
4 Huai ZY, Xian WF, Jiang LC, Chen WX. Submucosal injection solution for endoscopic resection in gastrointestinal tract: a traditional and network meta-analysis. *Gastroenterol. Res. Pract.* 2015; **2015**: https://doi.org/10.1155/2015/702768.
5 Uraoka T, Saito Y, Yamamoto K, Fujii T. Submucosal injection solution for gastrointestinal tract endoscopic mucosal resection and endoscopic submucosal dissection. *Drug Des. Devel. Ther.* 2008; **2**: 131–8.
6 Fujishiro M, Yahagi N, Kashimura K *et al.* Tissue damage of different submucosal injection solutions for EMR. *Gastrointest. Endosc.* 2005; **62**: 933–42.
7 Yandrapu H, Desai M, Siddique S *et al.* Normal saline solution versus other viscous solutions for submucosal injection during endoscopic mucosal resection: a systematic review and meta-analysis. *Gastrointest. Endosc.* 2017; **85**: 693–9.
8 Park S, Chun HJ, Kim CY *et al.* Electrical characteristics of various submucosal injection fluids for endoscopic mucosal resection. *Dig. Dis. Sci.* 2008; **53**: 1678–82.
9 Lorenzo-Zúñiga V, Boix J, Moreno de Vega V, Bon I, Marín I, Bartolí R. Endoscopic shielding technique with a newly developed hydrogel to prevent thermal injury in two experimental models. *Dig. Endosc.* 2017; **29**: 702–11.
10 Pop GA, de Backer TL, de Jong M *et al.* On-line electrical impedance measurement for monitoring blood viscosity during on-pump heart surgery. *Eur. Surg. Res.* 2004; **36**: 259–65.
11 Zhao TX, Jacobson B. Quantitative correlations among fibrinogen concentration, sedimentation rate and electrical impedance of blood. *Med. Biol. Eng. Comput.* 1997; **35**: 181–5.
12 Søndenaa K, Kjellevold KH. A prospective study of the length of the distal margin after low anterior resection for rectal cancer. *Int. J. Colorectal Dis.* 1990; **5**: 103–5.